Université d'Ottawa · University of Ottawa

To the Lighting One
and the genius of Armando

Abstract

The work presented in this thesis is primarly focused on the development of pre-fluorescent probes for carbon-centered radicals. Coumarin-TEMPO and quinoline-TEMPO adducts have been prepared by tethering a free radical nitroxide group such as 2,2,6,6-tetramethyl-1-piperidinyloxy (TEMPO) to coumarin and quinoline fluorophores through an ester bond. Some organic derivatives of the quinoline-TEMPO adduct are also presented. Intramolecular quenching of fluorescence due to a spin-exchange mechanism between the singlet excited state of the fluorophore and the doublet ground state of the nitroxide and the restoring of fluorescence due to coupling with a carbon-centered radical are the conceptual bases for this reaserach study. The sensors for radicals have been tested in radical trapping reactions employing common radical initiators such as 2,2`-azobisbutyronitrile, 1,3-diphenylacetone and tert-butyl peroxide in the presence of a good hydrogen donor. Carbon-centered radicals were produced by thermal and photochemical decomposition processes and the scavenging reactions were followed by monitoring fluorescence enhancements. Coumarin-TEMPO was then selected for an application in free radical polymerization. Employing the pre-fluorescent nitroxide-switch a novel methodology was developed and used to calculate the kinetic Arrhenius parameters and the corresponding bond dissociation energy for the terminal TEMPO group in the polystyrene-TEMPO capped polymeric chain. Quinoline-TEMPO was selected to detect photo-produced benzyl radicals in supramolecular systems. Sodium dodecyl sulfate was used to prepare micellar aggregates containing the pre-fluorescent probe and the radical initiator. Photolysis of the samples at 300 nm generated benzyl radicals and fluorescence growth was monitored via the radical coupling reaction by the sensor. The kinetics of trapping were slower than in homogenous solutions due to the presence of "cage effects" for the radical pairs produced within the constrained environment. Quinoline-TEMPO and 1,3-diphenylacetone were encapsulated in NaY zeolites in order to monitor carbon-centered radicals in the cavities of the aluminosilicate framework. Solid samples and polymeric

polymethylhydrosiloxane suspensions were photolyzed and fluorescence emission enhancements were monitored during the course of the reaction. Bisbenzyl biradicals, produced by photolysis of [3,3]-paracyclophane were detected employing quinoline-TEMPO as a pre-fluorescent probe. In the final part of this thesis the preparation of new organometallic compounds as single crystals using quinoline-TEMPO as a ligand for metals (Ni^{2+}, Co^{2+}, Eu^{3+}, La^{3+}) is described. The fluorescence spectrum of europium (III) potassium tetra-quinoline-TEMPO, obtained by excitation of the ligand part of the metal complex, showed an "antenna effect" resulting in a sharp metal-centered emission in the red part of the visible electromagnetic spectrum. The radical trapping reaction of 2-cyano-2-propyl radicals, produced by the thermal decomposition of 2,2'-azobisbutyronitrile, was observed by monitoring the behavior of the fluorescence emissions from the ligand and from the europium metal center. UV absorption spectral analysis of the dynamics of the reaction confirmed that during the course of the radical trapping reaction the organometallic complex degrades releasing diamagnetic coupled products of quinoline-TEMPO from the metal center.

Acknowledgments

During last two years I had a great opportunity to study radical chemistry in different systems and to explore novel areas of research. For this I would like to thank Professor Tito Scaiano who guided my research study, resulting in the achievement of reliable results. He is a great open-minded scientist that always allowed me to look for and investigate new possible areas of research. I also would like to thank all the members of the research group for their patience, advice and challenges which allowed me to build-up my perseverance. In particular I want to remember Olga Garcia Ballesteros, Alexis Aspee, Marius Gabriel Ivan and John Palfreyman for their outstanding contribution in this research project.

My special thanks are directed to the Reardon family because they helped me to feel at home here in Canada even if I belong to other places. In particular I would like to thank my great friend Damien Reardon who taught me everything I needed to crystallize my experience in Ottawa.

Table of contents

List of Figures

List of Schemes

List of Equations and Tables

List of Abbreviations

TEMPO (T•) : 2,2,6,6-tetramethylpiperidinyloxy free radical

4-hydroxy-TEMPO : 4-hydroxy-2,2,6,6-tetramethylpiperidinyloxy free radical

TMIO : 7,7,8,8-tetramethyl-*o*-quinodimethane

LFP : laser flash photolysis

EPR : electron paramagnetic resonance

DCC : 1,3-dicyclohexylcarbodiimide

DEA : 1-[dimethylamino)propyl]-3-ethylcarbodiimide hydrochloride

DMAP : dimethylaminopyridine

Coumarin-TEMPO (CUT•) : (3-coumarinoxyl)-2,2,6,6-tetramethylpiperidine-1-oxyl free radical

Quinoline-TEMPO : 4-(3-hydroxy-2-methyl-quinolinoyoxy)-2,2,6,6-tetramethylpiperidine-1-oxyl free radical

QTs-T : 4-(3-p-toluensulfonoxy-2-methyl-4-quinolonoyloxy)-2,2,6,6-tetramethylpiperidine-1-oxyl free radical

QMe-T : 4-(3-methoxy-2-methyl-4-quinolonoyloxy)-2,2,6,6-tetramethylpiperidine-1-oxyl free radical

Q10C-T : 4-(3-decylkoxy-2-methyl-4-quinolonoyloxy)-2,2,6,6-tetramethylpiperidine-1-oxyl free radical

Q-TH : 4-(3-hydroxy-2-methyl-4-quinolonoyloxy)-2,2,6,6-tetramethylpiperidine-1-hydroxyl

HPLC : High Performance Liquid Chromatography

AIBN : 2,2′-azobisbutyronitrile

DBK : 1,3-diphenylacetone

DTBP : tert-butyl peroxide

Q-TAIBN : 3-hydroxy-2-methyl-quinoline-4-carboxylic acid 1-(1-cyano-1-methyl-ethoxy)-2,2,6,6-tetramethyl-piperidin-4-yl ester

LFRP : living free radical polymerization

BDE : bond dissociation energy

EB-T : 2,2,6,6-tetramethyl-1-(1-phenylethoxy)-piperidine

PN-T : 1-(2,2,6,6-tetramethylpiperidine N-oxide)-1,3diphenylpropane

PS• : polystyrene macroradical

PS-T : Tempo-capped polystyrene

CU-T-PS : coumarin-TEMPO-capped polystyrene

SEC : size exclusion chromatography

PCP : [3,3]paracyclophan-2-one

BBB : 4,4'-(1,3-propanediyl)bisbenzyl biradical

CP : cyclophane

HDAC : hexadecyltrimethylammonium chloride

SDS : sodium dodecyl sulfate

PMHS : polymethylhydrosiloxane

Terpy-NIT : 2-[4'-(2,2':6',2''-teryridyl)]-(4,4,5,5-tetramethylimidazolinyl-3-oxide-1-oxyl

Terpy-IM : 2-[4'-(2,2':6',2''-teryridyl)]-(4,4,5,5-tetramethylimidazolin-1-oxyl

Ni-Q-T : nickel (II) bis-quinoline-TEMPO

Co-Q-T : cobalt (II) bis-quinoline-TEMPO

Eu-Q-T : europium (III) potassium tetra-quinoline-TEMPO

La-Q-T : lantanum (III) potassium tetra-quinoline-TEMPO

ISC : intersystem crossing

IC : internal conversion

CT : charge transfer

LMCT : ligand metal charge transfer

1 Introduction

1.1 Research objective

An important field in the study of photochemistry is the detection of carbon-centered radicals. These radicals have been detected, for several years, with the aid of different spectroscopic techniques and probes. Dr. Scaiano has a worldwide reputation in the field of photochemistry due to his research and understanding of radical chemistry. The project he asked me to pursue during my Masters program concerns the development of a sensor for radicals, which would simplify the monitoring of transients in solutions and in supramolecular systems. Construction of a suitable sensor requires, in general, the application of a well-accepted principle and in most cases will make use of molecular components whose characteristics and properties are well established. The concept we wanted to apply considers the use of an "on/off" switch of fluorescence emission covalently connected with the molecule responsible for the radiative transition (fluorophore). This switch has to quench fluorescence when it is attached to the fluorophore and be able to restore the signal after the formation of a sigma bond with the radical.

The molecule we decided to employ in order to satisfy the requirements of this concept is a nitroxide stable free radical, called TEMPO, which has been studied in the last few decades for its paramagnetic properties, as quencher of singlet and triplet states and as a trap for carbon-centered radicals. Quenching of excited states has been studied in intermolecular and intramolecular processes and it is well accepted that a nitroxide stable free radical tethered to a fluorophore almost entirely quenches the fluorescence due to the introduction, in the deactivation pathway of the excited state, of a fast channel to the ground state. This is the result of an electron exchange mechanism between the excited electron of the singlet state and the unpaired electron of the nitroxide moiety. The nitroxide group can then convert the paramagnetic non-fluorescent molecule to a

diamagnetic fluorescent compound by scavenging of a carbon-centered radical. This results in an easy methodology for the detection of carbon-centered radicals that makes use of a very sensitive spectroscopic technique like fluorescence spectroscopy. This study does not involve considerations of quantum yields and lifetimes of fluorescence because the main purpose is to be able to follow radical trapping and not to explain photophysical properties of the molecules developed.

1.2 Fluorescence: luminescence from the singlet state

The term luminescence refers to the emission of radiation. When an atom or a molecule absorbs electromagnetic radiation it is raised from its ground state to a higher electronic level excited state[1]. Every electronic state is characterized by its orbital electron configuration and its state multiplicity. State multiplicities are very important because they affect the nature of the emissions. If the state from which the emission originates has the same multiplicity of the state where the emission terminates the emission is called fluorescence, and if it is different, the emission is called phosphorescence. The electron evolution in an atom or molecule generates two types of magnetic momenta and mechanical angular momenta. One type is derived from the motion of the electron around the nucleus and the other from the "spin" of the electron. Quantization of the spin angular momentum makes it possible to symbolize the spin by a vector representation. Two orientations are possible, "spin-up" $\uparrow$ or "spin-down" $\downarrow$. In polyatomic molecules the polycentric orbitals are called molecular orbitals and the Pauli exclusion principle dictates that only two electrons can occupy the same orbital and the spin has to be opposite. The electronic state multiplicity is calculated from 2S+1 where S is the total spin quantum number, the sum of all the contributions of each electron. If the two outer shell electrons have opposite spin vectors the electronic state is called singlet state (S = 0) and if the spin have parallel spin vectors the state is called triplet state (S = 1). Usually the ground state for a molecule is a singlet state because both of the electrons are in the same molecular orbital with opposite spin. Upon irradiation the molecule jumps to a higher excited singlet state because highly probable transitions occur when $\Delta S =$

0 and the transition can occur to any of the excited states S_1, S_2, S_3, etc. A vibrational relaxation process with a lifetime ranging between 10^{-11} and 10^{-14} seconds is associated with each state and this brings the molecule to the lowest excited state S_1. The singlet excited state can deactivate to the singlet ground state with consequent fluorescence emission with a lifetime in the order of 10^{-7}-10^{-9} seconds. Otherwise radiationless processes can occur between the first excited singlet state and the lowest excited triplet state (intersystem crossing, 10^{-8} seconds). Internal conversion from the singlet to the ground state can also occur (10^{-5}-10^{-7} seconds) but this competes with the other faster processes therefore the complete quenching of fluorescence is extremely rare. From the triplet state the deactivation can proceed through phosphorescence emission or intersystem crossing to the ground singlet state with a lifetime between 10 and 10^{-3} seconds. The Jablonski diagram in Figure 1-1 shows the absorption of light (hν) and subsequent unimolecular deactivation processes (fluorescence, phosphorescence, internal conversion IC, intersystem crossing ISC).

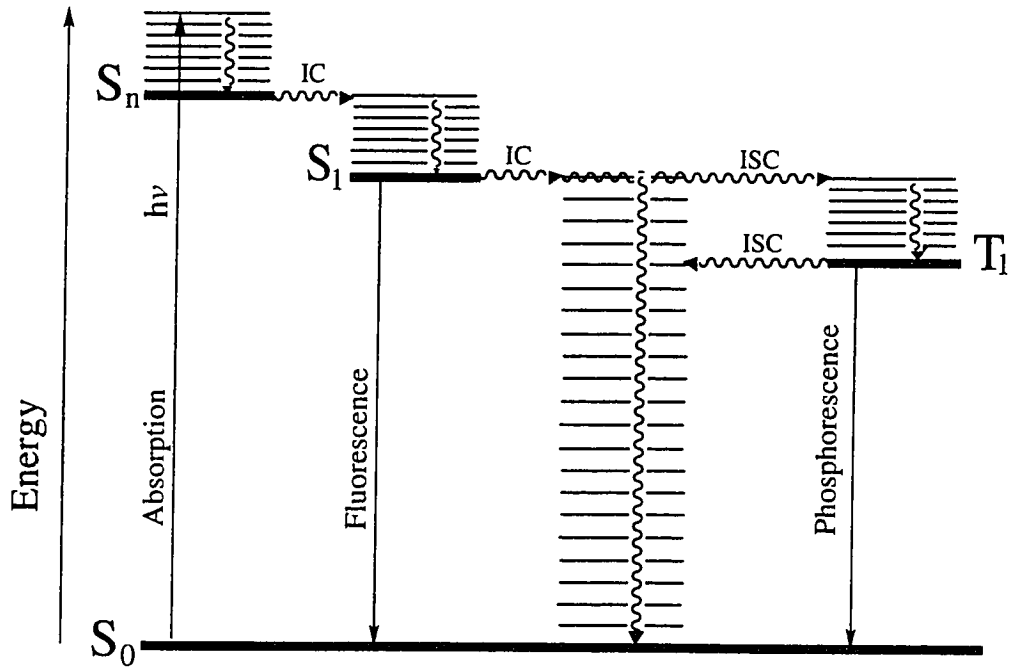

Figure 1-1 Jablonski diagram. Deactivation pathway of the excited states after absorption of a photon (hν).

The energy in the emission from the first singlet state, after several vibrational deactivation processes, is only a fraction of all the energy absorbed by the

molecule. Lower energy of the emitted photon is shown by the shift of the emission to longer wavelengths. Every measurement becomes a difference with zero background while in absorption spectrophotometry the result is a difference between two large signals. For this reason fluorescence spectroscopy is an analytical technique with a great sensitivity and specificity (fluorescence lifetimes). Trace contaminants in the order of parts per trillion can be detected in different systems in our environment and industries or in parts of our body. This makes detection of fluorescence an essential tool of analysis.

1.3 Nitroxides as persistent stable free radicals

Nitroxides are persistent free radicals in which an unpaired electron is delocalized between the nitrogen and the oxygen atom. Many different kinds of nitroxides are present in the literature including nitroxides with primary, secondary, and tertiary alkyl groups and with aryl, alkoxy and amino groups. Substituents derived from other elements of the higher periods are also known[2].

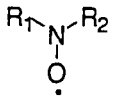

Scheme 1-1 Nitroxides. R^1 and/or R^2 = H, Me, n-, s- and t-alkyl, aryl, OR, SR, NR_2, PR_2, SiR_3, ML_n, (M = transition metal, L = ligand).

The stability of the free radical moiety derives from the unique resonance structure which can be written for the nitrogen-oxygen group in which three π-electrons are distributed over two atomic centers.

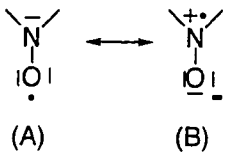

Scheme 1-2 Resonance structures for the nitrogen-oxygen group in nitroxides.

Two of the π-electrons occupy the low-lying bonding π-orbital, with a third one in the antibonding π*-orbital, thus yielding a net π-bonding of one electron. The N-O bond of the nitroxide group has a bond order of one and a half. This consists of a σ-bond and half of a π-bond as indicated by the bond energy of

approximately 100 kcal/mol[3]. For a single N-O bond and N=O double bond the energy is 53 kcal/mol and 145 kcal/mol respectively. The multiplicity of nitroxides is two and they are doublets in their ground state. In this thesis all the work has been done employing 2,2,6,6-tetramethylpiperidine-N-oxyl, also known as TEMPO, and in particular a derivative in which a 4-hydroxy-2,2,6,6-tetramethylpiperidinyloxy free radical, 4-hydroxy-TEMPO, is tethered to a fluorophore. The TEMPO free radical itself has attracted a lot of attention because of its properties as a quencher of singlet and triplet states, a scavenger of carbon-centered radicals and as a spin probe. The delocalization energy is in the order of 30 kcal/mol and for this reason dimerization of two molecules of TEMPO through formation of an O-O bond is highly unfavorable. The energy of 35 kcal/mol released when the bond is formed does not compensate for the loss of delocalization.

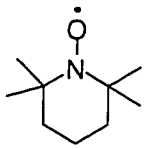

TEMPO, free radical

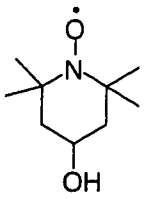

4-Hydroxy-TEMPO, free radical

Scheme 1-3 Nitroxides used for derivation in this application of paramagnetic pre-fluorescent probes.

1.4 TEMPO intermolecular quenching of singlet and triplet excited states.

The quenching of electronically excited states frequently involves either energy or electron transfer to an acceptor molecule. However, there are molecules which can efficiently quench singlet excited states and remain physically unchanged in the process. Simple molecules of this type are species with unpaired electrons which can enhance intersystem crossing without energy transfer by allowing overall spin conservation. Examples of these kinds of quenchers include paramagnetic ions and other paramagnetic molecules such as nitric oxide[4] and

molecular oxygen[5,6]. Molecular oxygen catalyzes intersystem crossing from the singlet to the triplet state and the triplet sensitizes the production of singlet oxygen. Nitric oxide is one of the simplest and stablest paramagnetic substances, which has been shown to play important roles in biological systems. It is an intra and intercellular signalling species; it controls and regulates the vascular tone, and it is a molecule that carries messages in the central nervous system[7]. Nitroxides are organic models for this molecule and nitric oxide for example can form a persistent radical 1,1,3,3-tetramethylisoindoline-2-oxyl free radical (TMIO) **2** through reaction with 7,7,8,8-tetramethyl-*o*-quinodimethane[8].

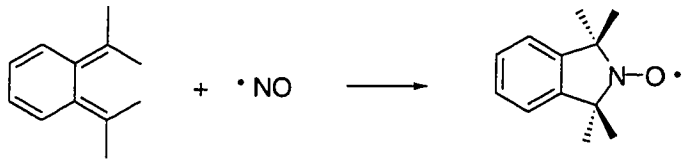

1 2

Scheme 1-4 Reaction scheme of nitric oxide with 7,7,8,8-tetramethyl-*o*-quinodimethane leading to 1,1,3,3-tetramethylisoindoline-2-oxyl free radical (TMIO).

TEMPO is an effective quencher of excited singlet states of organic molecules[9,10]. The rate constant k_q of quenching can be calculated from the Stern-Volmer relation which shows that the ratio of the fluorescence quantum yields both with and without the quencher is linearly dependent on the concentration of the quencher.

$$\frac{\Phi_f^0}{\Phi_f} = 1 + \frac{k_q[Q]}{k_f}$$

Equation 1-1 Stern-Volmer relation. The ratio of the quantum yields depends on the concentration of the quencher due to the Stern-Volmer coefficient $K_{SV} = k_q/k_f$.

The ratio of the quantum yields is equal to the ratio of the relative fluorescence intensities if the intensity of the absorbed radiation is identical for all the measurements. The slope of the plot of the fluorescence intensity ratio with and without the quencher (I_f^0/ I_f vs. the concentration of the quencher [Q]) is the Stern-Volmer coefficient, K_{sv}, equal to $k_q/k_f = \tau_f k_q$ and if the fluorescence lifetime

τ_f is known the rate constant of quenching can be obtained. The quenching rate constant for organic molecules[10,11] is in the order of 10^9-10^{10} M^{-1} s^{-1}, approximately diffusion controlled, and they show little variation upon changing the aromatic hydrocarbon. A variety of mechanisms are possible for the intermolecular quenching of singlet states by a stable free radical (doublet). They include spin exchange, charge transfer and energy transfer in the collision complex but rationalization of these components can be difficult. TEMPO has also been investigated as quencher of triplet states in which variations are observed when a different aromatic hydrocarbon is used[10]. The rate constant is obtained from laser flash photolysis studies of the decaying triplet signal in the presence of different amounts of quencher. The observed first order rate constant for triplet decay shows a linear dependence on TEMPO concentration where the resulting slope is the quenching rate constant.

$$k^T = k_0^T + k_q^T[\text{TEMPO}]$$

Equation 1-2 First order rate constant equation for intermolecular quenching of triplet excited states by TEMPO.

The mechanisms of triplet state quenching by nitroxides, which have been proposed to explain the deactivating interactions, are the same as the ones outlined for the singlet state case: charge transfer, energy transfer and spin exchange. Assigning the magnitude of each component of the deactivation pathway has been proven to be non-trivial, and hence complete understanding of this phenomenon has yet to be achieved.

1.5 TEMPO intramolecular quenching of singlet and triplet excited states.

The mechanism by which nitroxides quench singlet and triplet states has been the subject of many experiments for over 30 years. One of the most interesting efforts in order to understand the mechanism of singlet quenching was made by employing a fluorophore tethered to a free radical nitroxide[12,13]. Several naphthalene derivatives were synthesized and studied in terms of intramolecular fluorescence quenching (Scheme 1-5).

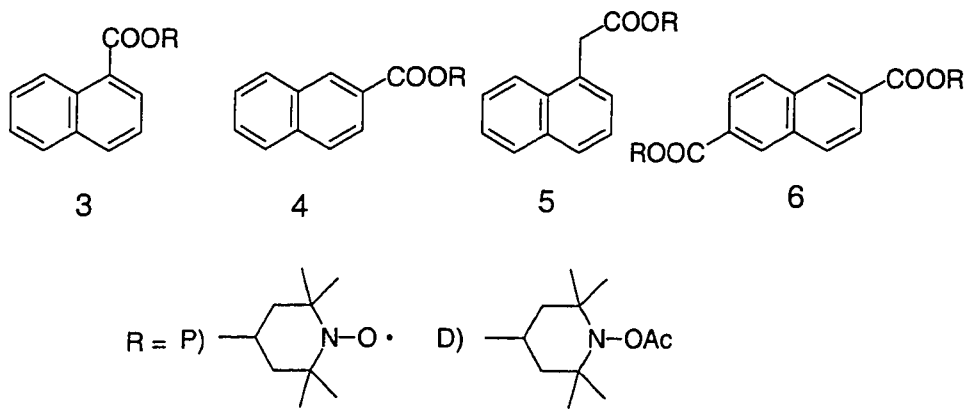

Scheme 1-5 Naphtalene-TEMPO adducts: P) paramagnetic species, D) diamagnetic species.

The paramagnetic free radical compound and the diamagnetic acetyl compound have both been studied to find their different fluorescence lifetimes and quantum yields. Fluorescence lifetimes are considerably diminished (by more than thirty times) when the diamagnetic molecule is exchanged with the paramagnetic one underlying the efficiency of intramolecular quenching of excited states by nitroxides. This kind of molecules offers a way of both studying the mechanism of nitroxide quenching in more detail and of establishing the distance dependence and possible importance of "through-bond" vs "through-space" interactions in the quenching. The expression "optical probe" appeared for the first time but only nine years later, when compound **3P** was used as a pre-fluorescent probe[14] for trapping carbon-centered radicals allowing all the potentials of this expression to be exploited. Primary radical concentrations generated by a laser pulse were detected using fluorescence detection. Fluorescamine-derivatized nitroxides (PROXYL and TEMPO adducts) **7A, 7B, 7C** are also present in the literature[15] (Scheme 1-6).

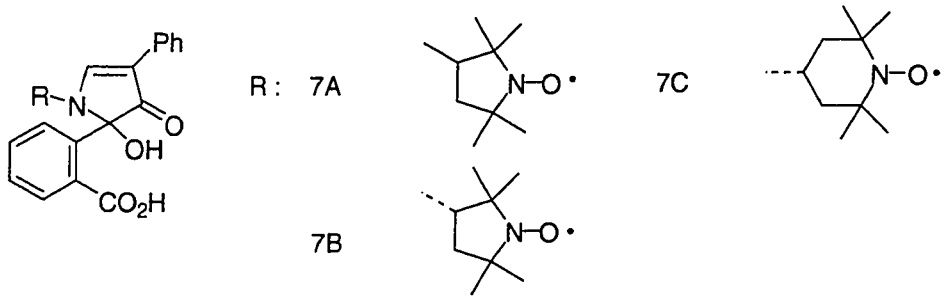

Scheme 1-6 Fluorescamine-derivatized nitroxides

These pre-fluorescent probes have been studied for the intramolecular quenching of excited singlet states in order to obtain information on the factors controlling the rates and distance-dependence of the quenching. Compounds **7A** and **7B** have hence been used to observe and quantify radicals in aqueous biological systems[16-18]. TEMPO free radical molecules have also been tethered to triplet sensitizers[19] in order to investigate the mechanism of quenching. Chemically induced dynamic electron polarization of the nitroxides[20,21] has been observed in the intermolecular quenching process of triplet states. This phenomenon was first observed in the 1980s when it was reported that electron spin systems in solution like the nitroxide doublet can become polarized in emission if triplet states of excited molecules are present[22]. Linking the nitroxide to the molecule, triplet quenching should be much faster and the spin polarization of the nitroxide more intense. Many TEMPO-labeled compounds are now studied for this fascinating phenomenon, including big and complex molecules such as fullerenes[23] and porphyrins[24]. A simpler molecule like 9-Oxo-9H-thioxanthenoxy-2,2,6,6-tetramethylpiperidine-1-oxyl free radical **8** has been synthesized and investigated in its intramolecular triplet quenching and compared with the intermolecular process. Laser flash photolysis and time-resolved electron paramagnetic resonance experiments showed that triplets were quenched by TEMPO via an intramolecular pathway. The reaction of quenching resulted in a spin polarized emission and this emission is much larger than in the intermolecular process.

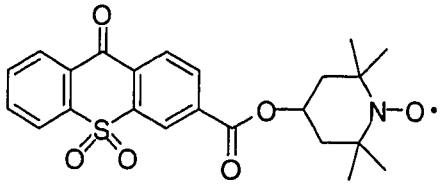

8

Scheme 1-7 9-Oxo-9H-thioxanthenoxy-2,2,6,6-tetramethylpiperidine-1-oxyl free radical.

The mechanism by which nitroxides intramolecularly quench singlet and triplet states has been assigned to an electron exchange mechanism between the doublet ground state of the quencher and the excited state of the sensitizer.

1.6 Nitroxides as carbon-centered radical scavengers.

Nitroxides are extremely important molecules for photochemists, as not only do they allow the quenching of singlet and triplet states, but they also couple with carbon-centered radicals. The formation of a bond between the nitroxide free radical and carbon-centered radicals has been extensively studied in terms of the rate constants of reaction[25-29] and in terms of the magnetic field effects on the interactions between radical pairs and nitroxides in solutions[30] and in supramolecular systems[31-34]. Laser flash photolysis (LFP) has been used by Ingold at the National Research Council of Canada in Ottawa for the determination of the absolute rate constant for the reactions of some carbon-centered radicals with both TEMPO and TMIO radical traps[25]. The carbon-centered radicals were produced by photolysis of symmetrically substituted ketones (a,Scheme 1-8), diacyl peroxides (b, Scheme 1-8), and tert-butyl peroxide in the presence of an hydrogen donor (c and d, Scheme 1-8). The rate constants of trapping were measured by monitoring the increased rate of decay of the carbon-centered radical produced with the laser pulse in the presence of different amounts of the nitroxide quencher. Plotting the experimental constant as a function of the concentration of quencher and by considering Equation 1-2, the rate constant of trapping by TEMPO was calculated as the slope of the linear fit.

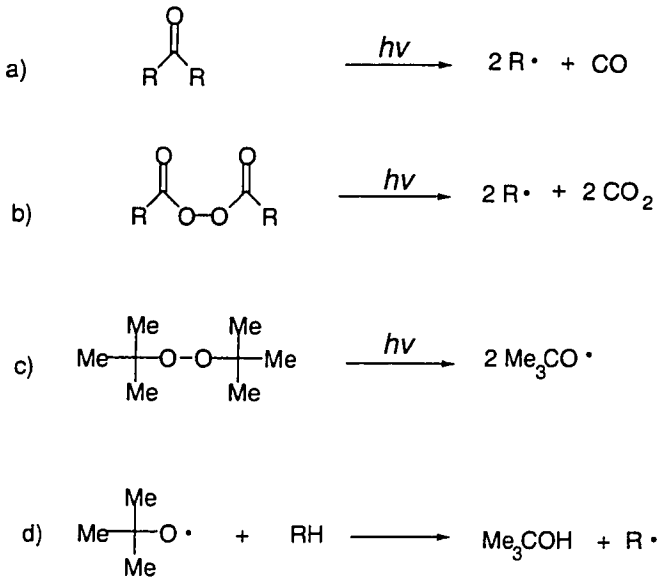

Scheme 1-8 Reaction showing the photolysis of a) symmetrical substituted ketones, b) diacyl peroxides, c) and, d) tert-butyl peroxide in the presence of a good hydrogen donor leading to generation of two carbon-centered radicals.

The absolute rate constants of the trapping of alkyl radicals are an order of magnitude slower than the rate constants for the bimolecular coupling reaction. For example TEMPO traps n-nonyl, tert-butyl, and benzyl radicals in isooctane at room temperature with rate constants of 1.2×10^9, 7.6×10^8, and 4.9×10^8 $M^{-1}s^{-1}$, respectively while the rate constants for the alkyl radical bimolecular self-reactions in comparable solvents are 2.4×10^{10} $M^{-1}s^{-1}$ for n-pentyl radicals, 7×10^9 $M^{-1}s^{-1}$ for tert-butyl radicals, and 5×10^9 $M^{-1}s^{-1}$ for benzyl radicals. The competition between radical trapping and bimolecular reaction can depend on the solvent used. Polarity and viscosity can affect the rate of the reaction therefore in order to allow the use of nitroxides as probes for these radicals the nature of any solvent dependence has been investigated[27]. A "radical-clock" has been used where the nitroxide radical trapping of a carbon-centered radical competes with a unimolecular rearrangement. Steric effects have also been observed using differently hindered nitroxide radicals[29,35] leading in some cases to cross-section rate constants less than 2×10^{-5} M^{-1} s^{-1}. The direct determination of the absolute rate constants of the reaction of scavenging by nitroxides was possible due to the high rates of reaction involved in these processes. This also allows the use of very low concentrations of the probe [(1×10^{-5})-(5×10^{-3}) M]. Nitroxides absorb strongly at the wavelength of photolysis and in these kinds of experiments light must be absorbed exclusively by the radical precursor.

1.7 Nitroxides as spin probes

Nitroxides are stable free radicals and the unpaired electron is a suitable moiety for electron paramagnetic resonance spectroscopy (EPR). The nitroxide EPR signal is very sensitive to the surrounding environment and the broadening of the peaks is representative of motional dynamics. For this reason molecules such as TEMPO and other nitroxides have been extensively used as spin labels for macromolecules such as proteins or macro structures such as membranes[36]. Every EPR spectrum is described by three parameters: the g-factor, which quantifies the interaction between the kinetic moments of the orbital movement of the electron and the moment of rotation about itself, the hyperfine coupling constant, which represents the interaction of the magnetic moments of the

electron and the nucleus ^{14}N (I=1), and the line widths. The first two parameters are averaged to a nonzero value for a molecule which is free to move but the EPR spectrum changes considerably when the motion of the molecule is slowed down. This provides information about the local environment of the probe, the constraint conditions and changes in the polarity. In addition, the unpaired electron of two different molecules of nitroxide can interact with each other by a magnetic dipolar interaction. This can be a long-range or a strong short-range interaction and can give information about distances in frozen or very viscous media. Nowadays, labeling of proteins, membranes, DNA and RNA is an effective tool in the investigation of the structure and dynamics of complex macromolecules in biological systems.

2 Preparation of pre-fluorescent probes

2.1 Introduction

The strategy we decided to follow for the synthesis of pre-fluorescent probes is an esterification of the carboxylic acid of a fluorophore with the alcohol derivative of the TEMPO free radical. When choosing a carboxylic acid, the obvious choice would be to choose a fluorophore with a high fluorescent quantum yield. Instead, the acid chosen was dictated by the availability of molecules in the laboratory at the beginning of this project and by the idea of having a starting material which has the potential to be easily modified. In this thesis coumarin-3-carboxylic acid **9** and 3-hydroxy-2-methyl-4-quinoline carboxylic acid **10** were used as starting materials for the reaction of coupling with 4-hydroxy-TEMPO.

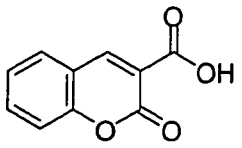

9

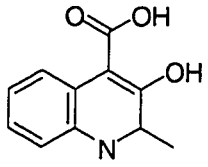

10

Scheme 2-1 Coumarin-3-carboxylic acid (9), 3-hydroxy-2-methyl-4-quinoline carboxylic acid (10).

Both carboxylic acid and 4-hydroxy-TEMPO were purchased from Aldrich and used as they were received. The parent structure of coumarin is not highly fluorescent unlike the derivatives coumarin 2, **11** and coumarin 343, **12**. Their fluorescent properties are due to delocalization of the lone pair on the nitrogen atom along the aromatic structure.

11 12

Scheme 2-2 Coumarin 2 (10), coumarin 343 (11).

2.2 Method of preparation

The esterification reaction takes place in the presence of 1,3-dicyclohexylcarbodiimide (DCC) or 1-[dimethylamino)propyl]-3-ethylcarbodiimide hydrochloride (DEA) and a catalytic amount of dimethylaminopyridine (DMAP). These molecules activate the carboxylic group, which is then transformed to the ester by attack of the alcohol on the activated adduct[37]. The activation happens through the attack of the carboxylic group which is made more nucleophilic by the presence of the substituted pyridine, to the diimidic group (Scheme 2-3). This activated ester intermediate **13** is then easily attacked by 4-hydroxy-TEMPO (Scheme 2-4).

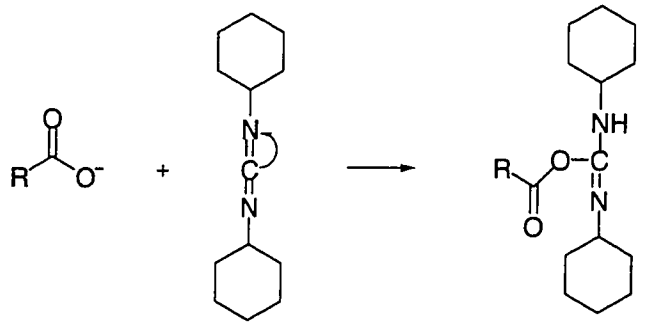

DCC 13

Scheme 2-3 Reaction for the activation of a carboxylic acid with 1,3-dicyclohexylcarbodiimide (DCC).

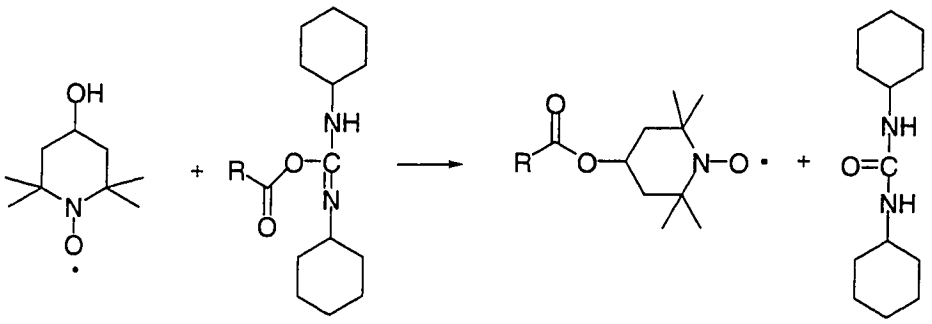

Scheme 2-4 Reaction for the nucleophilic attack of 4-hydroxy-TEMPO on the activated ester.

The coupling reaction of 4-Hydroxy-TEMPO with **9** was done using DCC at 60 °C under a nitrogen atmosphere yielding the pre-fluorescent probe 3-(coumarinoyloxy)-2,2,6,6-tetramethylpiperidine-1-oxyl free radical, which is also named coumarin-TEMPO.

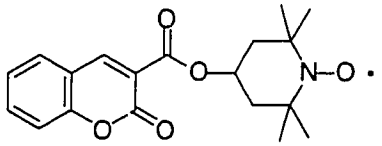

Scheme 2-5 3-(Coumarinoyloxy)-2,2,6,6-tetramethylpiperidine-1-oxyl free radical (coumarin-TEMPO).

DEA is used in a similar reaction with **10** as a substrate yielding the coupling product 4-(3-hydroxy-2-methyl-quinolinoyloxy)-2,2,6,6-tetramethylpiperidine-1-oxyl free radical, which is also named quinoline-TEMPO. The reaction mechanism of DEA is the same as for DCC but the polar groups of DEA allow the quinoline acid to dissolve in dichloromethane while DCC does not.

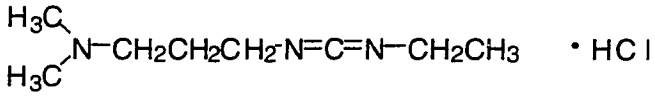

Scheme 2-6 1-[Dimethylamino)propyl]-3-ethylcarbodiimide hydrochloride (DEA).

This free radical derivative of quinoline contains in position 3 (Scheme 2-7) an interesting phenol group which can be easily modified by coupling reactions with other organic molecules.

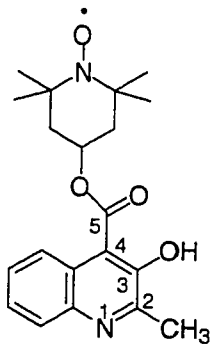

Scheme 2-7 4-(3-Hydroxy-2-methyl-quinolinoyloxy)-2,2,6,6-tetramethylpiperidine-1-oxyl free radical (quinoline-TEMPO).

The molecules we chose for this kind of derivatization were para-toluenesulfonyl chloride and two different alkyl bromides: methyl bromide and 1-bromodecane. Two nucleophilic substitution reactions were carried out employing quinoline-TEMPO in the presence of triethylamine or potassium carbonate as bases. The produced alkoxide form can attack the halogen substrates. In Scheme 2-8 the reaction scheme showing the preparation of 4-(3-p-toluenesulfonoxy-2-methyl-4-quinolinoyloxy)-2,2,6,6-tetramethylpiperidine-1-oxyl free radical (QTs-T) and in Scheme 2-9 the scheme for synthesizing 4-(3-methoxy-2-methyl-4-quinolinoyloxy)-2,2,6,6-tetramethylpiperidine-1-oxyl free radical (QMe-T) and 4-(3-decylkoxy-2-methyl-4-quinolinoyloxy)-2,2,6,6-tetramethylpiperidine-1-oxyl free radical (Q10C-T).

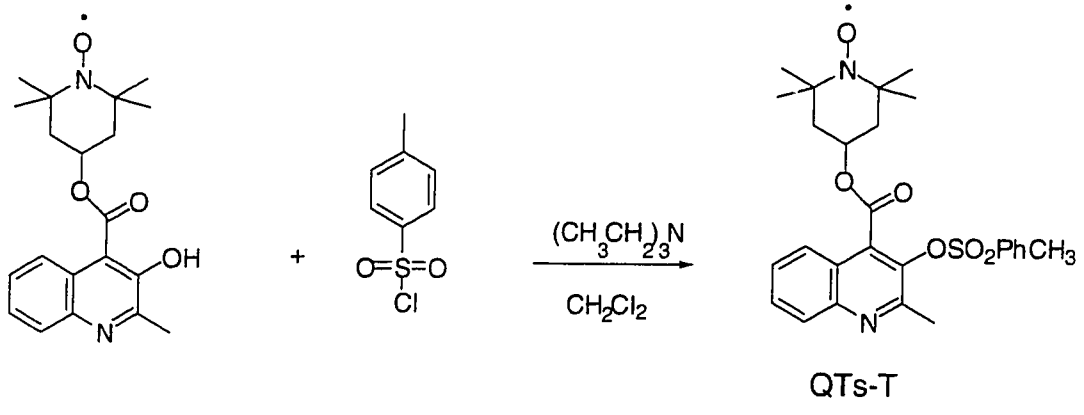

Scheme 2-8 Reaction of quinoline-TEMPO with p-toluenesulfonyl chloride in presence of triethylamine base leading to the synthesis of 4-(3-p-toluenesulfonyloxy-2-methyl-4-quinolinoyloxy)-2,2,6,6-tetramethylpiperidine-1-oxyl free radical (QTs-T).

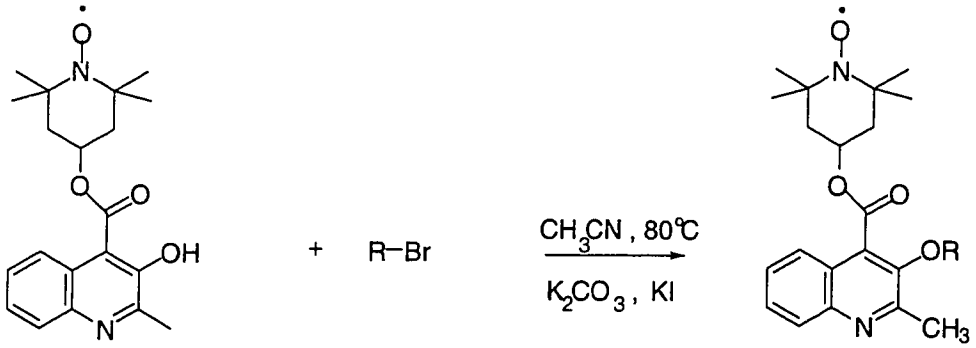

R : CH_3 QMe-T

$CH_3(CH_2)_8CH_2$ Q10C-T

Scheme 2-9 Reaction of quinoline-TEMPO with methyl bromide and 1-bromodecane in presence of potassium carbonate base and potassium iodide at 80 °C under a nitrogen atmosphere leading to the preparation of 4-(3-methoxy-2-methyl-4-quinolinoyloxy)-2,2,6,6-tetramethylpiperidine-1-oxyl free radical (QMe-T) and 4-(3-decyloxy-2-methyl-4-quinolinoyloxy)-2,2,6,6-tetramethylpiperidine-1-oxyl free radical (Q10C-T).

2.3 Synthesis

2.3.1 (3-Coumarinoyloxy)-2,2,6,6-tetramethylpiperidine-1-oxyl free radical (coumarin-TEMPO)

One gram (5.26 mmols) of coumarin-3-carboxylic acid was added to a three-necked round bottom flask containing 500 ml of dichloromethane under an argon atmosphere. To this mixture 0.1 equivalents of 4-dimethylaminopyridine (64 mg), 1 equivalent of DCC (1.08 g) and 1 equivalent of 4-hydroxy-TEMPO (906 mg) was added. The reaction was then stirred for 2 hours at 60 °C. After removal of the white precipitate, 1,3-dicyclohexylurea, the reaction mixture was washed three times with water. The organic solution was dried over magnesium sulfate and then concentrated. The residue was chromatographed on silica gel (hexane/ethyl acetate, gradient from 8:2 to 7:3) to obtain coumarin-TEMPO (1.17 g, yield 65 %, FW = 344). HPLC-MS (C-18 column, 100% acetonitrile) : 344, 191, 173,154,140, 124, 109,98, 89, 81, 69; RT=5.78 min. IR (KBr, cm^{-1}): 3409 (wb), 3079 (w), 3046 (w), 2992 (m), 2972 (m), 2938 (m), 1763 (s), 1613 (m), 1567 (m), 1489 (w),

1454 (s), 1377 (s), 1315 (m), 1297 (s), 1251 (s), 1241 (s), 1214 (s), 1178 (m), 1128 (s), 1012 (s), 994 (m), 955 (w), 923 (w), 866 (w), 798 (m), 784 (w), 757 (s).

2.3.2 *4-(3-Hydroxy-2-methyl-4-quinolinoyloxy)-2,2,6,6-tetramethylpiperidine-1-oxyl free radical (quinoline-TEMPO)*

One gram (4.92 mmols) of 3-hydroxy-4-methyl-2-quinoline carboxylic acid was added to 500 ml of dichloromethane at 60 °C under an argon atmosphere. The acid did not solubilize in dichloromethane but after adding 0.1 equivalents of 4-dimethylaminopyridine (60 mg), 1.2 equivalent of DEA (1.13 g) and 1 equivalent of 4-hydroxy-TEMPO (847 mg) the acid solubilized and the reaction mixture turned red. The reaction was stirred for 6 hours at 60°C and then washed 4 times with water. The organic solution was dried over magnesium sulfate and then concentrated. The residue was chromatographed on silica gel (hexane/ethyl acetate, gradient from 8:2 to 7:3) to obtain quinoline-TEMPO (1.22 g, yield 70%, FW = 357). HPLC-MS (C-18 column, 100% acetonitrile) : 357, 343, 204, 186, 172, 158, 140, 124, 109, 98, 83, 69; RT=7.81 min. IR (KBr, cm^{-1}): 3421 (wb), 2981 (m), 2947 (m), 2930 (m), 1651 (s), 1501 (w), 1465 (m), 1413 (s), 1372 (m), 1351 (m), 1327 (s), 1291 (m), 1216 (s), 1194 (s), 1180 (s), 1145 (s), 1036 (m), 1014 (m), 1003 (m), 992 (m), 981 (m), 892 (w), 809 (m), 768 (m), 745 (m), 677 (w), 641 (w). E.A. : C 65.32 %, H 7.36 %, N 7.6 %, O 15.44 %.

2.3.3 *4-(3-Methoxy-2-methyl-4-quinolinoyloxy)-2,2,6,6-tetramethylpiperidine-1-oxyl free radical (QMe-T)*

One half gram (1.4 mmols) of quinoline-TEMPO was added to 300 ml of acetonitrile at 80 °C under an argon atmosphere. To this solution, 0.5 equivalents of K_2CO_3 (96 mg), 1 equivalent of KI (232 mg) and 1 equivalent of methyl bromide (133 mg) was added and the mixture was stirred for 4 hours. After evaporation of the solvent the desired methylated compound was purified by silica gel chromatography (hexane/ethyl acetate, isocratic 8:2), (0.44 g, yield 85 %, FW = 371). HPLC-MS (C-18 column, 100% acetonitrile) : 371, 341, 218, 200, 170, 157, 140, 124, 109, 98, 81, 69; RT= 6.88 min. IR (KBr, cm^{-1}): 3000 (m), 2971 (m), 2943 (m), 1721 (s), 1588 (w), 1501 (m), 1464 (m), 1446 (m), 1402 (m), 1386 (m), 1363 (m), 1341 (m), 1324 (m), 1289 (s), 1229 (s), 1179 (m), 1154 (m), 1135 (m), 1112 (m), 1024

(w), 1012 (m), 979 (m), 970 (m), 908 (w), 868 (w), 741 (w), 776 (s), 725 (w), 684 (w), 634 (w).

2.3.4 *4-(3-Decyloxy-2-methyl-4-quinolinoyloxy)-2,2,6,6-tetramethylpiperidine-1-oxyl free radical (Q10C-T)*

One half gram (1.4 mmols) of quinoline-TEMPO was added to 300 ml of acetonitrile at 80 °C under an argon atmosphere. To this solution 0.5 equivalents of K_2CO_3 (96 mg), 1 equivalent of KI (232 mg) and 1 equivalent of 1-bromodecane (309 mg) were added and the mixture was stirred for 4 hours. After evaporation of the solvent the desired alkylated compound Q10C-T was purified by silica gel chromatography (hexane/ethyl acetate, isocratic 8:2), (0.56 g, yield 80 %, FW = 497). HPLC-MS (C-18 column, 100% acetonitrile) : 497, 344, 326, 203, 186, 154, 140, 124, 109, 98, 81, 69; RT=17.08 min. IR (Nujol, cm^{-1}): 3448 (wb), 3046 (w), 1732 (s), 1501 (w), 1463 (m), 1414 (m), 1342 (m), 1326 (m), 1289 (s), 1222 (s), 1192 (m), 1167 (m), 1141 (m), 1116 (m), 1086 (w), 1042 (w), 1014 (w), 982 (w), 965 (w), 938 (w), 893 (w), 865 (w), 809 (w), 765 (m), 739 (m), 678 (w), 636 (w).

2.3.5 *4-(3-p-toluenesulfonoxy-2-methyl-4-quinolinoyloxy)-2,2,6,6-tetramethylpiperidine-1-oxyl free radical (QTs-T)*

One half gram (1.4 mmols) of quinoline-TEMPO and 1 equivalent of p-toluenesulfonyl chloride (267 mg) was dissolved in 200 ml of dichloromethane under an argon atmosphere. One equivalent of triethylamine (0.2 ml) was added and the reaction mixture was stirred for 1 hour at room temperature. After evaporation of the solvent the desired compound QTs-T was purified by silica gel chromatography (hexane/ethyl acetate, isocratic 8:2), (0.62 g, yield 90 %, FW = 496). HPLC-MS (C-18 column, 100% acetonitrile) : 496, 358, 340, 186, 155, 140, 124, 109, 91, 81, 69; RT= 7.2 min. IR (KBr, cm^{-1}): 3454 (wb), 2980 (m), 2948 (m), 2938 (m), 1773 (s), 1597 (w), 1501 (w), 1462 (w), 1374 (s), 1352 (m), 1321 (w), 1286 (m), 1231 (s), 1190 (m), 1179 (s), 1138 (w), 1102 (w), 1084 (s), 1042 (w), 1005 (w), 986 (m), 959 (w), 922 (m), 902 (w), 873 (w), 818 (m), 807 (m), 778 (s), 730 (m), 672 (s), 643 (m).

2.4 UV absorption spectra of the pre-fluorescent probes

The absorption spectra of the molecules have been acquired in cyclohexane, benzene and ethanol at five different concentrations inside a 1x1 cm quartz cell. The instrument used was a CARY IE UV spectrophotometer. The extinction coefficients ε_λ have been obtained from the Lambert-Beer equation, $Abs=\varepsilon_\lambda cl$ (concentration mol/L, l optical path of 1 cm) and they are reported in Table 2-1. Extintion coefficients are given in units of M^{-1} cm^{-1}.

Coumarin-TEMPO	ε_{310nm}	ε_{330nm}	ε_{350nm}
Benzene	8663	7322	5826
Ethanol	9273	7884	5202

Quinoline-TEMPO	ε_{310nm}	ε_{330nm}	ε_{350nm}
Cyclohexane	7565	7460	6182
Benzene	4795	5626	5948
Ethanol	7128	8547	6218

QMe-T	ε_{310nm}	ε_{330nm}	ε_{350nm}
Cyclohexane	4893	2337	189
Benzene	2008	3988	< 50
Ethanol	4730	2393	< 50

Q10C-T	ε_{310nm}	ε_{330nm}	ε_{350nm}
Cyclohexane	4771	2823	844
Benzene	4306	2835	771
Ethanol	4301	2874	539

QTs-T	ε_{310nm}	ε_{330nm}	ε_{350nm}
Cyclohexane	1366	897	19.4
Benzene	4846	3561	112
Ethanol	4714	3101	< 50

Table 2-1 Extinction coefficients ε_λ (M^{-1} cm^{-1}) of quinoline-TEMPO, QMe-T, Q10C-T, QTs-T, QMe-T, coumarin-TEMPO respectively in cyclohexane, benzene, ethanol at 310, 330, 350 nm.

As previously reported for **3P** and **4P** the absorption spectra of the probes are insensitive to solvent polarity[12]. The absorption spectrum of quinoline-TEMPO in the three different solvents does not show relevant changes as shown in Figure 2-1.

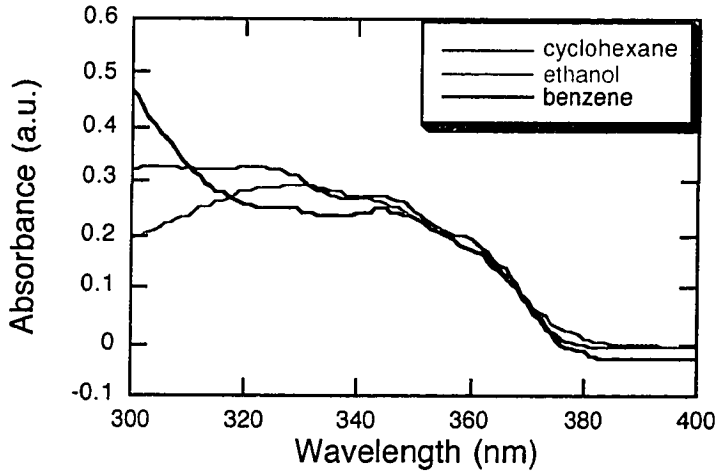

Figure 2-1 Absorption spectrum of quinoline-TEMPO (0.047 mM) in cyclohexane, ethanol, benzene.

If the spectra of the four derivatives of quinoline are compared, only quinoline-TEMPO differs significantly from the other derivatives. The absorption extends 40 nm further into the red and this is due to the hydrogen bond between the phenol hydrogen in position 3 and the carbonyl group in position 4, which increases conjugation in the aromatic system (Figure 2-2).

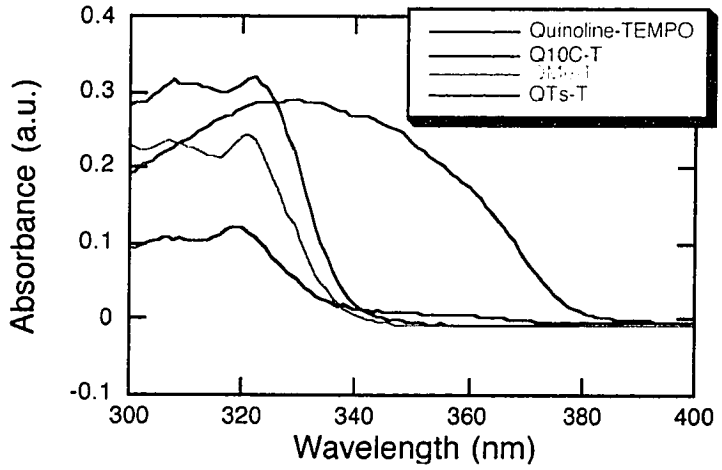

Figure 2-2 Absorption spectrum of quinoline-TEMPO (0.0472 mM), Q10C-T (0.0539 mM), QMe-T (0.0473 mM), QTs-T (0.0465 mM) in ethanol.

In Fifure 2-3 the absorption spectrum of coumarin-TEMPO in ethanol is shown.

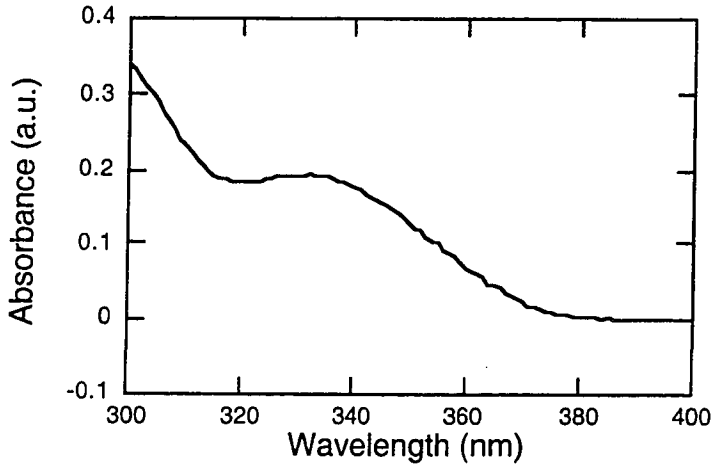

Figure 2-3 Absorption spectrum of coumarin-TEMPO (0.023 mM) in ethanol.

2.5 Preparation of diamagnetic quinoline-TEMPO hydroxylamine

In order to obtain the diamagnetic derivative of quinoline-TEMPO the reduction of the nitroxide group was studied. The first good hydrogen donor we considered was tributyltin hydride[38]. The reaction was done in ether without previously degassing the sample and it was possible to follow the reaction of formation of the fluorescent diamagnetic hydroxylamine with the fluorimeter by injecting different aliquots of the hydride to an etheric solution of the pre-fluorescent probe. The growth of fluorescence intensity was followed by exciting the sample at 350 nm and then monitoring at 400 nm during the time of the reaction. Apart from an application in zeolite supramolecular system (Chapter 4.5.1) all fluorescence experiments presented in this thesis have been performed by using a Photon Technology International PTI Fluorimeter.

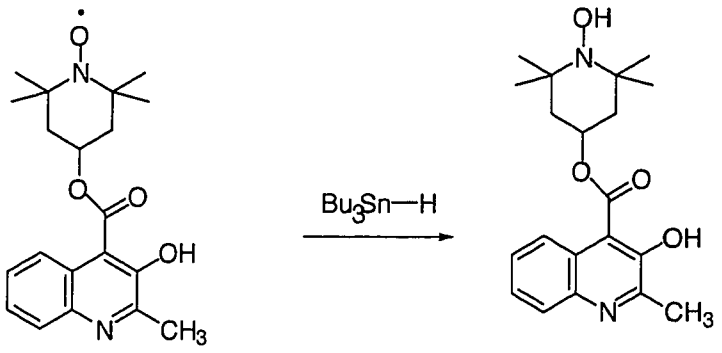

Scheme 2-10 Reaction of quinoline-TEMPO reduction by tributyltin hydride leading to 4-(3-hydroxy-2-methyl-4-quinolinoyloxy)-2,2,6,6-tetramethylpiperidine-1-hydroxyl (Q-TH).

In Figure 2-4 the formation of the diamagnetic hydroxylamine Q-TH is shown, which occurs due to the addition of different quantities of the hydride (62 and 20 mM).

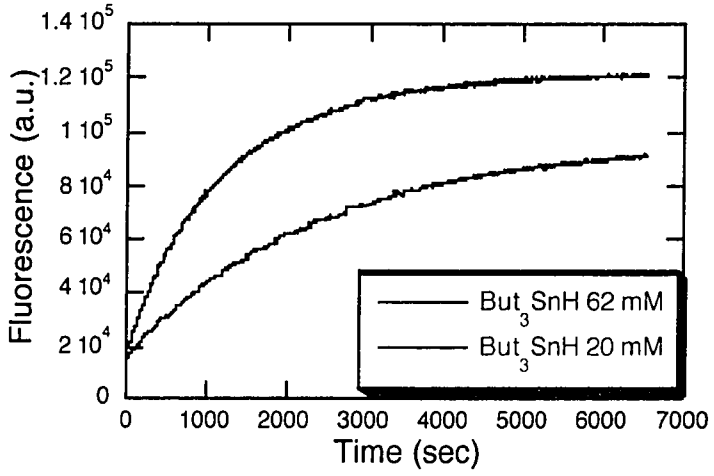

Figure 2-4 Fluorescence growth monitored at 400 nm (ex 350 nm) during the reaction in ether between quinoline-TEMPO (0.023 mM) and tributyltin hydride 62 mM and 20 mM.

In the actual preparation, this kind of reaction was avoided because organotin compounds are undesirable to work with due to the difficulties to separate the desired product from the metal. A different method to reduce quinoline-TEMPO was used. This method is a general procedure for mild reduction of nitro compounds[39]. The conditions used in the reference paper were repeated with the only difference being an increase in the solvent volume; thus, 300 mg (0.84

mmol) of the probe was dissolved in 30 ml of methanol under nitrogen atmosphere and then 30 mg of palladium (10 wt. % on activated carbon) and 260 mg (4.1 mmol) of ammonium formate were added (Scheme 2-11). The reactions were stirred for five hours at room temperature.

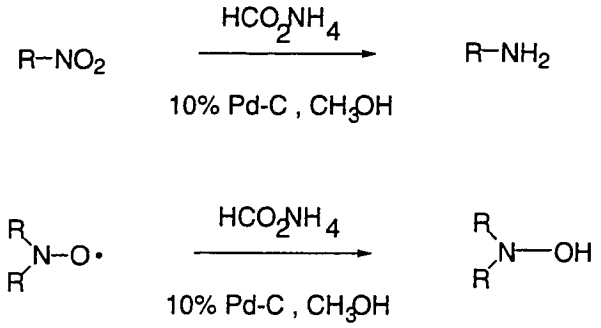

Scheme 2-11 Reaction showing the reduction of nitro compounds and nitroxides by ammonium formate/palladium (10 wt. % on activated carbon) in methanol.

The work-up of the reaction consisted of a filtration of the solution and subsequent evaporation of the solvent. Acetonitrile was added to extract the desired product leaving the unreacted ammonium formate on the bottom of the flask. Using this procedure 4-(3-hydroxy-2-methyl-4-quinolinoyloxy)-2,2,6,6-tetramethylpiperidine-1-hydroxyl (Q-TH) was quantitatively prepared. HPLC-MS (C-18 column, 100% acetonitrile) : 358, 343, 204, 186, 158, 140, 124, 98, 83, 74; RT = 9.07 min. IR (KBr, cm^{-1}): 3258 (sb), 2991 (m), 2970 (s), 2936 (m), 1656 (s), 1600 (w), 1464 (w), 1416 (s), 1386 (m), 1361 (m), 1347 (m), 1325 (s), 1291 (m), 1236 (m), 1213 (s), 1146 (s), 1046 (w), 1029 (w), 997 (m), 963 (m), 955 (m), 932 (w), 891 (w), 810 (s), 770 (s), 748 (m) 686 (w). ^{1}H NMR (500 MHz, $CDCl_3$, TMS) δ 8.57 (m, 1H), 8.0 (m, 1H), 7.5 (m, 2H), 5.54 (m, 1H), 2.7 (m, 3H), 2.21 (m, 1H), 1.94 (m, 4H), 1.29 (s, 12H). ^{13}C NMR (500 MHz, $CDCl_3$) δ 171,1, 155.5, 153.7, 142.2, 129.6, 127.7, 126.1, 124.4, 123.8, 108.7.

2.6 Crystal structures

2.6.1 *4-(3-hydroxy-2-methyl-4-quinolinoyloxy)-2,2,6,6-tetramethylpiperidine-1-oxyl free radical (quinoline-TEMPO)*

Red crystals were obtained from saturated acetonitrile solutions of quinoline-TEMPO kept in the refrigerator at –20 °C and from isopropanol saturated solutions at room temperature. The crystal system is monoclinic and triclinic respectively. The geometry of quinoline-TEMPO is the same in both of the structures but the tridimensional packing is different. The most important observations concern the planarity of the aromatic rings, the presence of a hydrogen bond between the phenolic hydrogen and the carbonyl and the cyclohexyl chair conformation of the TEMPO moiety.

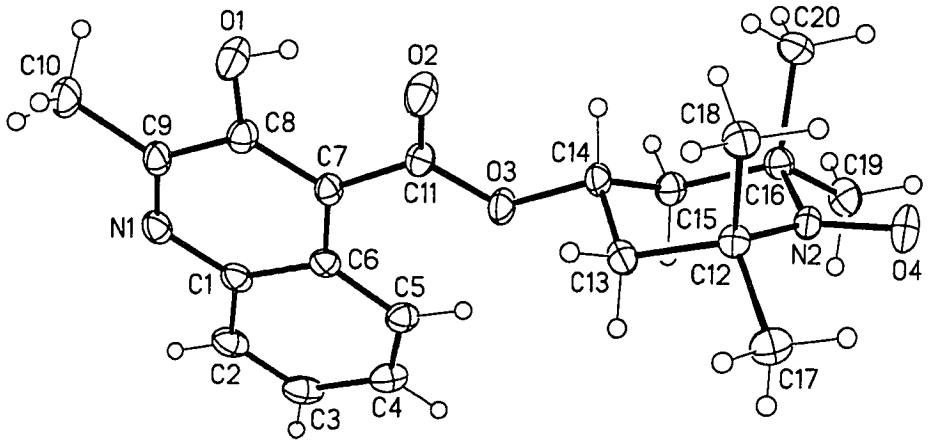

Figure 2-5 Crystal structure of (3-hydroxy-2-methyl-4-quinolinoyloxy)-2,2,6,6-tetramethylpiperidine-1-oxyl free radical (quinoline-TEMPO).

Crystallographic analysis allowed the determination of a distance between O (1) and O (2) of 2.52 Å. This value is less than the reported maximum distance of 2.7 Å between two oxygen atoms involved in hydrogen bonds[40]. In Table II of the Appendix a list of selected bonds and angles is reported. The crystal structure shows the planarity of the aromatic system of the quinoline moiety. A difference in the bond length between N (1) – C (9) = 1.305 (2) Å and N (1) – C (1) = 1.376 (2) Å can be attributed to the presence of the methyl group. The carbonyl group is positioned in front of the phenolic group and hydrogen bonding is present. It is important to mention the distance O (1) – C (8) = 1.3467 Å (19) because it will be

compared to the same bond distance in QTs-T. The nitroxide group in the cyclohexyl group reports a bond length of N (2) – O (4) = 1.2863 (16) Å.

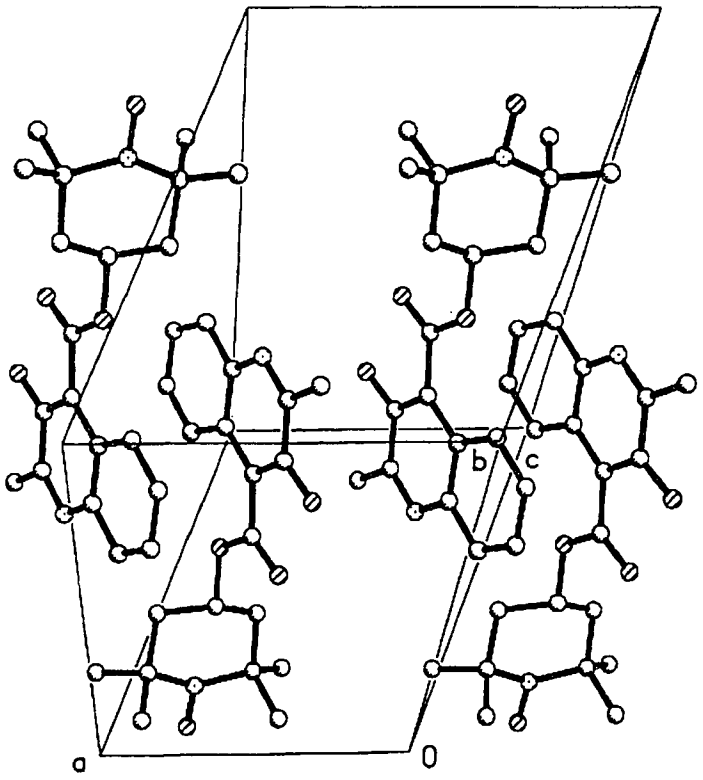

Figure 2-6 Quinoline-TEMPO (monoclinic) unit cell.

The unit cell of the monoclinic quinoline-TEMPO is composed of two molecules which are positioned with the aromatic systems in front of each other and antipallel to each other (Figure 2-6).

2.6.2 *4-(3-hydroxy-2-methyl-4-quinolinoyloxy)-2,2,6,6-tetramethylpiperidine-1-hydroxyl (Q-TH).*

Transparent crystals of QT-H were obtained from saturated acetonitrile solutions kept in the refrigerator at –20 °C. The crystal structure of Q-TH is almost identical to the structure of quinoline-TEMPO. In Table IV of the Appendix a list of selected bonds and angles is reported. The important difference between the two structures is the bond distance in the nitroxide group. The presence of an oxygen-hydrogen bond in the hydroxylamine reduces the double bond caracter of the nitroxide group leading to a longer bond length N (2) – O (4) = 1.447 (2) Å.

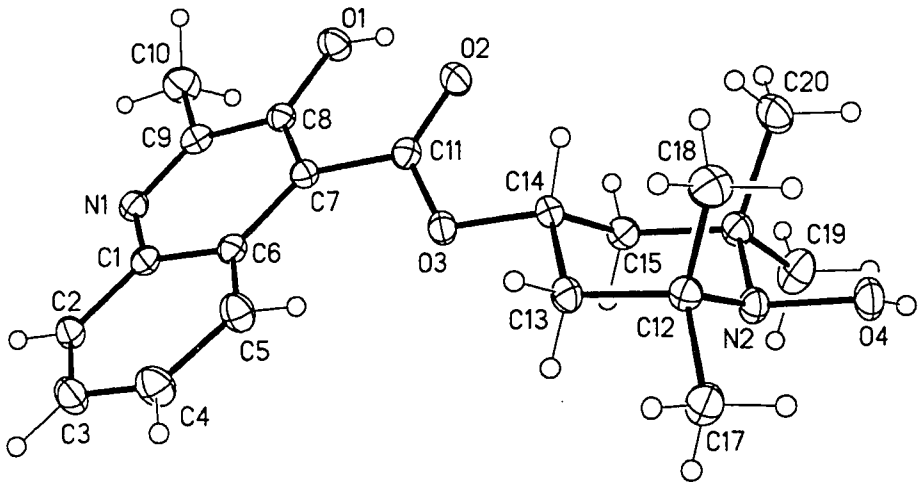

Figure 2-7 Crystal structure of 4-(3-hydroxy-2-methyl-4-quinolinoyloxy)-2,2,6,6-tetramethylpiperidine-1-hydroxyl (QT-H).

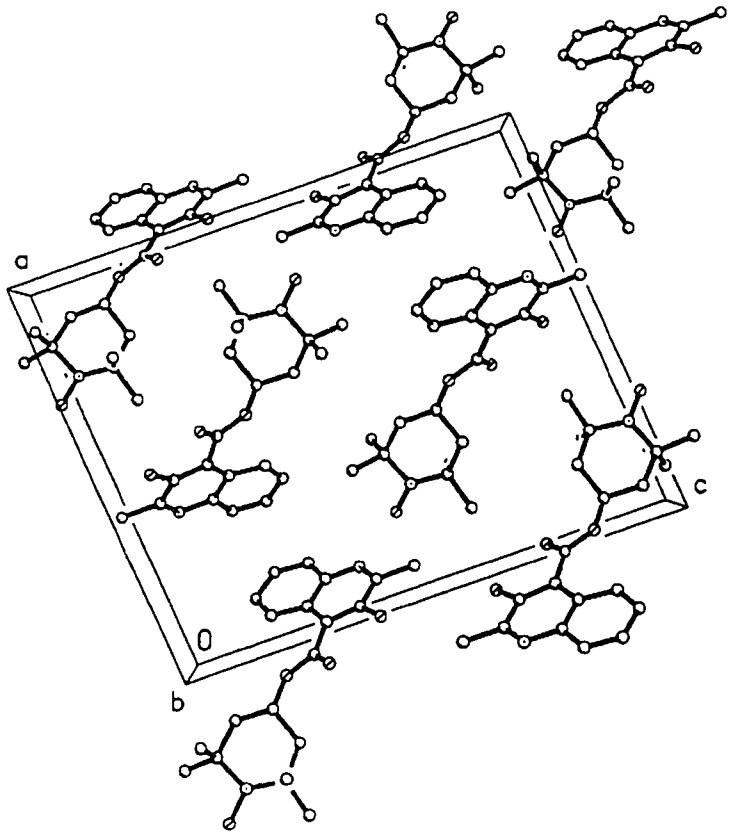

Figure 2-8 Q-TH unit cell.

The unit cell of Q-TH (Figure 2-8) is composed of two molecules and differs from the unit cell of quinoline-TEMPO due to the fact that the hydroxylamine group is

positioned in front of the nitrogen atom of the quinoline aromatic ring in another molecule of an adiacent cell. The aromatic systems of two molecules of the same unit cell are not in front of each other anymore. The packing is probably due to a hydrogen bond between different molecules in the crystal lattice.

2.6.3 *4-(3-p-toluenesulfonoxy-2-methyl-4-quinolinoyloxy)-2,2,6,6-tetramethylpiperidine-1-oxyl free radical (QTs-T)*

The crystal structure of QTs-T is similar to the structure of quinoline-TEMPO. In Table IV of the Appendix a list of selected bonds and angles is reported. The important difference to be noticed is the bond length O (1) – C (8) = 1.402 (2) Å which is greater than the same bond length in quinoline-TEMPO O (1) – C (8) = 1.3467 (19) Å due to the formation of a sigma bond with a sulfur atom which is more electronegative than hydrogen. The other consideration for this structure regards the position of the carbonyl group with respect to O (1). Rotation of the C (7) – C (11) bond interrupts the conjugation present in quinoline-TEMPO due to hydrogen bonding. This is also responsible for different absorption spectra.

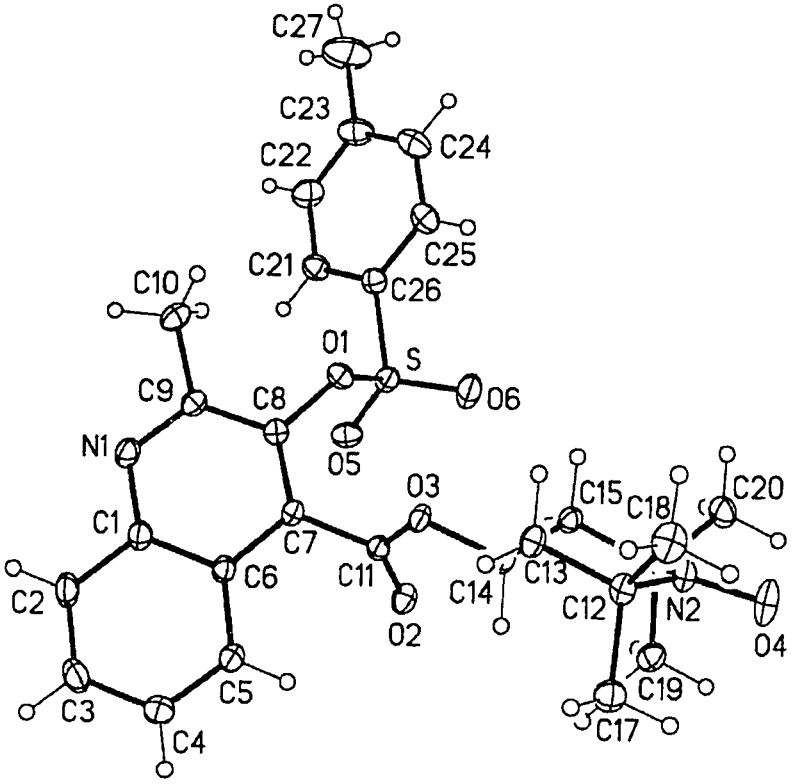

Figure 2-9 Crystal structure of 4-(3-p-toluenesulfooxy-2-methyl-4-quinolinoyloxy)-2,2,6,6-tetramethylpiperidine-1-oxyl free radical (QTs-T).

3 Fluorescence detection of radicals in homogenous solutions

3.1 Introduction

Carbon-centered radicals have been under investigation for a long time. They are present in nature in the gas phase, liquid environments, and solid states. They may be reactive intermediates, which can be produced and sometimes controlled in applications such as free-radical polymerization[41], they are suitable reactive species for intramolecular reactions in organic synthesis[38] and they are reactive intermediates in many important biochemical processes as both constructive and destructive agents. The detection and quantification of free radicals in solution allows access to information about the rates of production and the interactions between radicals. The study of free radicals is not an easy task due to their reactivity (rate constants for self-reaction are in the range 10^7-10^9 M^{-1} s^{-1}) and consequent low concentrations (typically < 10^{-7} M). The pre-fluorescent probes that are presented in this thesis are designed to be sensors for this kind of radicals. The nitroxide moiety in these molecules allows almost diffusion controlled reaction with carbon-centered radicals and the principle of restoring the quenched fluorescence by trapping of a radical is a facile methodology for detection. To demonstrate the efficiency and the potential of these molecules it was necessary to use a system in which radicals are constantly produced. Carbon-centered radicals in homogenous systems such as an organic solvent or water can be produced in several ways. It is possible to use light or heat as energy source to produce homolytic bond breakages in organic molecules. The energy is related to the wavelength λ of the light and for example a quantum at 270 nm is equivalent to 106 kcal/mol, which is enough to break the majority of bonds in organic molecules. Raising the temperature increases the vibrational energy of a molecule. This internal energy can then be dissipated by collision and

dispersion in the medium or by homolytic fission of one or several bonds. In this part of the thesis the pre-fluorescent probes are tested in the radical trapping reaction and the course is followed by monitoring fluorescence enhancements. The sources of radicals have been chosen from some of the most commonly used radical initiators: 2,2`-azobisbutyronitrile (AIBN), 1,3-diphenylacetone (DBK) and tert-butyl peroxide (DTBP) in the presence of a good hydrogen donor. In order to obtain valuable kinetic data, the absorption spectra of the radical initiators and the pre-fluorescent probes has to be taken in consideration. In experiments observing the thermal decomposition of a radical initiator in the presence of a pre-fluorescent probe the excitation wavelength has to be chosen to obtain the maximum emission from the sensor. At this wavelength the absorbance of the probe must be between 0.1 and 0.2 (a.u.), otherwise the solution loses its transparency, and the concentration of initiator cannot be so high as to compete for photons with the probe. Instead in photodecomposition experiments the light at the wavelength of photolysis has to be almost exclusively absorbed by the initiator, so to avoid the side reactions of decomposition of the probe. Also the excitation wavelength for fluorescence detection has to be in a region where only the sensor absorbs. In this way the fluorescence emission becomes a transparent tool for the detection of carbon-centered radicals. All the experiments presented in this section have been performed on samples degassed by bubbling nitrogen in order to remove molecular oxygen. Oxygen reacts at close to the diffusion control limit with carbon-centered radicals[38] leading to the production of oxygen center radicals which are unreactive towards nitroxides.

3.2 Radical initiators

3.2.1 Thermal initiation of 2,2`-azobisbutyronitrile

Azo compounds are organic molecules in which decomposition occurs through the breaking of two C—N bonds with the consequent releasing of a stable nitrogen molecule and the generation of two carbon-centered radicals[38]. The activation energy for this decomposition process is moderately low and is dependent on the type of radicals being formed. The production of carbon-

centered radicals with these molecules can be initiated by using heat or light. For azomethane, the activation energy is 51 kcal/mol and it decomposes only at temperatures near 400 °C; however for AIBN the activation energy is only 31 kcal/mol.

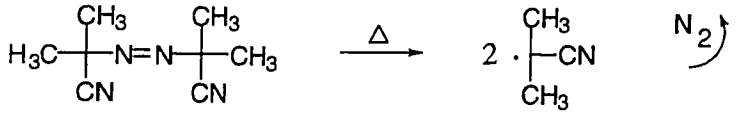

Scheme 3-1 Thermal decomposition of 2,2`-azobisbutyronitrile (AIBN) leading to the production of two 2-cyano-2-propyl radicals.

The low activation energy of ~30 kcal/mol for this process can be easily attributed to the elimination of a very stable molecule such as nitrogen. AIBN decomposes strictly by first-order kinetics at essentially the same rate in a variety of solvents, with no evidence of induced chain reactions. Hence, by suitable structural changes, substances with a wide variety of decomposition rates are available. The 2-cyano-2-propyl radical is able to abstract only weakly bonded hydrogens (allylic or benzylic hydrogen, thiol, tin hydride) so there is no evidence of a reaction with common solvents. AIBN and other radical azo initiators are widely used for their moderate decomposition temperatures but their efficiency as initiators is reduced by an appreciable amount of cage recombination reactions (l~ 20%). All five of the pre-fluorescent probes presented in the previous section were tested in the trapping reaction of the 2-cyano-2-propyl radical generated by thermal decomposition of AIBN in benzene. The absorption properties of the initiator were also evaluated. AIBN absorbs with a maximum at 350 nm. Figure 3-1 shows absorbances at three wavelengths (310, 330, 350 nm) as a function of AIBN concentration. The extinction coefficients have been calculated from the slope of the linear fit. AIBN extinction coefficient values are 3.04 M^{-1} cm^{-1} at 310 nm, 7.91 M^{-1} cm^{-1} at 330 nm and 10 M^{-1} cm^{-1} at 350 nm.

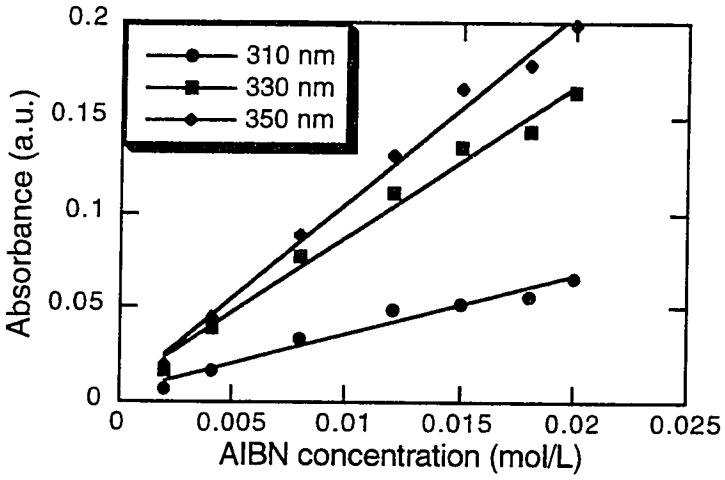

Figure 3-1 Dependence of the AIBN absorption intensity on the concentration at different wavelengths.

3.2.2 *Photochemical initiation of 1,3-diphenylacetone giving benzyl radicals*

Ketones are another class of organic radical initiators. By photolysis of certain ketones it is possible to generate through homolytic cleavage of a C—C bond, an alkyl radical and an acetyl radical. The latter frequently converts to an alkyl radical through the elimination of carbon monoxide (Scheme 3-2). One of these molecules is 1,3-diphenylacetone (DBK). Photodecarbonylation proceeds via a two-step mechanism and photolysis in benzene solution (λ_{ex}> 300 nm, room temperature) results in a quantitative yield of CO and 1,2-diphenylethane[42].

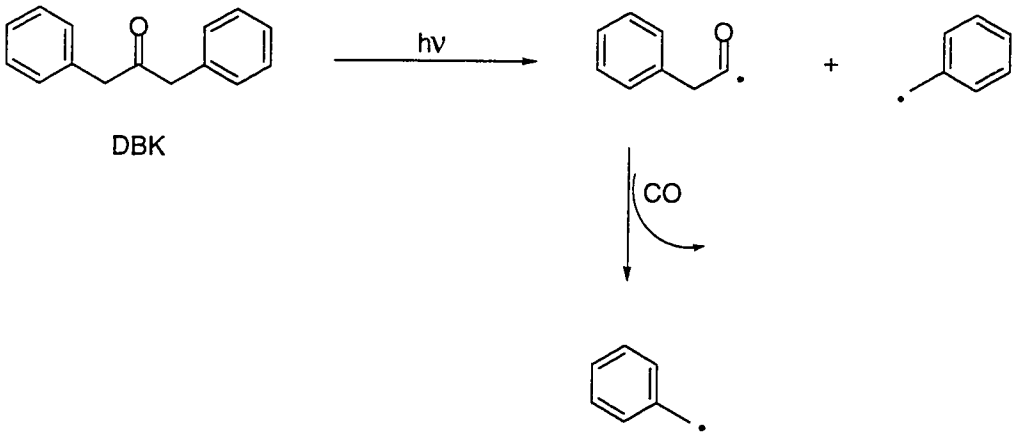

Scheme 3-2 Reaction showing the photolysis of 1,3-diphenylacetone (DBK) leading to generation of acyl and benzyl radicals.

The two-step mechanism has been proven by the radical trapping of benzyl and phenyl acetyl radicals with TEMPO. Irradiation at 313 nm of a solution with a 1:1.9 molar ratio of the ketone and the nitroxide produces 1-(2,2,6,6-tetramethylpiperidine N-oxide)-phenylmethane **14** and 1-(2,2,6,6-tetramethylpiperidine N-oxide)-phenylacetate **15** in a 3:2 ratio (Scheme 3-3).

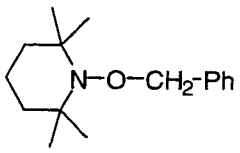

14

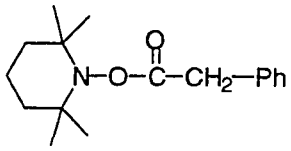

15

Scheme 3-3 1-(2,2,6,6-tetramethylpiperidine N-oxide)-phenylmethane (14) and 1-(2,2,6,6-tetramethylpiperidine N-oxide)-phenylacetate (15).

In solution, the photolysis of DBK produces efficiently random benzyl free radicals. The radicals of the triplet geminate pair quickly escape from the solvent cage before intersystem crossing to the more reactive singlet pair occurs. Nitroxides have offered the possibility of studying the competition between bond formation and the alternative spin exchange pathway of the interaction between triplet radical pairs and the doublet of the nitroxide. When a doublet nitroxide approaches a triplet radical pair a spin exchange mechanism may occur with the conversion of the triplet state to a singlet state (Scheme 3.4). The singlet state of the radical pair can then easily proceed in the spin-allowed recombination process. An "antiscavenging effect" for nitroxides like TEMPO has been observed[43] when the concentration of the nitroxide is increased above the value of ca. 0.1 M even if the trap has a scavenging rate constant close to the diffusion rate.

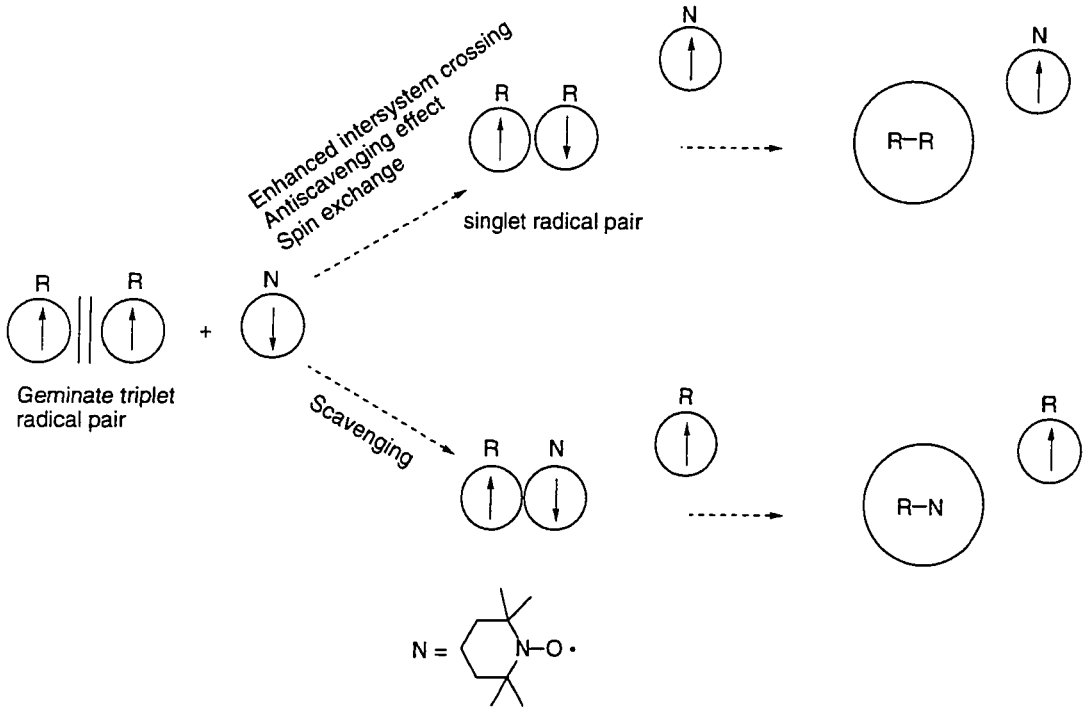

Scheme 3-4 Interactions between a triplet radical pair and a nitroxide doublet: enhanced intersystem crossing and radical scavenging.

In the experiments described in the next few paragraphs quinoline-TEMPO has been used in a concentration which is 4000 times lower than 0.1 M and the spin exchange mechanism cannot compete with the radical trapping. Benzene was chosen as the solvent for the experiments in which the concentration of initiator was varied. The absorptive properties of the photoinitiator have been investigated in benzene in order to choose the right range of concentrations of initiator. DBK absorbs below 350 nm (Figure 3-2) and at the irradiation wavelength of 300 nm the value of the extinction coefficient ε_λ is 539 M^{-1} cm^{-1} (Figure 3-3). Quinoline-TEMPO is a suitable molecule for these experiments because at the excitation wavelength of 350 nm there is no absorptive interference with the initiator. Instead, the derivative compounds absorb at a lower wavelength coincident with the radical initiator band and they have not been considered for this experiment.

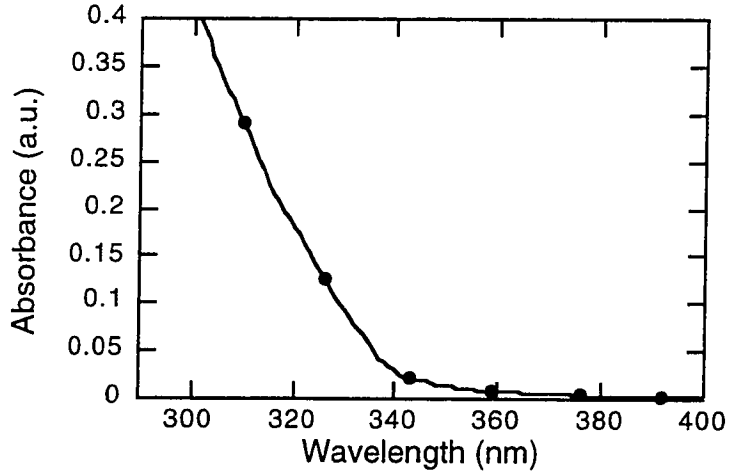

Figure 3-2 DBK (0.9 mM) absorption spectrum in benzene.

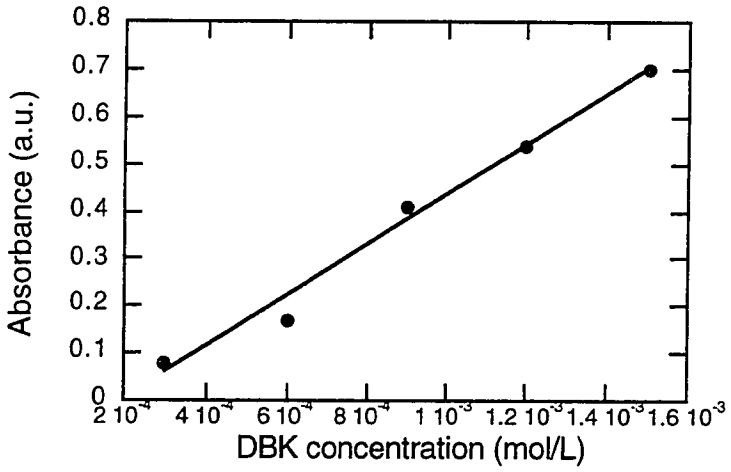

Figure 3-3 DBK extinction coefficient plot in benzene at 300 nm.

3.2.3 *Photolysis of tert-butyl peroxide in presence of a hydrogen donor.*

Peroxides are widely used as photo or thermal initiators of alkoxy radicals[38]. Depending on the system in which they are employed the radicals which are generated by an energetic favorable process can initiate chain reactions, transfer or addition reactions or may also be trapped and converted to diamagnetic species. The O—O bond of peroxides has dissociation energies between 25 and 40 kcal/mol and can be easily broken thermally or photolytically. When the alkoxy radical is formed it can undergo an exothermic hydrogen transfer

reaction, if a good hydrogen donor is present, producing a carbon-centered radical. Peroxides are characterized by a first-order rate constant for the cleavage reaction but the experimental half-life is a little shorter than those expected from the first-order rate constant due to induced reactions that accelerate the disappearance rate of peroxide. Quinoline-TEMPO has been tested in the trapping reaction of cyclohexyl radicals using tert-butyl peroxide (DTBP) as a photochemical source of alkoxy radicals in cyclohexane as solvent. The oxygen centered radicals abstract hydrogen from the cyclohexane ring with consequent production of a carbon-centered cyclohexyl radical (i, ii, Scheme 3-5).

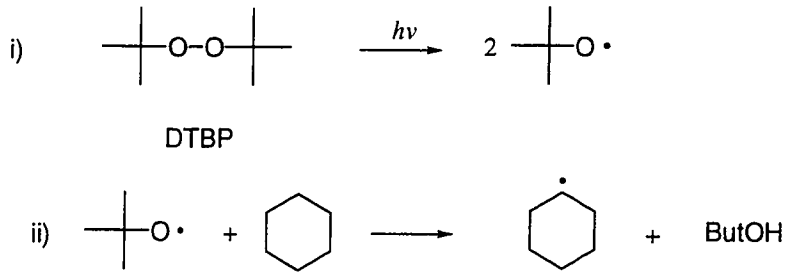

Scheme 3-5 Reaction showing the photodissociation of tert-butyl peroxide (DTBP) (i) and the hydrogen abstraction from cyclohexane by tert-butoxyl radical (ii).

3.3 Results and discussion

3.3.1 Scavenging of the 2-cyano-2-propyl radical

Quinoline-TEMPO was employed in a concentration of 0.025 mM; a complete study using different amounts of AIBN has been carried out at a temperature of 60 °C in benzene. The only product of the reaction is the coupled compound formed by quinoline-TEMPO and 2-cyano-2-propyl radical. In a first experiment the concentration of the radical initiator was varied between 20 mM and 1.2 mM. Nitrogen gas was bubbled into each sample for at least 20 minutes to allow complete removal of molecular oxygen. Fluorescence was monitored in situ exciting at 350 nm and monitoring at 400 nm.

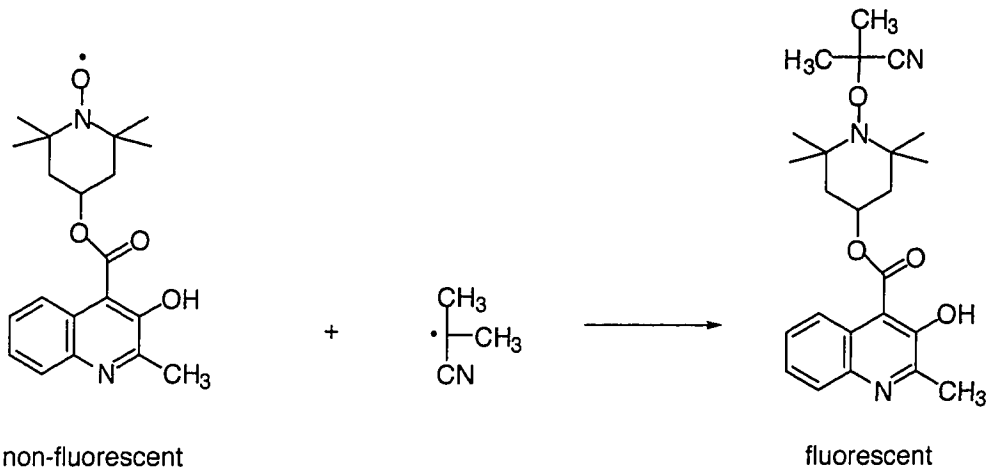

Scheme 3-6 Reaction showing the formation of the diamagnetic fluorescent product of coupling between quinoline-TEMPO and 2-cyano-2-propyl radical.

Figure 3-4 shows how the end of the reaction is reached at different times when the concentration of the initiator is changed and that when higher concentrations of AIBN are used the final fluorescence value is considerably different from the samples with lower concentrations. This due to the fact that after 1000 seconds only a small portion of the AIBN present in the system has been decomposed and the absorbance at the excitation wavelength is still so high that the initiator competes with the probe for photons; thus, the emission is not representative of the concentration of the diamagnetic compound.

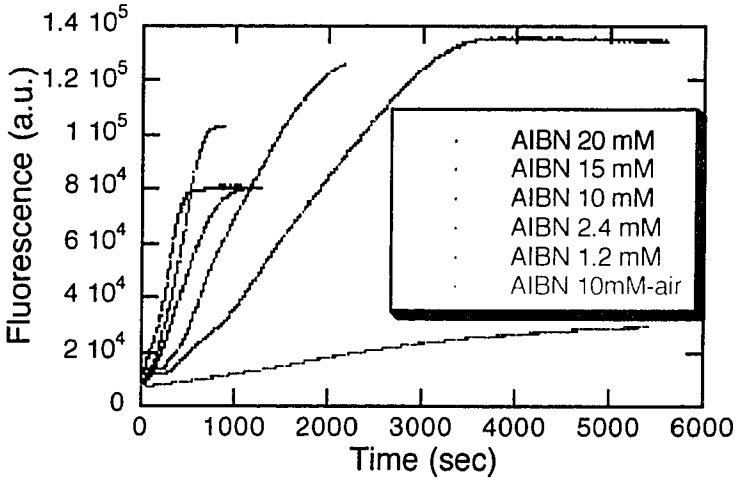

Figure 3-4 Fluorescence growth due to the scavenging of the 2-cyano-2-propyl radical by quinoline-TEMPO (0.025 mM). T = 60 °C. AIBN concentration range 1.2-20 mM. λ_{ex} 350 nm, λ_{em} 400 nm.

The plot also shows the kinetic trace for the reaction with a 10 mM concentration of AIBN in air. The sample was not degassed with nitrogen and the rate of the reaction is dramatically lower because of the competition of the diffusion-controlled reaction of oxygen with carbon-centered radicals to form peroxyl and alkoxy radicals. In a second experiment the concentrations of AIBN were varied between 4 mM and 0.2 mM (Figure 3-5) and in this case the end of the reaction is reached at different times but with consistent final fluorescence intensities, except for the AIBN concentration of 4 mM. This means that AIBN does not compete for photons with quinoline-TEMPO until the concentration is raised to a value higher than 2 mM. The decomposition of AIBN occurs with first-order kinetics but the kinetics of fluorescence growth are linear. This is indicative of the fact that every time a radical is formed it is trapped by the probe and thus the slope is representative of the initial rate of radical formation.

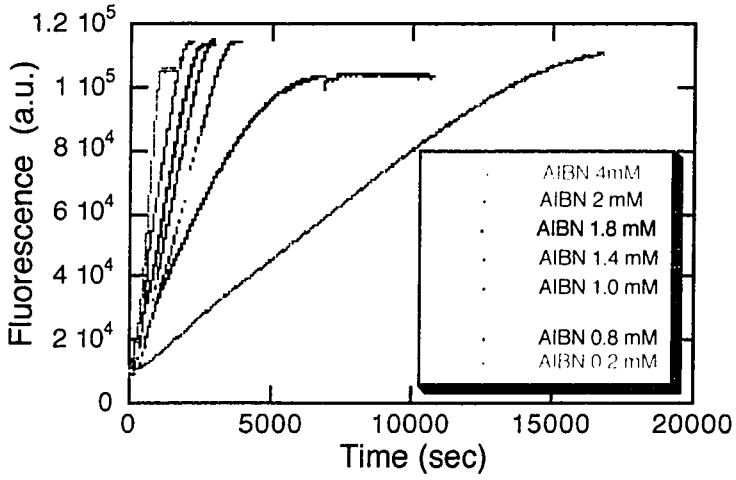

Figure 3-5 Fluorescence growth due to the scavenging of the 2-cyano-2-propyl radical by quinoline-TEMPO (0.025 mM). T = 60 °C. AIBN concentration range 0.2-4 mM. λ_{ex} 350 nm, λ_{em} 400 nm.

When plotting the slope obtained from the linear fit of the data as a function of the concentration of AIBN a linear dependence is observed (Figure 3-6).

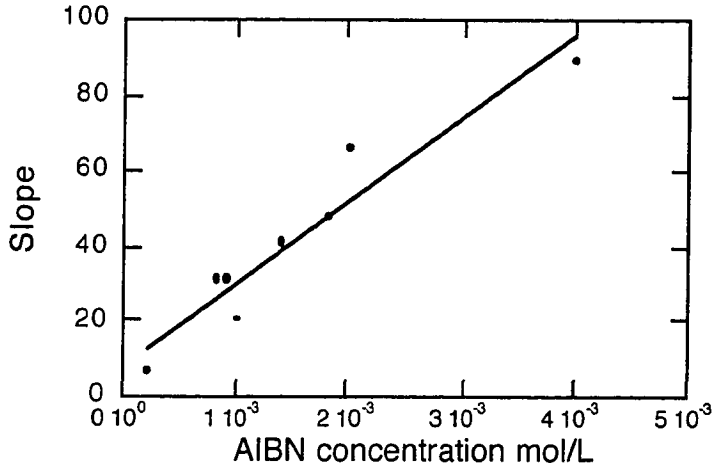

Figure 3-6 Graph of the slope values from the linear fit of the kinetics of radical trapping as a function of the concentration of AIBN radical initiator.

The other probes were also tested in this reaction. Figure 3-7 shows the fluorescence signal observed during the reactions of Q10C-T, QTs-T and QMe-T with AIBN (2 mM) upon excitation at 300 nm and monitoring at 400 nm.

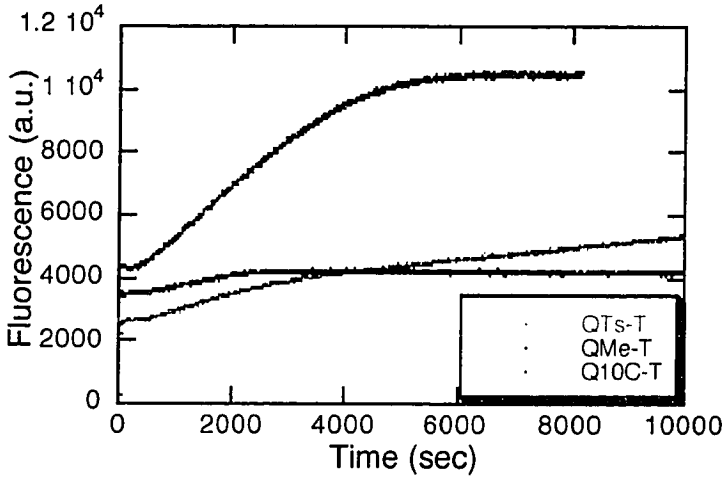

Figure 3-7 Fluorescence growth due to the radical trapping of the 2-cyano-2-propyl radical by Q10C-T (0.02mM), QMe-T (0.023 mM), QTs-T (0.024 mM). T = 60 °C. AIBN concentration 2 mM. λ_{ex} 300 nm, λ_{em} 400 nm.

Fluorescence emission grows during the radical trapping reaction for all the quinoline-TEMPO derivatives. The enhancement in fluorescence is much smaller than in the case of the radical trapping reaction by quinoline-TEMPO. The presence of an alkyl group or a p-toluenesulfonyl group on the oxygen in position 3 of quinoline-TEMPO eliminates the hydrogen bonding between the

phenolic group and the carbonyl group in position 4. The intramolecular hydrogen bonding in quinoline-TEMPO plays an important role for the reactivity of the molecule and for the fluorescence quantum yield of the diamagnetic product of radical trapping. It increases conjugation of the aromatic system of the molecule and the additional delocalization of electrons is responsible for the different optical properties of quinoline-TEMPO in comparison with the derivatives. The absorption spectra of quinoline-TEMPO and its derivatives, which are shown in Figure 2.2, already displayed the turning off of the additional conjugation due to the presence of a substituent. In QMe-T, Q10C-T and QTs-T, rotation of the carbonyl group out of the plane of the aromatic system probably occurs with consequent reduction of the conjugation in the aromatic system. This hypothesis is supported by the crystallographic analysis of quinoline-TEMPO and QTs-T (Chapter 2.6). In solid state it has been shown that the presence of the tosyl group makes the carbonyl group rotate out of the plane of the aromatic system.

The experiments with coumarin-TEMPO were carried out by varying both the concentration of the initiator and the temperature. In the first experiment two different concentrations of AIBN were used (2 mM and 5 mM, Figure 3-8). In the second experiment, using a concentration of AIBN of 2 mM, kinetic data was acquired at four different temperatures within the range of 50 °C and 65 °C (Figure 3-9). The rate of the reaction increases with the temperature and this is expected due to the faster production of radicals in the system. The sample holder inside the fluorimeter permits experiments at different temperatures but because it is placed close to the lenses high temperatures were avoided. Coumarin-TEMPO was found to contain a diamagnetic impurity. The trapping of carbon-centered radicals in this case allowed firstly the monitoring of the decrease of fluorescence due to of the disappearance of the diamagnetic hydroxylamine impurity by hydrogen abstraction and secondly the increase in fluorescence from the trapping reaction (Scheme 3-7, 3-8).

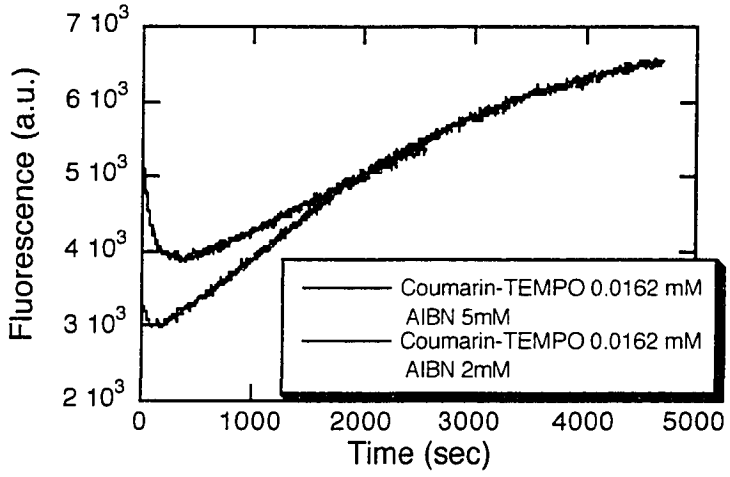

Figure 3-8 Fluorescence growth due to the scavenging of the 2-cyano-2-propyl radical by coumarin-TEMPO (0.0162 mM). T = 65 °C. AIBN concentrations 2-5 mM. λ_{ex} 330 nm, λ_{em} 420 nm.

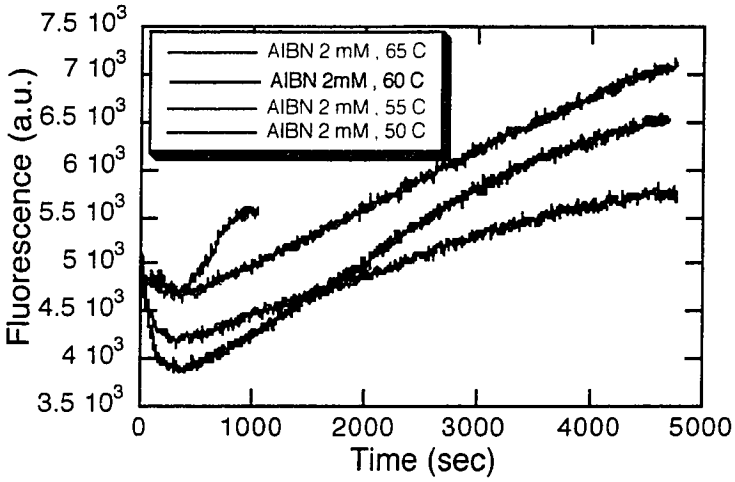

Figure 3-9 Fluorescence growth due to the scavenging of the 2-cyano-2-propyl radical by coumarin-TEMPO (0.0162 mM). T = 65, 60, 55, 50 °C. AIBN concentrations 2 mM. λ_{ex} 330 nm, λ_{em} 420 nm.

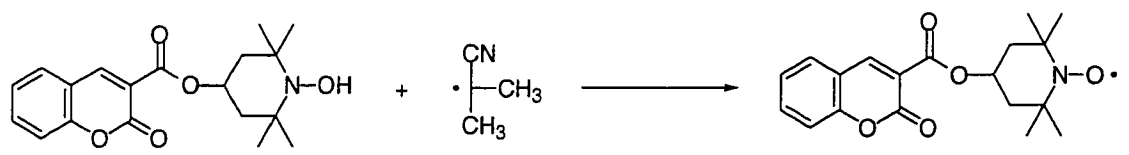

fluorescent non-fluorescent

Scheme 3-7 Reaction showing the hydrogen abstraction from Q-TH by the 2-cyano-2-propyl radical leading to formation of the paramagnetic coumarin-TEMPO.

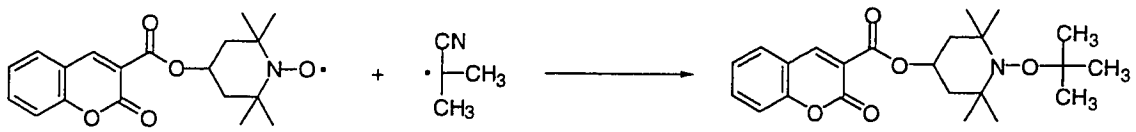

non-fluorescent fluorescent

Scheme 3-8 Reaction showing the trapping of the 2-cyano-2-propyl radical by coumarin-TEMPO giving a diamagnetic fluorescent product.

The reaction time necessary for the complete consumption of coumarin-TEMPO is longer (5000 sec) than in the case of quinoline-TEMPO (2000 sec). This suggests that the difference in the structure of this derivative of the TEMPO moiety changes the reactivity of the nitroxide group even if substitutions on the fourth position of the cyclohexyl group should not affect the reactivity. For this reason a clear explanation of this result cannot be proposed.

3.3.1.1 Synthesis of the diamagnetic alkoxyamine (Q-TAIBN) from quinoline-TEMPO and 2-cyano-2-propyl radical

300 mg of quinoline-TEMPO (0.84 mmols) was dissolved in 100 ml of acetonitrile under a nitrogen atmosphere at 70 °C. To this solution 250 mg of 2,2`-azobisbutyronitrile was added and the solution was stirred for ten hours. After evaporation of the solvent the yellow precipitate was washed three times with methanol to remove the side product of the reaction obtained from the bimolecular self-reaction of two 2-cyano-2-propyl radicals. The desired product 3-hydroxy-2-methyl-quinoline-4-carboxylic acid 1-(1-cyano-1-methyl-ethoxy)-2,2,6,6-tetramethyl-piperidin-4-yl ester (Q-TAIBN) was then filtered and recrystallized in acetonitrile at –20 °C quantitatively yielding white crystals. HPLC-MS (C-18 column, 100% acetonitrile) : 358, 342, 204, 186, 172, 158, 140, 124, 109, 98, 82, 69; RT = 8.00 min. IR (KBr, cm^{-1}) : 2980 (m), 2948 (m), 1652 (s), 1602 (w), 1463 (m), 1411 (s), 1383 (m), 1368 (m), 1351 (m), 1331 (s), 1289 (m), 1235 (m), 1218 (s), 1187 (s), 1144 (s), 1085 (w), 1038 (w), 1017 (m), 998 (m), 981 (w), 955 (m), 930 (w), 890 (w), 851 (w), 809 (m), 768 (s), 745 (m), 682 (w), 642 (w). ^{1}H NMR (500 MHz, $CDCl_3$, TMS) δ 12.05 (s, OH), 8.56 (m, 1H), 8.0 (m, 1H), 7.52 (m, 2H), 5.5 (m, 1H), 2.70 (m, 3H), 2.17 (m, 1H), 1.94 (m, 4H), 1.35 (s, 12H). ^{13}C NMR (500 MHz, $CDCl_3$) δ 171.1, 155.4, 153.6, 142.1, 129.6, 127.6, 125.5, 124.0, 123.8, 108.5, 69.4, 60.4, 44.5, 34.0, 27.2, 25.0, 21.18, 20.35.

3.3.2 *Quinoline-TEMPO trapping of benzyl radicals*

When DBK is photolyzed in the presence of the pre-fluorescent probe the benzyl radicals can couple with the free radical moiety of the nitroxide resulting in a fluorescent diamagnetic product.

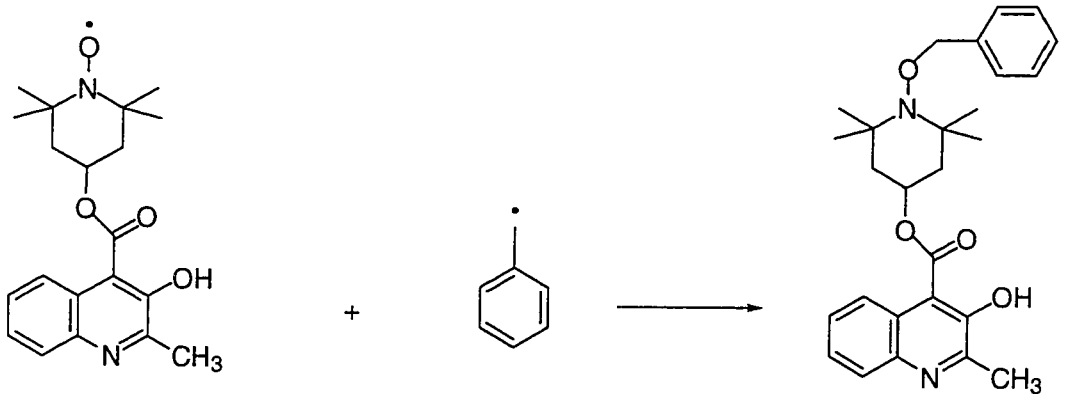

non-fluorescent *fluorescent*

Scheme 3-9 Reaction showing the scavenging of benzyl radicals by quinoline-TEMPO leading to a fluorescent coupled product.

Quinoline-TEMPO was employed in this experiment in a concentration of 0.0232 mM in benzene and the concentration of radical initiator was varied between 0.3 mM and 1.5 mM. Each sample was photolyzed for 5 or 10 seconds with one lamp at 300 nm and the fluorescence emission spectrum was collected at each interval using an excitation wavelength of 350 nm. All the photolysis experiments presented in this thesis have been performed by using a 300 nm Rayonet Photochemical Reactor Lamp (Ultraviolet co.). At the irradiation wavelength the probe has an absorbance of 0.1 and the radical initiator 0.3. The use of only one lamp placed at a distance of 10 cm from the quartz cell containing the sample allows a consideration of shielding effects even if the difference in absorbance is minimal. The product of the reaction can tolerate a certain amount of energy and the relationships proposed in these experiments concluded in satisfactory results. The concentration of DBK cannot be too high because at the excitation wavelength the probe has to exclusively absorb the incident light. Figure 3-10 shows the fluorescence increase at five seconds intervals of irradiation when

DBK is employed as a concentration of 0.9 mM until the maximum intensity is reached in 50 seconds.

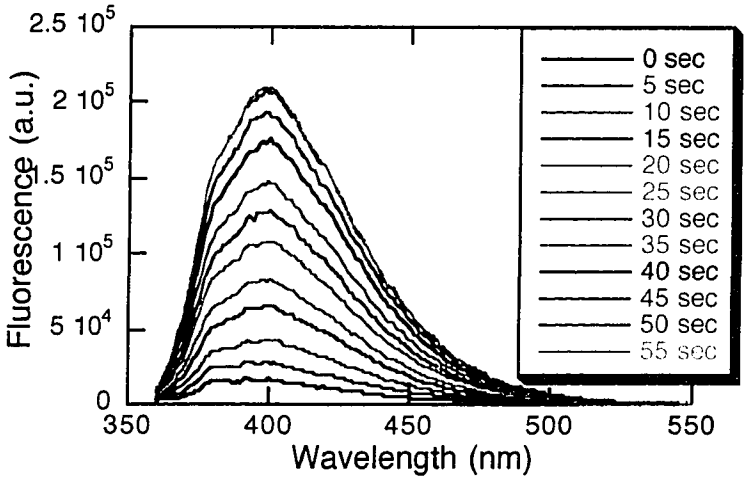

Figure 3-10 Emission spectrum of the trapping reaction of benzyl radicals produced by photolysis at 300 nm of DBK (0.9 mM) in the presence of quinoline-TEMPO (0.0232 mM), at five seconds intervals. Fluorescence is monitored by excitation at 350 nm.

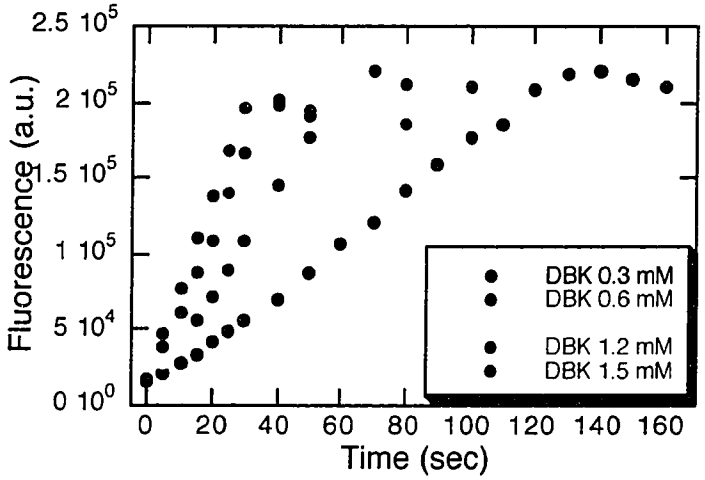

Figure 3-11 Fluorescence growth due to the radical trapping of benzyl radicals generated by photolysis at 300 nm of DBK (0.3, 0.6, 0.9, 1.2, 1.5 mM) in the presence of quinoline-TEMPO (0.0232 mM). λ_{ex} 350 nm, λ_{em} 400 nm.

Figure 3-11 shows the growth of the fluorescence intensity monitored at 400 nm for five samples containing different amounts of radical initiator. From these results it is possible to observe the efficiency of the probe as an optical sensor for carbon-centered radicals. The evolution of fluorescence has also been followed after reaching the plateau of the reaction. Photolysis of the diamagnetic product

caused formation of non-fluorescent products leading to a complete depletion of fluorescence after 4000 seconds of irradiation at 300 nm.

3.3.2.1 Solvent effects

The solvent in the reaction was varied using carbon tetrachloride, cyclohexane, benzene, pyridine, acetonitrile, ethanol and methanol. The reactivity of quinoline-TEMPO was found to be dependent on the type of solvent used in the reaction. The difference in reactivity can be attributed to different solvations of the probe or to changes in the extinction coefficient or changes in the quantum yield of decomposition of DBK.

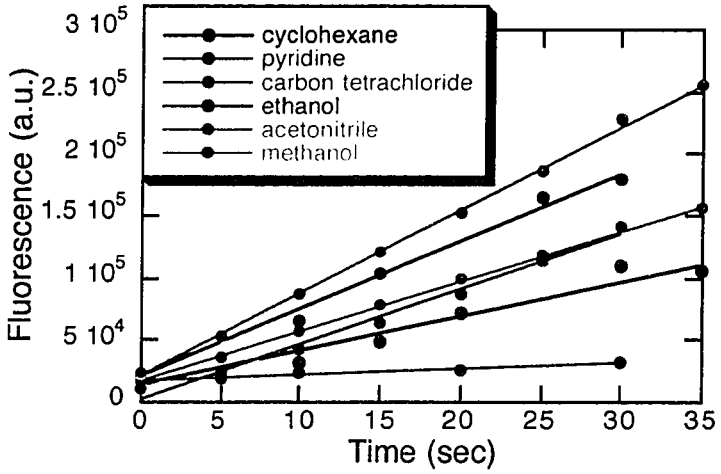

Figure 3-12 Solvent influence on the fluorescence growth due to the radical trapping of benzyl radicals generated by photolysis at 300 nm of DBK (0.9 mM) in the presence of quinoline-TEMPO (0.0232 mM). λ_{ex} 350 nm, λ_{em} 400 nm. Solvents: tetrachlorocarbon, cyclohexane, benzene, pyridine, acetonitrile, ethanol, methanol.

In 1992 Ingold used the spectroscopic technique of laser flash photolysis to monitor the quenching of the absorption of the benzyl radical in the presence of TEMPO. Benzyl radicals generated by photolysis of 1,3-diphenylacetone decay with pseudo-first-order kinetics and variations of the experimental first-order rate constant with changing TEMPO concentrations were linear. From the slope of the linear fit the absolute rate constant for the TEMPO trapping of benzyl radicals was calculated. The experiments were done in different solvents and the results for some of the solvents[27] are shown in Table 3-1.

Solvent	$k_T/(10^7\ M^{-1}\ s^{-1})$
Cyclohexane	41 ± 2
Benzene	18 ± 1
Acetonitrile	9.5 ± 0.7
Ethanol	15 ± 1
Methanol	13 ± 1

Table 3-1 Second order rate constants for the trapping of benzyl radicals by TEMPO in different solvents. Values obtained by laser flash photolysis.

The kinetic traces in Figure 3-12 can be fitted with a linear equation. The slopes extrapolated from this treatment of the data are shown in Table 3-2. They have an increasing trend going from a non-polar solvent to a polar one. This behavior is not in accordance with the trend seen for the values reported by Ingold for TEMPO but this can be attributed to the fact that TEMPO differs from the pre-fluorescent probes for a more limited structure and also probably due to different solvation properties. It is also possible that the efficiency of the photolysis of DBK is different in different solvents. This possibility can affect the rate of radical production leading to different kinetics for trapping reactions in different solvents. Pyridine is the solvent giving the slowest rate of trapping and interactions of the base group with the probe can be considered as responsible for this effect.

Solvent	Slope
Carbon tetrachloride	3542
Cyclohexane	3015
Benzene	3823
Pyridine	470
Acetonitrile	4105
Ethanol	5398
Methanol	6745

Table 3-2 Slope values of the linear fit of the fluorescence growth due to the radical trapping of benzyl radicals generated by photolysis of DBK (0.9 mM) at 300 nm in the presence of quinoline-TEMPO (0.0232 mM). λ_{ex} 350 nm, λ_{em} 400 nm.

3.3.3 *Cyclohexyl radical trapping with quinoline-TEMPO*

Photolysis of tert-butyl peroxide in cyclohexane as a solvent produces cyclohexyl carbon-centered radicals very efficiently and in the presence of quinoline-TEMPO pre-fluorescent probe the radical trapping reaction occurs with the consequent formation of a diamagnetic product (Scheme 3-10).

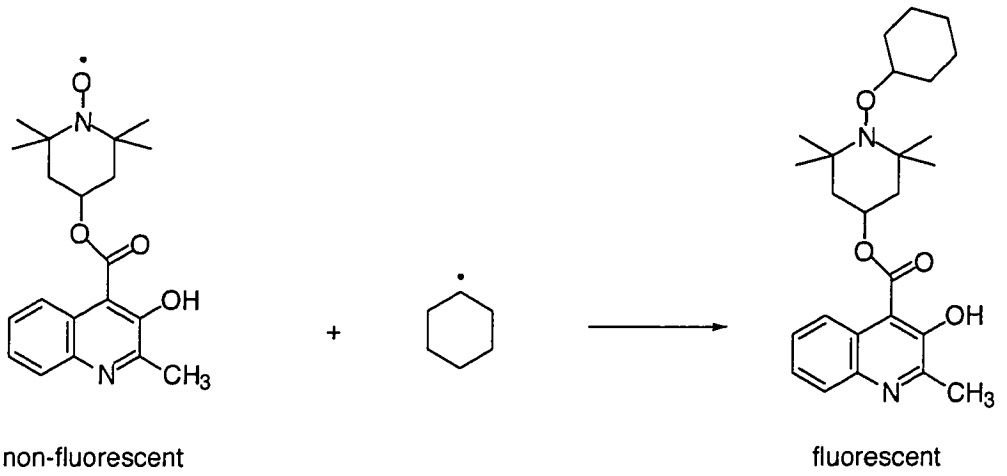

Scheme 3-10 Reaction showing the radical coupling between quinoline-TEMPO and cyclohexyl radicals produced by the photolysis of tert-butyl peroxide in cyclohexane.

The trapping reaction of the cyclohexyl radical with quinoline-TEMPO shows an increase in the fluorescence for 40 seconds with a maximum intensity at 391 nm (Figure 3-13).

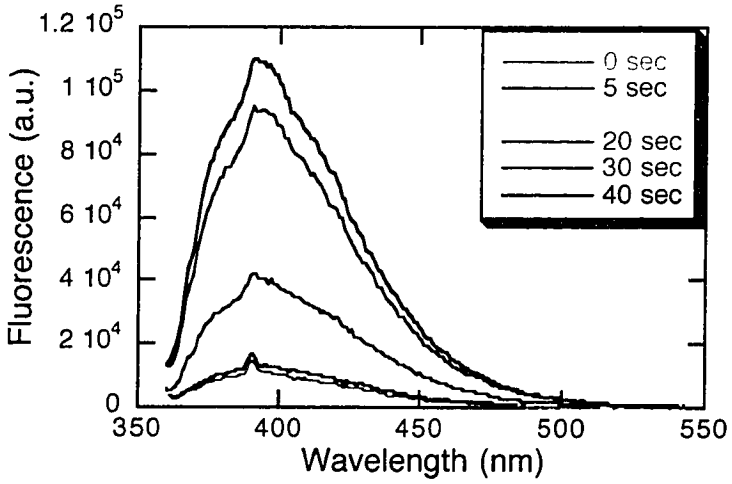

Figure 3-13 Fluorescence growth due to the radical trapping of cyclohexyl radicals produced by photolysis at 300 nm of DTBP (10%) in cyclohexane in the presence of quinoline-TEMPO (0.025 mM). λ_{ex} 350 nm, λ_{em} 360-550 nm.

Figure 3-14 shows the fluorescence intensity at 391 nm changing with time.

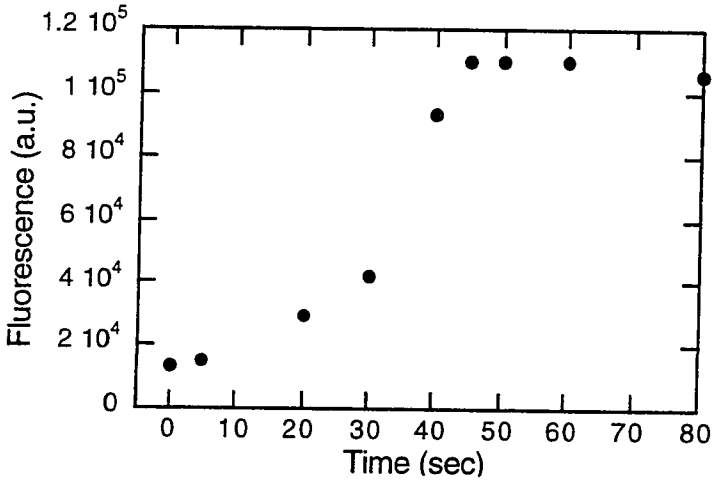

Figure 3-14 Fluorescence growth monitored at 390 nm (λ_{em} 350 nm) due to the radical trapping by quinoline-TEMPO (0.025 mM) of cyclohexyl radicals produced by the photolysis at 300 nm of DTBP (10%) in cyclohexane.

3.4 Experimental section

3.4.1 Thermolysis of 2,2`-azobisbutyronitrile in the presence of the pre-fluorescent probes. Sample preparation

When the samples are prepared the absorption characteristics of the probe and of the initiator have to be considered. The probe used in the fluorimetric experiment must have a concentration such that the absorbance at the excitation wavelength is between 0.1 and 0.2. In this way the kinetic data are not affected by the phenomena of self-absorption. The excitation and the emission wavelengths vary for the five probes: quinoline-TEMPO λ_{ex}= 350 nm λ_{em} = 400 nm, QMe-T λ_{ex} = 300 nm λ_{em} = 400 nm, Q10C-T λ_{ex} = 300 nm λ_{em} = 400 nm, QTs-T λ_{ex} = 300 nm λ_{em} = 400 nm, coumarin-TEMPO λ_{ex} = 330 nm λ_{em} = 420 nm. The reactions are all done in benzene and from the extinction coefficients previously reported the working concentration of the probes have been chosen at around 0.025 mM for the quinoline probes (A_{bs} ~ 0.15) and 0.016 mM for coumarin-TEMPO (A_{bs} ~ 0.12). From the values of the extinction coefficients of AIBN in benzene at the three working wavelengths it is possible to consider that at concentrations higher than 2 mM shielding phenomena could generate a

fluorescence signal that is not representative of the fluorescent molecules present in the system. All the samples were prepared by adding microlitre quantities of a stock solution of the probe and AIBN to a 4.0 ml of benzene in a 1x1 cm quartz cell. The solutions were then degassed with a high flow of nitrogen until the solution reached a volume of 3 ml.

The kinetics of the reaction were obtained by exciting and following the emission at fixed wavelengths and using a time-based program. Measurements were taken every five seconds.

3.4.2 *Photolysis of 1,3-diphenylacetone in the presence of quinoline-TEMPO. Sample preparation.*

The concentration of the probe used is 0.0232 mM. The preparation of the sample is the same as described for the AIBN experiments. A stock solution 0.092 M of the photoinitiator in benzene was used and different amounts were added to the reaction solution before degassing. Photolysis was always performed with one lamp at 300 nm at which the ketone has an extinction coefficient of 539 M^{-1} cm^{-1}. The cell was placed at a distance of 10 cm from the light source in all the photolysis experiments presented in this thesis. Five different concentrations of DBK between 0.3 mM and 1.5 mM were used in the presence of quinoline-TEMPO in benzene and in these conditions the initiator absorbs most of the light. The experiments in different solvents were done using the same procedure as described above.

3.4.3 *Photolysis of tert-butyl perxide in cyclohexane in the presence of quinoline-TEMPO. Sample preparation*

Quinoline-TEMPO was used in a concentration of 0.25 mM (A_{bs}= 0.15). Tert-butyl peroxide was used as 10 % by volume. The sample was degassed as previously reported and irradiated for short time with one lamp at 300 nm inside the photoreactor. The emission spectrum was taken after 5, 10, 20, 30 and 40 seconds with excitation at 350 nm and then the monitoring of the fluorescence between 360 and 550 nm.

3.5 Conclusions

The pre-fluorescent probes tested in coupling reactions with carbon-centered radicals produced in homogenous solution by thermal and photodecomposition of suitable radical initiators has shown successful results. Fluorescence growth has been monitored with varying experimental conditions which influence the amount of radicals produced with time (concentration of radical initiators and temperature). The reported results support the mechanism of the quenching of the fluorophore fluorescence due to an electron exchange mechanism between the singlet excited state and the TEMPO doublet and the restoring of the emission signal due to radical coupling with a carbon-centered radical. Previous considerations regarding the absorption of molecules within the reactive system resulted in a methodology being developed for a clear detection of radicals. The use of only one lamp for experiments of photodecomposition of radical initiators has allowed the preparation of samples with varying amounts of DBK which in turn shield the probe enough to avoid side reactions of decomposition until the sensor is totally consumed. Quinoline-TEMPO derivatives showed a reduced fluorescence enhancement at the end of the radical trapping reaction due to the removal of the hydrogen bonding in quinoline-TEMPO. The conjugation in the aromatic system is reduced by the presence of substituents on the oxygen in the third position. This leads to lower quantum yields of fluorescence in comparison with quinoline-TEMPO. Coumarin-TEMPO was found to contain a diamagnetic hydroxylamine impurity which, in presence of the 2-cyano-2-propyl radical, was converted to the paramagnetic form due to hydrogen abstraction. This process was observed from the decrease of the fluorescence signal which then increases due to the radical trapping reaction of the coumarin-TEMPO free radical. The applications we wanted to achieve with this methodology employing quinoline-TEMPO and coumarin-TEMPO adducts have been selected in the field of free radical polymerization, detection of radicals in supramolecular systems and monitoring of biradical intermediates during the photodecomposition of cyclic ketones.

4 Applications

4.1 Introduction to nitroxide mediated free radical polymerization

Since 1980 nitroxides have been very prominent in the field of free-radical polymerization as they contain the possible ability to control the polymerization process. Conventional radical polymerization is an important industrial process, which allows the production of polymers with high molecular weight at mild conditions but with the great disadvantages of not controlling the structure of the macro polymer, the degree of polymerization or the polydispersity. Nitroxides offer the possibility of controlling the growing chain and limiting the bimolecular recombination reaction responsible for the irreversible chain termination. The main beneficial characteristic of nitroxides is their ability to activate and deactivate the growing macro radical at high temperatures. By adding the monomer in different steps it is possible to obtain further polymer growth and build copolymers with a defined structure[44-46]. Rizzardo was the first to investigate both the reaction of benzoyloxy radicals and tert-butoxy radicals with styrene in the presence of nitroxides[47] and was able to produce low molecular weight products. In 1993 Georges discussed the preparation of low-polydispersity polystyrene by "living free radical polymerization"[45,48]. In Scheme 4-1 the mechanism of polymerization of styrene in the presence of TEMPO is displayed. The radical initiator is benzoyl peroxide, which decomposes at high temperatures to form benzoyloxy radicals, which then abstract hydrogen from the double bond of styrene with the consequent formation of a reactive benzyl radical. Benzyl radicals start the polymerization by chain addition to the double bond of another molecule of styrene in the propagation step. Nitroxides react with carbon-centered radicals with a rate constant close to diffusion control and hence trap the growing radical chain efficiently. At a temperature of 125 °C the capping of the growing radical chain is

reversible[49,50] and in the presence of a monomer the radical chain can grow until the substrate is totally consumed. Under these conditions the macro radical has a lesser probability of encountering another radical chain and undergoing self-termination. The process consists of activation and deactivation steps of the polymer radical through a mechanism of cap separation and cap formation. This kind of polymerization is called "living" free radical polymerization because the growing radical, also called the "dormant" radical can be controlled through its addition to another monomer or by trapping with the nitroxide.

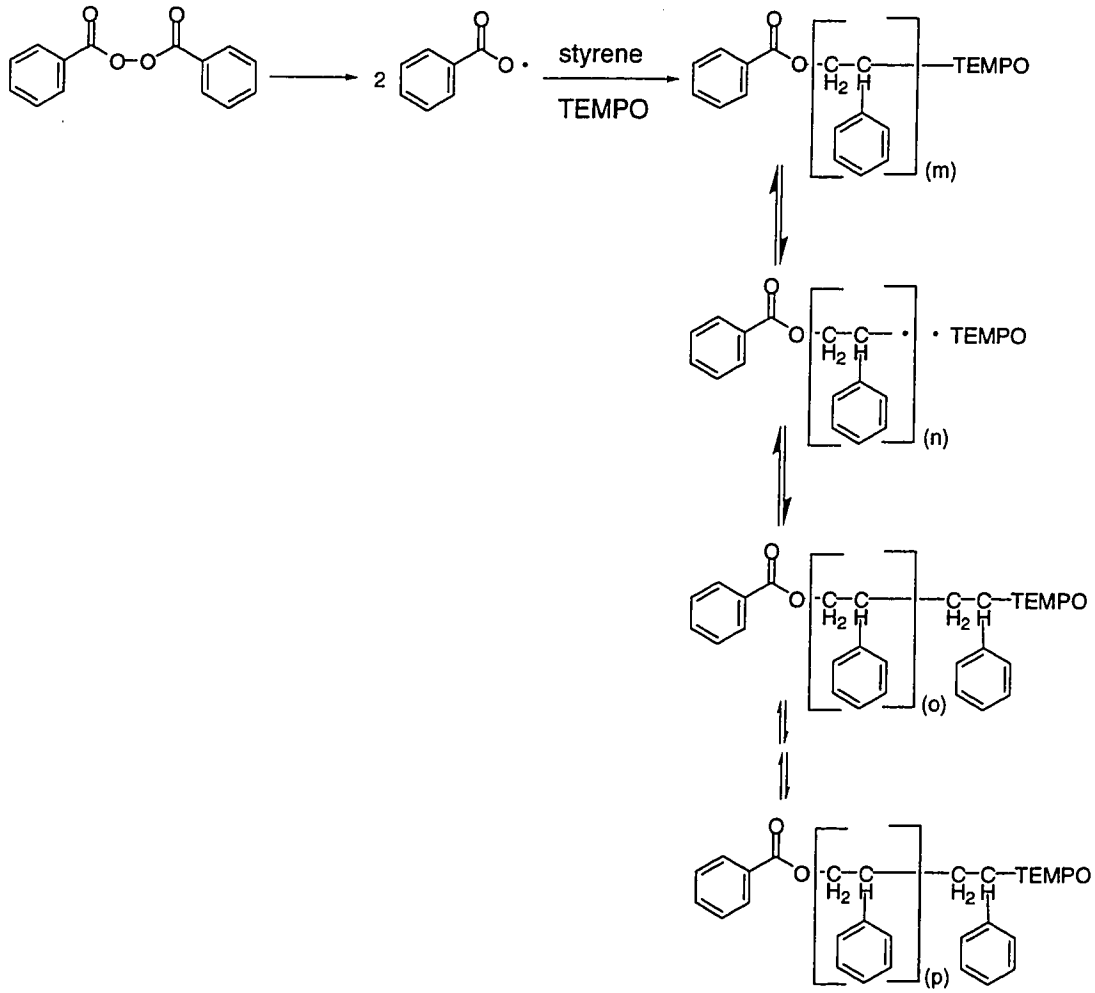

Scheme 4-1 Free radical polymerization of styrene in presence of TEMPO free radical trap employing benzoyl peroxide as a radical initiator.

The overall dynamics of LFRP (Living Free Radical Polymerization) is determined by the cap cleavage reaction and the small concentrations of nitroxide that accumulate in the system. Researchers have been looking for

information about the key step in the reversible capping of the polymer in terms of the activation energy of bond breaking and the bond dissociation energy. A variety of nitroxide-based initiators have been reported by our group[51,52] and by others[53]. These kind of molecules decompose at high temperatures producing a carbon-centered radical and a nitroxide free radical which in presence of a styrene monomer act as an initiating radical and a scavenger respectively. The stoichiometric production of nitroxide relative to the initiating radical is an advantage which results in every chain end being capped with a nitroxide, ultimately resulting in low polydispersities polymers. The properties of the polymer can be interpreted using unimolecular initiators as a model if it is assumed that the C-O bond dissociation energy at the capped polymer end is similar to those in other benzylic systems. Will Skene, a PhD student in Dr. Scaiano's group prior to the beginning of this project, studied a series of alkoxyamine initiators which mimic the end chain[50] (Scheme 4-2).

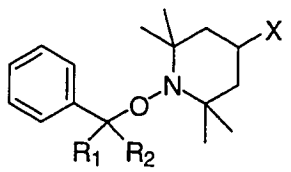

I : $R_1 = R_2 = X = H$

II : $R_1 = X = H$; $R_2 = CH$

III: $R_1 = R_2 = CH$; $X = H$

IV: $R_1 = R_2 = H$; $X = OH$

Scheme 4-2 Radical initiators mimicking the polymer chain end constituted by TEMPO and substituted benzylic moieties.

He studied the kinetics of thermal cleavage of these compounds under irreversible conditions. In reversible conditions the activation energies for the reverse reaction have to be taken into consideration and this can lead to more complicated kinetic data. Conditions of irreversibility can be obtained by performing the decomposition of the initiators in the presence of a large excess of another nitroxide. The trap was used in concentrations seven times greater than the radical initiator. In this way the carbon-centered radical generated by thermolysis of the initiator is trapped by the added scavenger before it can recombine with another benzyl radical in a reaction representative of the self-termination process (Scheme 4-3). k_c was determined by analyzing the products of this reaction at different times using HPLC. (High Performance Liquid

Chromatography). From the Arrhenius plot for the decomposition of the molecules a BDE (Bond Dissociation Energy) between 25 and 31 kcal/mol were calculated.

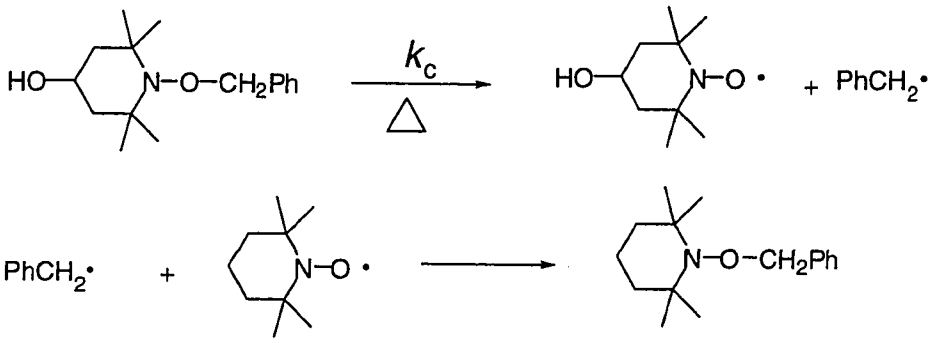

Scheme 4-3 Reaction showing the reversible coupling of benzyl radicals with TEMPO at high temperatures.

2,2,6,6-Tetramethyl-1-(1-phenylethyoxy)-piperidine (EB-T) and 1-(2,2,6,6-tetramethylpiperidine N-oxide)-1,3diphenylpropane (PN-T) are good mimic reagents for the nitroxide-capped polystyrene and they lead to bond dissociation energies of 28.4 kcal/mol[50] and 28.0 kcal/mol[35] respectively.

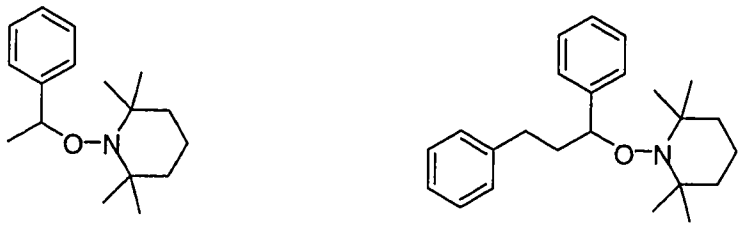

EB-T **PN-T**

Scheme 4-4 2,2,6,6-tetramethyl-1-(1-phenylethyoxy)-piperidine (EB-T), 1-(2,2,6,6-tetramethylpiperidine N-oxide)-1,3diphenylpropane (PN-T).

4.2 Kinetics of cap separation in nitroxide-regulated "living" free radical polymerization

The aim of this study was to determine the bond dissociation energy of the native polymeric system employing one of the pre-fluorescent probes presented in this thesis. This project was the product of collaboration with Olga Garcia Ballesteros. The coumarin-TEMPO (CU-T•) paramagnetic adduct was used in the

detection of polystyrene macroradicals. When a TEMPO-capped polystyrene produced by LFRP is thermally decomposed in the presence of the probe the resulting macroradical (PS• polystyrene macroradical) can be trapped by either TEMPO (T•) or by CU-T• with essentially the same kinetics (Scheme 4-5). By choosing the concentration to favor conditions of irreversibility the trapping of the probe is favored.

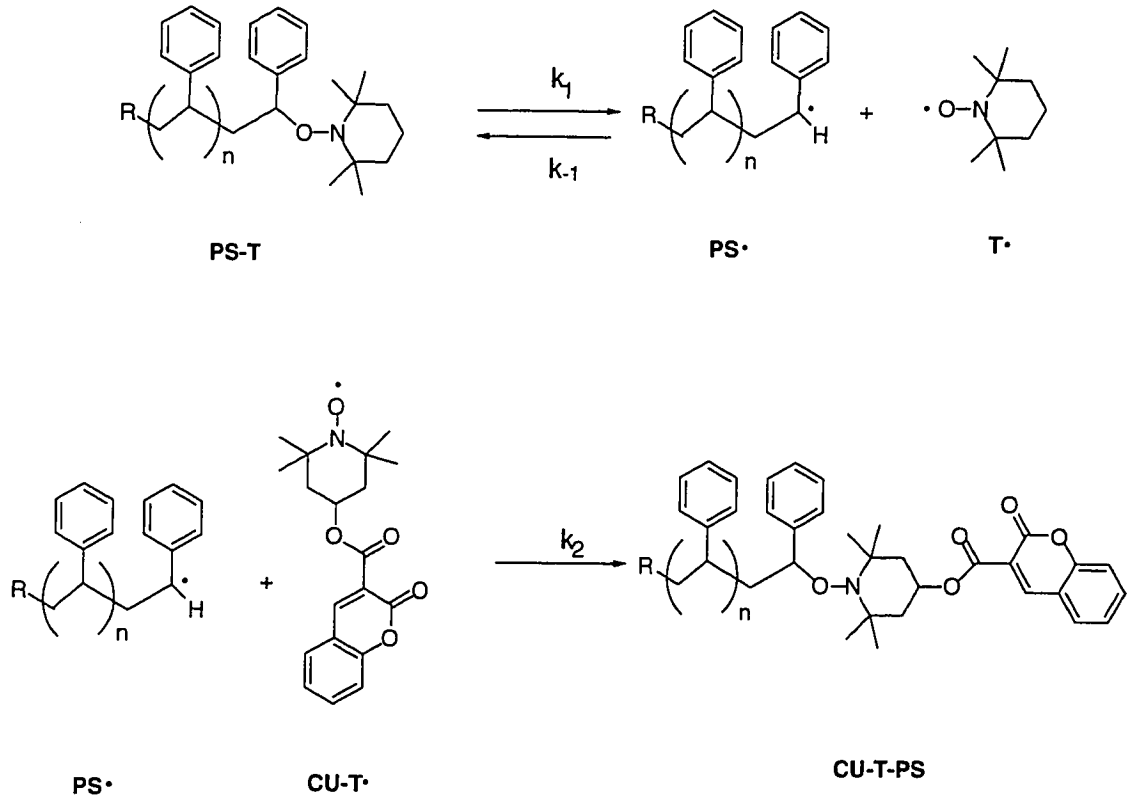

Scheme 4-5 Reversible uncapping of polystyrene-TEMPO adduct at high temperatures leading to formation of the macroradical PS• and consequent radical trapping by coumarin-TEMPO (CU-T•).

Every trapping reaction of a carbon-centered radical causes the switching of the sensor to its fluorescent form CU-T-PS allowing the detection of the radical by following the increase in fluorescence. Rates of radical formation at different temperatures as a function of time were estimated with this methodology. From this the kinetic Arrhenius parameters and the corresponding bond dissociation energy for the terminal TEMPO group in the polymeric chain were calculated.

4.2.1 Results and discussion

Polystyrene-TEMPO was prepared in a nitroxide-regulated radical polymerization using a unimolecular initiator derived from radical coupling of a benzyl radical with a nitroxide. A similar strategy was employed by Turro et al.[54] to prepare end-labeled monodisperse polymers. The reactions of coumarin-TEMPO (1.5×10^{-4} M) and polystyrene-TEMPO (1.5×10^{-6} M) were studied in temperatures ranging between 90 °C and 130 °C with chlorobenzene as a solvent. This solvent offered a suitable temperature range while other solvents, like acetonitrile and ethylbenzene, had inadequate temperature ranges or they showed reactivity towards the nitroxide at 125 °C. All the plots in Figure 4-1 show enhancement in fluorescence upon radical trapping under nitrogen or air atmosphere at different temperatures. From these plots it is possible to observe the presence of small levels of diamagnetic impurities. Measurements are normally based on the difference; the fluorescence enhancement upon radical trapping and the absolute concentrations of CU-T• are not necessary for the calculations. From every single plot of product formation a constant rate was obtained. At all temperatures the growth of fluorescence shows the same kinetic behavior, consisting of a first rapid increase until a plateau is reached. The exception is the plot at 90 °C at which the plateau was not reached in the time examined. The rate of fluorescence increases as the temperature of the system increases. From the experiments under air it is possible to observe that the fluorescence intensity increases slower than when the system is under nitrogen and that the plateau is lower. Carbon-centered radicals react with oxygen at close to the diffusion control rate producing peroxyl radicals and it is known that molecular oxygen inhibits radical-induced polymerization because of its high reactivity towards carbon-centered radicals. This result supports the mechanism of interaction between carbon-centered radicals and the pre-fluorescent probe.

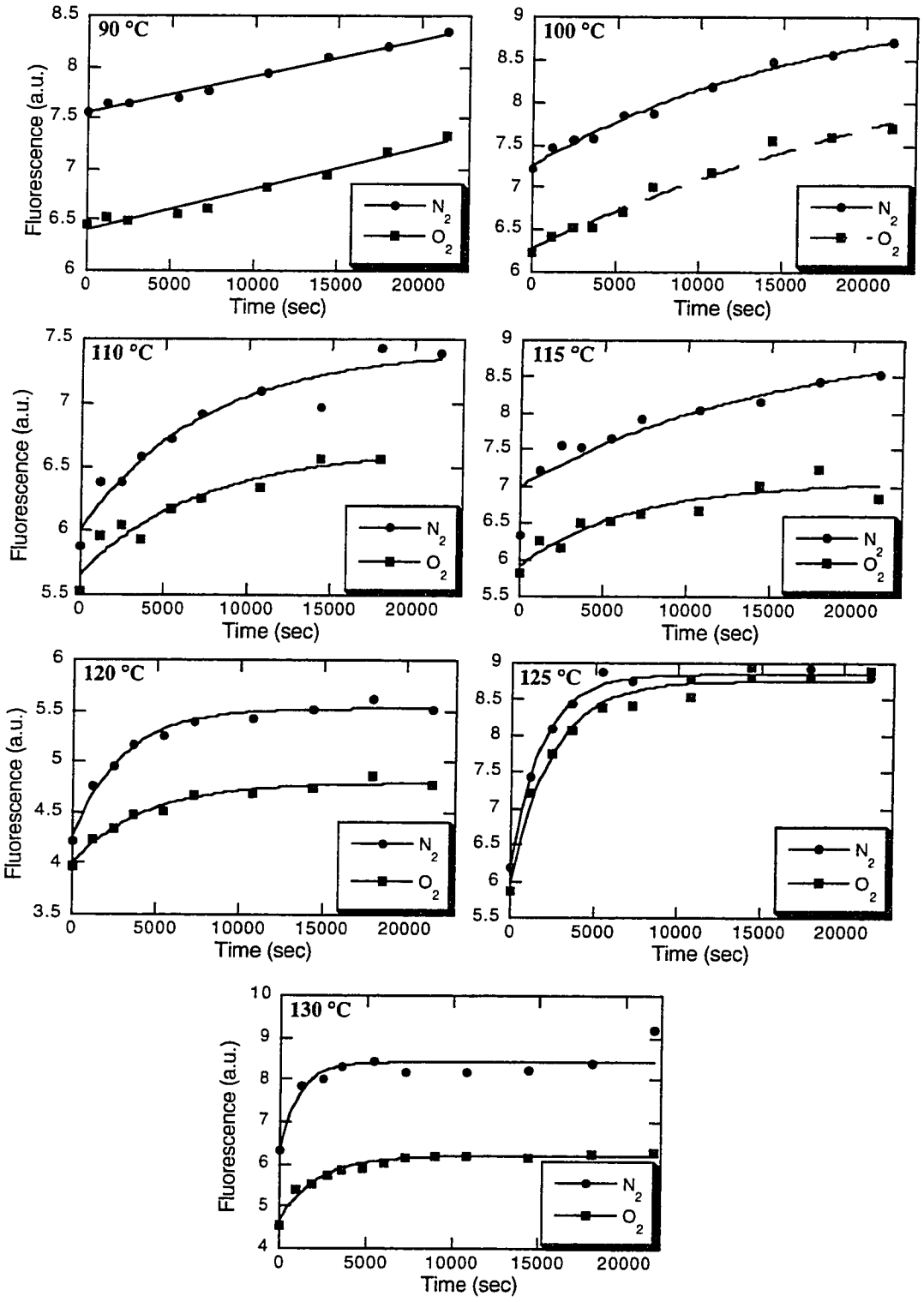

Figure 4-1 Fluorescence growth due to the radical trapping of polystyrene macroradicals PS• (PS-T 1.5 x 10^{-6} M) by quinoline-TEMPO (1.5 x 10^{-4} M) in chlorobenzene under both a nitrogen and an oxygen atmosphere at different temperatures (90, 100, 110, 115, 120, 125, 130 °C).

All the plots were fitted with a first-order growth equation apart from the experiments at 90 °C where a linear equation was applied. From the experimental rate constants at a range of temperatures, it is possible to obtain the activation parameters for cap separation and from them to estimate the desired C-O bond dissociation energy. The Arrhenius equation plot for the reaction under nitrogen and under air is shown in Figure 4-2.

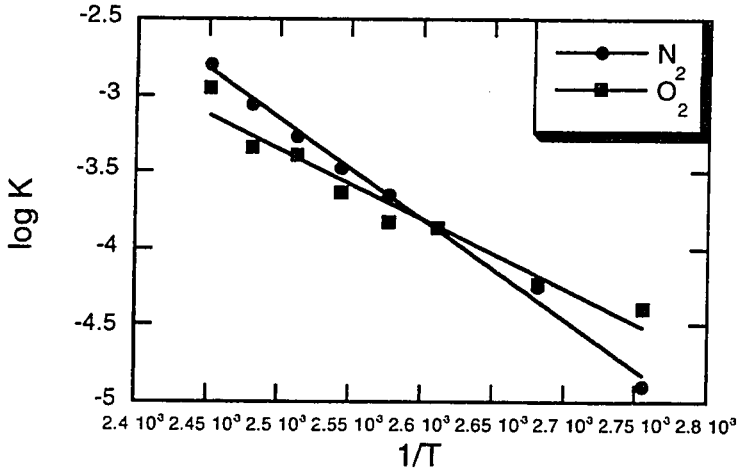

Figure 4-2 Arrhenius plot for the determination of the activation parameters for C-O bond cleavage in the polystyrene-TEMPO capped polymer chain synthesized by the LFRP process.

The plot yields a pre-exponential factor (log A/s^{-1}) = 13.3 which is related to the structure of the transition state and an activation energy E_a= 30.2 kcal/mol which is necessary for C-O bond cleavage. This value is comparable with a reported activation energy value of 30.3 kcal/mol for PN-T[51]. Subtracting from this value 2.3 kcal/mol for the activation energy for radical trapping[28] the bond dissociation energy in PS-T can be estimated to be 27.9 kcal/mol. Information about the transition state of the reaction is contained in the pre-exponential factor. The value is consistent with other measurements for PN-T and EB-T[50,51] model compounds and with homolytic bond cleavage processes for similar reactions. The relatively high value indicates that the transition state is similar to the products and that it has gained degrees of freedom.

4.2.2 *Experimental section*

4.2.2.1 Synthesis of the thermal initiator: 2,2,6,6-tetramethyl-1-(1-phenylethyoxy)-piperidine (EB-T)

The conditions used for the photochemical synthesis of the initiator are described in the literature[54]. One equivalent (1 g) of TEMPO was dissolved in 5 mass equivalents of tert-butyl peroxide (2.8 ml). Tert-butyl peroxide was previously purified by passing it through neutral alumina. To the red-orange solution 30-35 ml of ethylbenzene was added. In this system ethylbenzene acts as both a solvent and a reagent and the mechanism of formation of carbon-centered benzyl radicals is the same as the one reported in Scheme 4-1. The solution was placed in a Pyrex test tube and purged with nitrogen for 30 minutes. Then the Pyrex tube was placed inside a photoreactor and irradiated for 5 days at 300 nm with broad-band lamps until the color turned from orange to yellow. The solution was evaporated by bubbling nitrogen through the sample and then completely dried under vacuum. The product was recrystallized from methanol yielding white crystals in a yield greater than 90 %.

4.2.2.2 Nitroxide-mediated "living" free radical polymerization of styrene

Freshly distilled styrene was used as a solvent and as a monomer for the free radical polymerization process. The thermal initiator in a ratio of 1:100 was dissolved in styrene and the mixture, after purging with nitrogen, was flame-sealed in a 7 mm Pyrex glass tube. The sample was then heated in a thermo stated aluminum block at 125 ± 1 °C for 22 hours. After cooling of the sample, the residual styrene was evaporated under vacuum and the resulting polymer was precipitated with methanol. The analysis of the polymer was done using size exclusion chromatography (SEC) injecting a tetrahydrofuran solution of the white precipitate. A Waters Styragel HR3 column and a Varian refraction index detector were employed. The molecular weight and polydispersities were determined in relation to polystyrene molecular weight standards. LFRP is a suitable method for the production of low polydispersity polymers. The average molecular weight (M_w) was 16780 and the polydispersity 1.23.

4.2.2.3 Temperature dependence study

The experiments at different temperatures were carried out by adding an excess of CU-T• (1.5×10^{-4} M) to a chlorobenzene solution of PS-T. The samples were purged with nitrogen for 30 minutes and sealed in a 1 x 1 cm quartz cell. The samples were then heated in a thermo stated paraffin bath in a dark oven and removed at different times. The sample was cooled in an ice bath to stop the reaction. The oil was cleaned from the cuvettes using ethanol. Emission scans were then recorded with the fluorimeter. The excitation wavelength was set at 350 nm to allow selective excitation of the probe. Size exclusion chromatography coupled with fluorescence detection proved that the polymer was labeled with the chromophore.

4.3 Fluorescence detection of 4,4'-(1,3-propanediyl)bisbenzyl biradical by quinoline-TEMPO

Biradicals have been recognized as reactive intermediates in thermal and photochemical reactions. Direct evidence of the formation of a biradical has been obtained from radical trapping reactions and more direct methods such as electron paramegnetic resonance[55] and laser flash photolysis[56]. The lifetimes of triplet biradicals are usually controlled by intersystem crossing, which depends on the conformations of the biradical[57-60]. The behavior of long-chain acyl-alkyl biradicals has been investigated in order to understand the interactions between the radical termini[55]. Dr. Font, a post-doctorate researcher in our group, has previously studied by LFP the chemical behavior of 4,4`-(1,2-ethanediyl)bisbenzyl biradicals produced by photolysis of [3,2]paracyclophan-2-one[61]. He then prepared (1,n-alkanediyl)-homologous with longer tethers and he studied their behavior by means of LFP. Employing the quinoline-TEMPO pre-fluorescent probe we wanted to study the radical trapping of bisbenzyl biradicals (BBB) produced by the photodecomposition of [3,3]paracyclophan-2-one (PCP) by means of fluorescence spectroscopy. The photochemistry of radical formation is a Norrish type I process in which the excitation of the cyclic ketones leads to the homolytic cleavage of the α-bond of the carbonyl moiety. Analysis of the

photolysate by ^{1}N-NMR and GC/MS have shown decarbonylated cyclophanes (CP) to be the only products of the reaction (Scheme 4-6).

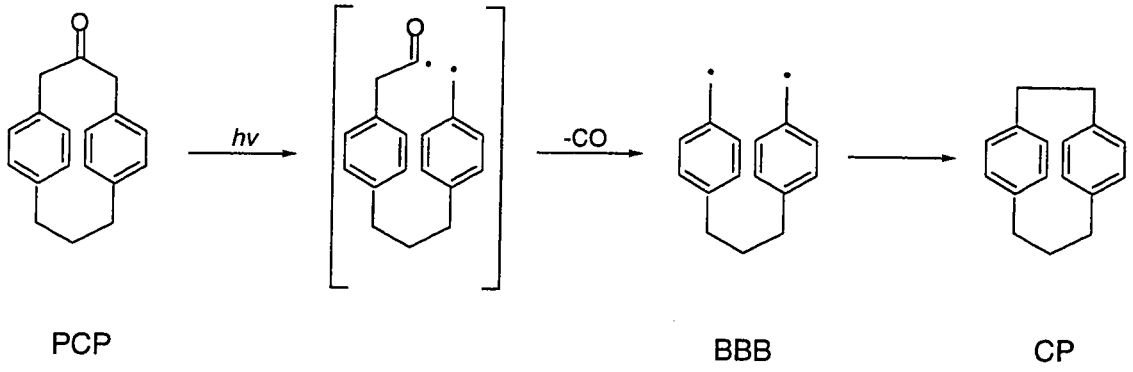

Scheme 4-6 Reaction showing the photolysis of [3,3]paracyclophan-2-one (PCP) leading to the production of 4,4`-(1,3-propanediyl)bisbenzyl biradical (BBB) as an intermediate and the decarbonylated cyclophane (CP) as final product.

This mechanism is consistent with the fast decarbonylation of aromatic ketones. Upon irradiation of the cyclic ketone a triplet biradical BBB is generated. Intersystem crossing to the singlet biradical rapidly occurs with consequent formation of product CP. LFP has offered an important tool to understand the behavior of biradicals intermediates, allowing the detection of the transient and the measurement of the lifetime (3.9 μs). Biradicals are suitable substrates for radical scavengers and it is well known that paramagnetic substances like nitroxides readily quench triplet biradicals[62]. For this reason quinoline-TEMPO was chosen to test this intermediate. Radical trapping of BBB by the pre-fluorescent probe leads to a diamagnetic product with the result being a growth of the fluorescence emission. The radical sensor in this application opens a further insight into the behavior of these intermediates. The radical scavenging process is in fact in competition with intersystem crossing from the triplet biradical which depends on the chain length.

4.3.1 Results and discussion

The pre-fluorescent probe was used in the same concentration as in the experiment with DBK and with PCP having a concentration of 1 mM. The samples were irradiated with one lamp at 300 nm and emission scans were collected at different times until quinoline-TEMPO was completely consumed.

In Figure 4-3, the growth of fluorescence at 400 nm during the reaction of trapping of the biradical BBB is shown. The excitation wavelength is fixed at 350 nm where only quinoline-TEMPO is able to absorb the incident light. The plateau of the reaction is reached after almost 2000 seconds. The kinetic trace has been fitted with a first order growth equation resulting in a constant rate of trapping equal to 1.07×10^{-3} sec^{-1}.

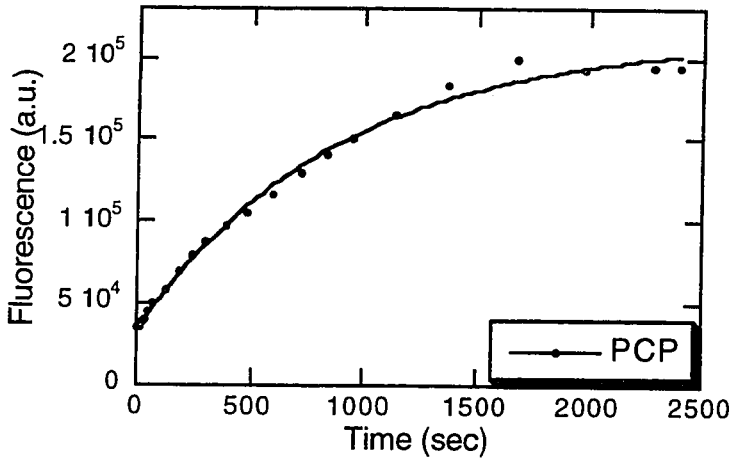

Figure 4-3 Fluorescence growth due to the radical trapping by quinoline-TEMPO (0.0232 mM) of bisbenzyl biradicals BBB produced by the photolysis of PCP (1 mM) at 300 nm.

The initial slope of the fluorescence growth is shown in Figure 4-4. The plot has been fitted with a linear equation and it is compared with the radical trapping of benzyl radicals. The slope of the linear fit represents the rate constant of the initial production of radicals. This result introduces the possibility of investigating the behavior of biradical intermediates by employing pre-fluorescent probes. Intersystem crossing from the triplet to the singlet biradical depends on the chain length and on the conformation of the biradical. Repeating these experiments with [3,n]paracyclophan-2-ones having different chain lengths will reveal the different intersytem crossing components of the quenching of the biradical intermediates if the rate of the radical trapping results different for each cyclic ketone.

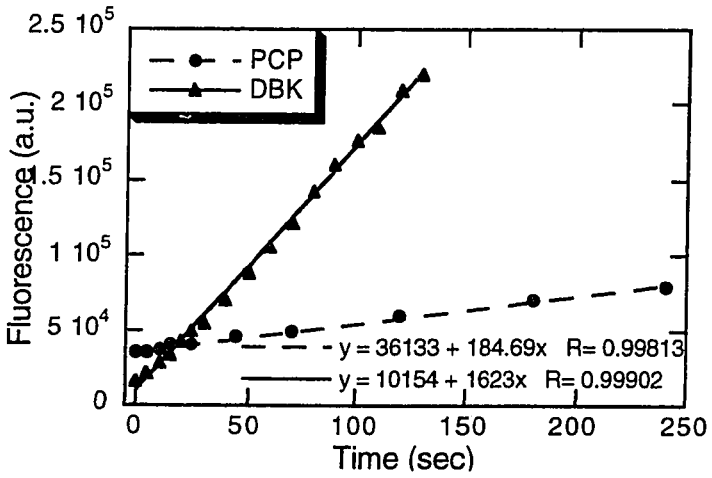

Figure 4-4 Linear fit of the initial slope of the fluorescence growth due to the radical trapping by quinoline-TEMPO (0.0232 mM) of benzyl and bisbenzyl biradicals BBB produced by the photolysis of DBK (0.9 mM) and PCP (1 mM) at 300 nm. λ_{ex} 350 nm, λ_{em} 400 nm.

4.3.1.1 Experimental

The sample has been prepared using the same procedure as in the experiments showing the trapping of benzyl radicals, which were produced by photodecomposition of DBK (Chapter 3.4.2). The concentration of PCP was chosen to be 1 mM in the presence of quinoline-TEMPO in a concentration of 0.0232 mM. In these concentrations PCP has an absorbance of 0.3 at 300 nm and the sensor 0.11. One lamp at 300 nm is used to irradiate the cell. Fluorescence growth is monitored by exciting the sample at 350 nm where only quinoline-TEMPO absorbs.

4.4 Radical trapping of benzyl radicals in SDS micelles

Detergents like sodium dodecyl sulfate can form amphiphilic aggregates in water called micelles when they are used above the critical micellar concentration. Micelles are characterized by a hydrocarbon-like interior, an ionic polar surface and an aqueous exterior. Radical pairs have been photogenerated and studied for their recombination process into a micellar environment. The dynamics of triplet radical pairs generated by photolysis of unsymmetric ketones has been investigated by laser flash photolysis[31], product studies[63] and magnetic

isotope effects[32,33]. By using an unsymmetric dibenzyl ketone the ratios of the three possible products of recombination were obtained in both homogenous solutions and in a micellar hexadecyltrimethylammonium chloride (HDAC) environment. When two radicals R_1• and R_2• are produced in homogenous solutions they rapidly become random free radicals and the products of recombination are representative of reencounters trajectories. Instead in the hydrophobic environment of micelles, the two radicals are constricted in a reduced dimensional space. This reduces the number of random free radicals that can be formed. Scheme 4-7 shows the possible formation of three different products in the photolysis of an unsymmetric ketone.

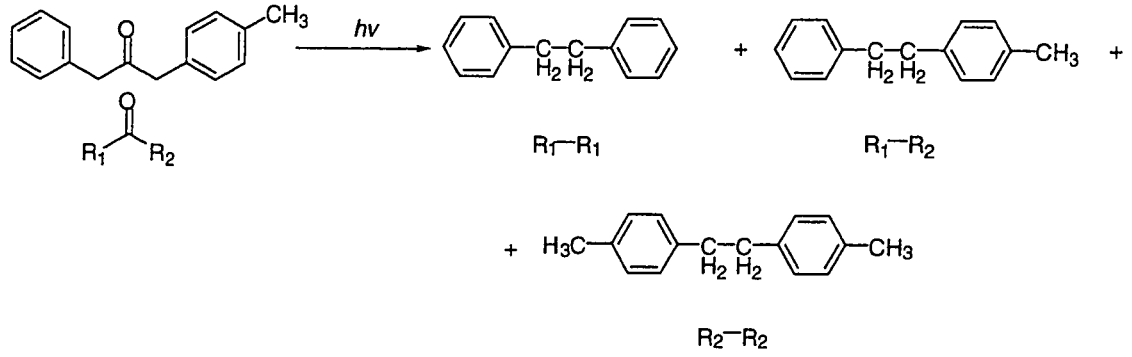

Scheme 4-7 Reaction showing the photolysis of unsymmetric ketone leading to a combination of coupling products.

The ratios of the products were studied at different surfactant concentrations and the values R_1-R_1 25 %, R_1-R_2 50 %, R_2-R_2 25 % remained constant until a concentration of hexadecyl ammonium chloride of ~3 x 10^{-3} M was added[63]. Indeed these ratios are the result of a statistical distribution of products which varies when the change in environment changes the photochemical reaction pathway. In order to explain the non-statistical distributions of the products it is possible to consider a model (Scheme 4-8) in which a primary radical pair formed in the solvent cage by α-cleavage is composed of an acyl radical and a benzyl radical. Together they can recombine or produce a secondary radical pair, through fast decarbonylation, which leads to two benzyl radicals originating from the same molecule of DBK. The radicals can then either recombine in the solvent cage or escape to become random free radicals. This model cannot be considered in homogenous systems because of the fast escape of the radicals out

of the solvent cage. In micelles instead the amphiphilic environment slows down the production of random radicals, hence increasing the number of possibilities available for the self-reaction of the primary and secondary radical pairs. The result is a non-statistical distribution of the products of the reaction with an increase of the percentage of product R_1-R_2. The latter, if the concentration of surfactant is raised, increases until it reaches 98 % at a concentration of HDAC of ~6×10^{-3} M.

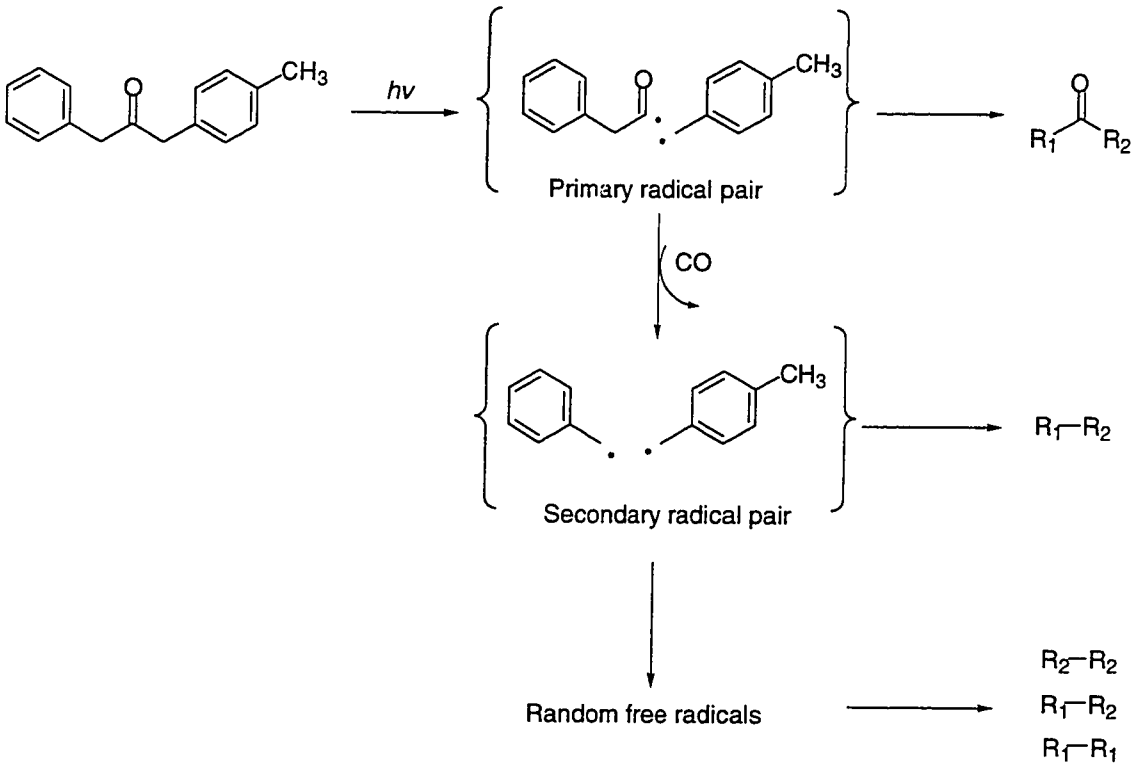

Scheme 4-8 The photolysis reaction of an unsymmetric dibenzylketone in a constrained medium.

The experiment of fluorescence detection of benzyl radicals was carried out employing quinoline-TEMPO as a pre-fluorescent probe and a concentration of sodium dodecyl sulfate (SDS) of ~0.2 M. Under these conditions the radicals formed by photolysis quickly recombine inside the "super cage" of micelles slowing down trapping by the probe in relation to homogenous solution due to the competition with the enhanced bimolecular self-reaction [31,33,34].

4.4.1 Results and discussion

Quinoline-TEMPO does not show any solubility in water but it has a great affinity for the amphiphilic media of the surfactant. The probe and the radical were added to an SDS water solution 0.02 M and stirred overnight. Two solutions were prepared with a fixed amount of quinoline-TEMPO (2.8×10^{-5} M, Abs=0.2 at 340 nm in hexane) and different concentrations of DBK (0.7, 2.8×10^{-3} M, A_{bs}=0.25, 1.00 at 300 nm in hexane). After bubbling nitrogen for at least twenty minutes the samples were irradiated at 300 nm for time intervals ranging from five to thirty seconds. Fluorescence emission was monitored at each interval excitating the sample at 340 nm. The radical initiator lightly absorbs in this region and only at high concentrations it is able to compete for photons with the sensor.

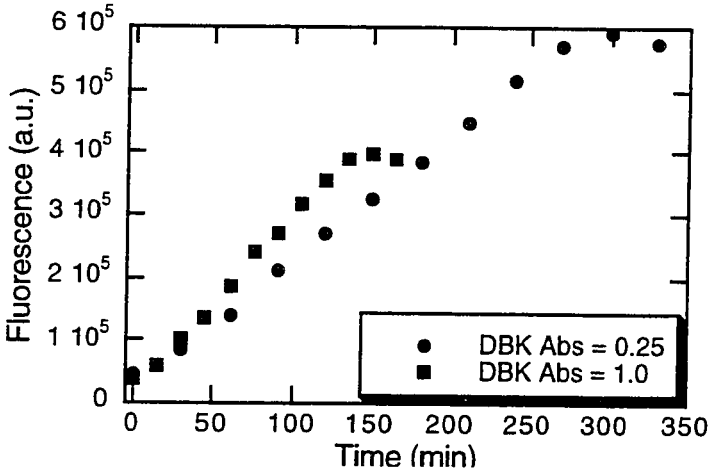

Figure 4-5 Fluorescence growth due to the radical trapping in SDS micelles (0.2 M) of benzyl radicals generated by the photolysis at 300 nm of DBK (Abs at 290 nm: 0.25, 1.0) in the presence of quinoline-TEMPO (Abs at 340 nm = 0.2). λ_{ex} 340 nm, λ_{em} 400 nm.

The result of fluorescence detection of benzyl radicals in SDS micelles is shown in Figure 4-5. It can be observed that it takes longer for the plateau to be reached than in homogenous solutions and the final value of fluorescent intensity decreases at higher concentrations of 1,3-diphenylacetone. Because of the simultaneous absorption of quinoline-TEMPO and DBK at the excitation wavelength of 340 nm, high concentrations of the radical initiator decrease the amount of photons reaching the pre-fluorescent probe. This results in lower fluorescence intensity of the diamagnetic coupling product as the concentration

of DBK is increased. The radical trapping reaction of benzyl radicals in SDS micelles by quinoline-TEMPO results in a slower rate than the radical trapping reaction in homogenous solutions. This can be attributed to the presence of "cage effects" for the radical pairs generated within the micellar aggregates. Due to the environment, benzyl radical pairs are not allowed to quickly separate and become random radicals. Intersystem crossing of the triplet radical pairs to the singlet radical pairs and consequently to products of recombination is in competition with the radical trapping reaction by quinoline-TEMPO. This leads to a longer time required for the reaction to saturate the fluorescence signal from the probe. Quinoline-TEMPO could be used in this reaction system varying the concentration and the type of surfactant in order to evaluate the effects of caging of radical pairs. Lowering the concentration of surfactant would increase the amount of radicals escaping from the solvent cage. This would lead to higher constant rates for the radical trapping reaction with quinoline-TEMPO until there is no longer a difference with the rates of trapping in homogenous systems.

4.4.2 Experimental

The sample was prepared by overnight stirring of 576 mg of sodium dodecyl sulfate (SDS) in 10 ml of water in the presence of 50 μL of a hexane solution 5.6 mM of quinoline-TEMPO and 1.5, 6.0 mg of DBK respectively. From this solution, 3 ml of solution was taken and placed inside a 1x1 cm quartz cell. The samples were degassed with a low flow of nitrogen for at least 20 minutes. No evaporation of solvent was observed during this procedure. The cells were photolyzed by using one lamp at 300 nm.

4.5 Fluorescence detection of benzyl radicals in NaY zeolites

Zeolites are crystalline aluminosilicates consisting of repeat units composed of an internal core surrounded by nanosized cages or channels. The repetition of the units creates a three-dimensional framework in which molecules can intercalate in a small window on the external surface or move randomly through the internal surface. Zeolites are characterized by an enormous internal surface that allows absorbing of large quantities of guest molecules. Depending on the

structure the molecules are allowed to pass from the external to the internal surface. The framework of the zeolite is a rigid structure constituted of $[SiO_4]^{-4}$ and $[AlO_4]^{5-}$ tetrahedral which share their edges. Al has a lower valence than Si and this results in a net negative charge, which is balanced by the presence of a cation (H^+, Na^+, Ca^{2+} etc.). The behavior of radical pairs has been studied inside the cavities of zeolites using aryl alkyl ketones[64-67]. As in the case of micelles, unsymmetric radical photoinitiation has been used to evaluate the influences of the environment on the dynamics of the reaction. The zeolite structure limits the diffusion of the radical pairs and avoids the escape of random radicals leading to a non-statistical distribution of the products of coupling reactions. This phenomenon is named the cage effect (Equation 4-1) and can be expressed in the following manner (R_1, R_2 ref. Chapter 4.4):

$$\% \text{ cage effect} = \frac{R_1{-}R_2 - (R_1{-}R_1 + R_2{-}R_2)}{R_1{-}R_1 + R_1{-}R_2 + R_2{-}R_2}$$

Equation 4-1 Equation showing the percentage of the cage effect expressed as a ratio of geminate radical pairs which undergo recombination.

This represents the percentage of geminate radical pairs that undergo recombination. Nitroxides have been used as triplet quenchers inside zeolites[68] and they also have the potential to be studied as radical scavengers. In this project the objective of the research was to develop a method for the fluorescence detection of carbon-centered radicals inside the zeolite cavities. This study was done in collaboration with Dr. Alexis Aspee`, who provided the expertise for both this and other systems (liposomes). 1,3-Diphenylacetone and quinoline-TEMPO were included inside a NaY zeolite (Figure 4-6) and, during intervals of photolysis, fluorescence growth was detected once again. The intensities of the next plots have a different intensity scale because we used an older Perkin Elmer Fluorimeter with a front face sample holder. Zeolites are powders and the emission from the host molecules has to be detected from the diffuse reflection of the beam.

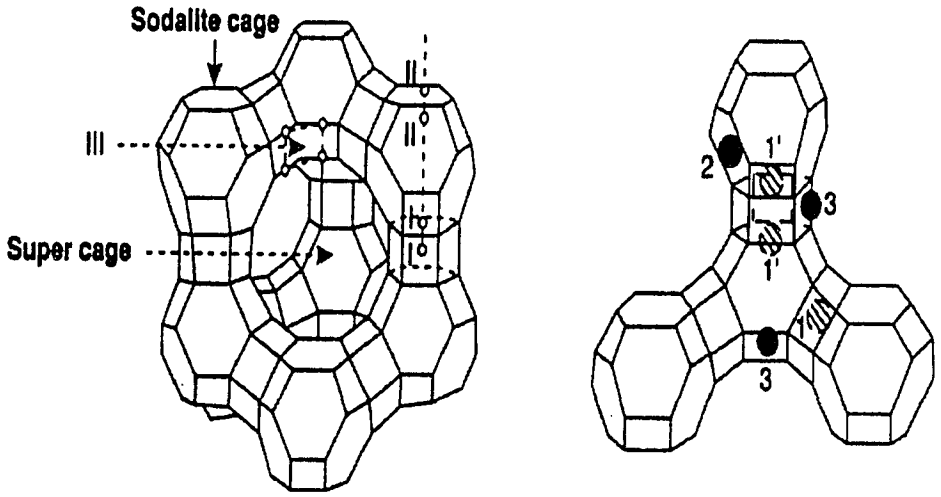

Figure 4-6 NaY zeolite

4.5.1 Results and discussion

The NaY zeolite was activated by heating at 500 °C in order to eliminate all the water present in the polar cavities. DBK was included in the framework by stirring at room temperature an organic suspension of the zeolite. After, quinoline-TEMPO was included by refluxing the suspension for several hours. The use of heat assists the entry of molecules of the probe inside the internal surface; this is an indication of molecular dimensions that are similar to the opening of the windows (7.4 Å) and the size of the supercages (13 Å) of the zeolite. Not all of the guest molecules can insert into the framework, hence it is possible to calculate an occupancy number which describes the average number of molecules per cavity. Considering the fact that NaY zeolites have 0.6 mmol of cavities per gram[69], it is possible to determine the amount of DBK or quinoline-TEMPO that did not enter the zeolite from the filtrate of the organic suspension and therefore the occupancy number(s) can be easily calculated. In the first experiment, the radical initiator and the sensor were incorporated giving occupancy numbers of 0.45 and 0.07. The solid samples were placed in a flat 7 x 3 mm cell and fluorescence spectra were collected with the front detector technique. The samples were irradiated with a 300 nm lamp for 1, 4 and 18 hours. Figure 4-7 shows the growth in fluorescence during photolysis of the sample. The trapping reaction showed an extremely slow rate.

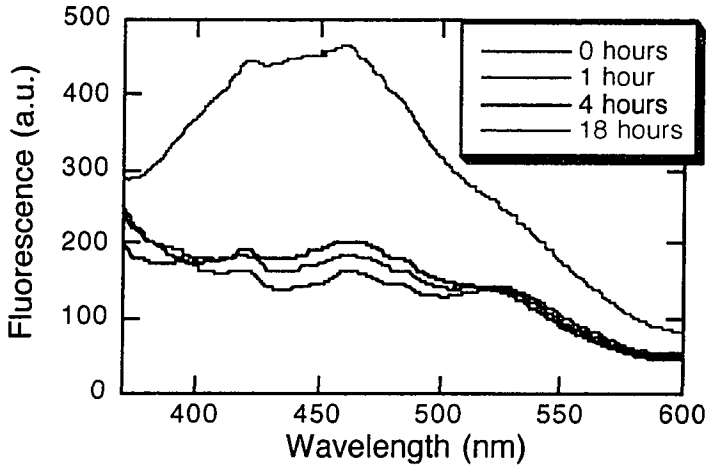

Figure 4-7 Fluorescence growth due to the radical trapping by quinoline-TEMPO of benzyl radical produced by the photolysis at 300 nm of NaY[DBK (s = 0.45, molecule/cavity) and quinoline-TEMPO (s = 0.07)] after 1, 4, 18 hours.

Eighteen hours of irradiation were required to reach a maximum in the fluorescence intensity. This indicated that most of the incident light of irradiation had been scattered by the surface of the zeolite. For this reason we decided to disperse the zeolite powder in polymethylhydrosiloxane (PMHS). In this suspension more light can reach the core of the zeolite producing a more efficient fragmentation of the dibenzyl ketone. DBK and quinoline-TEMPO were included with an occupancy of 0.2 and 0.04, respectively. Quinoline-TEMPO was completely consumed after 150 minutes of irradiation as shown in Figure 4-8.

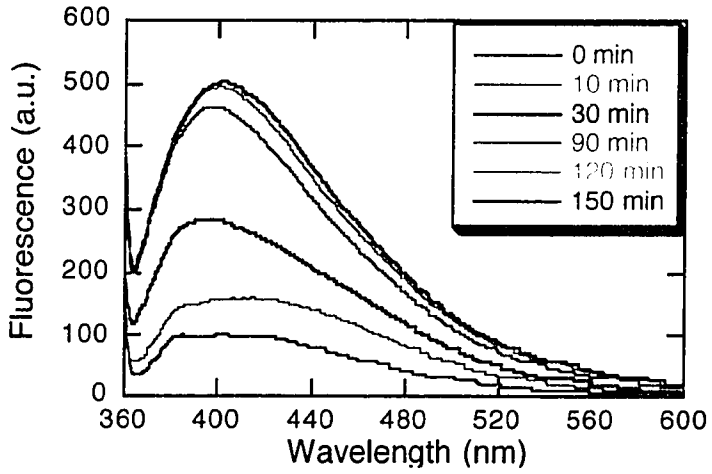

Figure 4-8 Fluorescence growth due to the radical trapping by quinoline-TEMPO of benzyl radicals produced by photolysis at 300 nm of NaY [DBK (s = 0.2, molecule/cavity) and quinoline-TEMPO (s = 0.04)] /polymethylhydrosiloxane suspension after 0, 10, 30, 90, 120, 150 minutes.

The time required to obtain saturation of the signal from the radical sensor has been considerably reduced by the application of this method. This is the result of a lower light scattering by the polymer suspension of zeolite, in comparison with the solid sample. From the results obtained it is not possible to make considerations about cage effects because of the light scattering component for the rate of decomposition of the radical initiator. This was not the main purpose of this application, which was instead to obtain evidence of trapping of the radicals by the probe inside the cavities.

4.5.2 Experimental

NaY zeolite (0.625 g) was activated by heating in an oven at 500 °C for 12 hours. After evaporation of water present in the framework 0.5 g was obtained. DBK was incorporated by stirring 0.5 g of NaY and 0.0315 g DBK in 7 ml of hexane-dichloromethane solution (5:2) at room temperature for 8 hours. The occupancy number **(s)** was calculated from the amount of DBK left in the solution after filtration of the zeolite and after two washings with hexane. The resulting powder was then added to 7 ml of hexane-dichloromethane solution (5:2) containing 0.0224 g of quinoline-TEMPO. The suspension was refluxed at 70 °C for 30 hours. The occupancy number was calculated from the amount of probe left in the solution after filtration and two washings with hexane. The samples were irradiated by one lamp at 300 nm. Fluorescence was detected using a Perkin Elmer fluorimeter LS-50 and the spectra were collected by a front face technique. The solid sample and the PMHS suspension were placed at 45° to the incident light and the line of the detector. The incident beam hits the surface of the sample and reflects to the detector at an angle of 90°.

5 Europium single emission probe. Organometallic nitroxides

5.1 Introduction

Nitroxide based ligands for metal complexation has been obtained in previous years with great attention being given to the possibility that they offer in the building of magnetic molecular objects. The high spin properties of the material synthesized by this approach are usually studied for the temperature dependence of the magnetic susceptibility[70,71]. Recently novel terpyridine-based nitroxide complexes have been synthesized and used as a ligand for transition metals like zinc, copper and nickel[72].

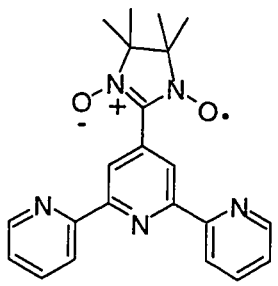

terpy-NIT

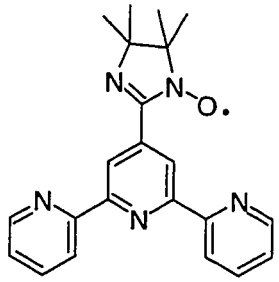

terpy-IM

Scheme 5-1 2-[4′-(2,2′:6′,2″-terlyridyl)]-(4,4,5,5-tetramethylimidazolinyl-3-oxide-1-oxyl (terpy-NIT) and 2-[4′-(2,2′:6′,2″-terlyridyl)]-(4,4,5,5-tetramethylimidazolin-1-oxyl (terpy-IM).

The complexation of the metal occurs through the three nitrogen centers of the tripyridine moiety. A p-pyridyl nitronyl nitroxide has been previously employed for the coordination of a tetraphenylporphinatozinc (II) and the time-resolved electron paramagnetic resonance spectrum has been reported[71]. The nitronyl-nitroxide is the famous Ullman stable free radical[73]. This very stable nitroxide is very easy to prepare and it has also the ability to form metal-nitronyl nitroxide chains as molecular wires[74] complexing through the basic radical group with

acidic metal centers. A similar behavior in the complexation of metals is reported for TEMPO[75]. TEMPO can act as a ligand for metals because it acts as a Lewis base in coordination chemistry.

In this final part of this dissertation a new paramagnetic ligand for metals is presented. Quinoline-TEMPO is a compound with three potential sites for complexation in its structure: the free radical NO group, the nitrogen atom of the aromatic ring and the enolic group between carbon 3 and carbon 5 (Scheme 2-7). This section of the structure is very similar to the tautomeric enolic form of acetylacetonate (2,4-pentadione), which is a very good ligand for the efficient preparation of organometallic compounds (Scheme 5-2).

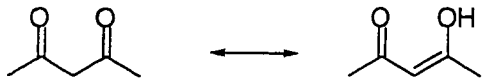

Acetylacetonate (2,4-pentadione) enolic form

Scheme 5-2 Acetylacetonate (2,4-pentadione) keto-enol tautomerism.

The strategy for complexing metal atom centers was directed towards the use of quinoline-TEMPO in the presence of a base and suitable inorganic salt. Deprotonation of the phenolic group activates the enolic form which can then bind to the metal atom forming the metal complex. All the synthetic attempts to obtain the product of complexation have always been directed to find a procedure for the synthesis of crystals that can be analyzed by X-ray crystallography. The paramagnetic properties of quinoline-TEMPO do not allow characterization by NMR spectrometry and this renders other analytical techniques useless when complicated organometallic compounds are analyzed. Quinoline-TEMPO is a molecule with a great tendency to crystallize but in order to obtain X-ray suitable crystals the product has to be isolated in a clean media where it can slowly crystallize.

5.2 The synthetic pathway

The first coupling reactions used were suggested by the literature, with one in particular being the preparation of vanadium (IV) oxy(acetylacetonate) from

vanadyl sulfate, acetylacetonate and sodium carbonate in water[76]. This compound precipitates while gaseous CO_2 is produced and then can be recrystallized from chloroform yielding blue-green crystals. Quinoline-TEMPO is not soluble in water but potassium carbonate is basic enough to abstract the hydrogen from the phenol hydrogen allowing solubilization and formation of the potassium salt. By the addition of vanadyl sulfate to an aqueous solution of quinoline-TEMPO and potassium carbonate, CO_2 was produced with simultaneous precipitation of a green compound. After filtration the product did not show any solubility in most of the organic solvents. For this reason I tried to prepare crystals in situ using a technique of layering two different solvents containing the components of the reaction. Layering 10 ml of water containing 50 mg of quinoline-TEMPO (0.14 mmol) and 21 mg of potassium carbonate (0.15 mmol) and 10 ml of an ethanol solution containing 15 mg of vanadyl sulfate (0.07 mmol) resulted in green crystals being produced at the interface. These crystals could not be resolved by X-ray crystallography due to their low quality. Potassium tert-butoxide was then employed as a base instead of potassium carbonate and nitrates of different metals were tested in layering experiments with water and alcohols as solvents. Several reactions were tested by layering 10 ml of water containing 100 mg of quinoline-TEMPO (0.28 mmol) in a test tube with 31 mg (0.28 mmol) of potassium tert-butoxide, 10 ml of isopropanol and finally 1 ml of ethanol containing 41 mg (0.14 mmol) of nickel nitrate hexahydrate. The intermediate value of the density of ethanol makes the metal salt reach the interface between water and 2-propanol and immediately start a reaction of formation of two products which are both different colors to the starting materials. Quinoline-TEMPO is red and the potassium salt solution is orange, nickel nitrate is an intense green color and at the interface between layers the formation of both a white and a yellow precipitate was observed. After a couple of days the white compound slowly began to sink and the yellow compound had dissolved in the upper isopropanol layer and crystallized in single yellow units. This diffusion in isopropanol of the hypothetical complex occurred also in the case of cobalt nitrate and this observation influenced the use of only isopropanol as a solvent for the reaction. 2-Propanol dissolves nitrates, quinoline-TEMPO and potassium tert-butoxide which through abstraction of a

hydrogen forms tert-butanol. The side product of the reaction (potassium nitrate) is insoluble in isopropanol and this allows, after filtration, to isolate and crystallize the product in a clean media.

5.3 Synthesis

5.3.1 Nickel (II) bis-quinoline-TEMPO(Ni-Q-T)

One half gram of quinoline-TEMPO (1.4 mmol) was dissolved in 200 ml of isopropanol in the presence of 157 mg of potassium tert-butoxide (1.4 mmol). To this solution 203 mg of $Ni(NO_3)_2.6H_2O$ (0.7 mmol) was added resulting in the immediate formation and precipitation of KNO_3. After filtration of a quantitative amount of potassium nitrate (140 mg) the isopropanol solution was evaporated until saturation occured. After four days yellow crystals were obtained. IR (KBr, cm^{-1}) : 3631 (w), 3374 (mb), 2975 (m), 2935 (m), 1632 (s), 1604 (m), 1544 (w), 1469 (m), 1416 (m), 1366 (m), 1330 (s), 1299 (s), 1241 (w), 1208 (s), 1178 (m), 1152 (s), 1043 (w), 1017 (w), 1000 (w), 979 (w), 958 (w), 896 (w), 875 (w), 804 (w), 769 (m), 748 (w), 680 (w), 564 (w). E.A. : C 58.21 %, H 7.64 %, N 6.07 %, O 16.79, Ni 5.62 %.

5.3.2 Cobalt (II) bis-quinoline-TEMPO (Co-Q-T)

One half gram of quinoline-TEMPO (1.4 mmol) was dissolved in 200 ml of isopropanol in the presence of 157 mg of potassium tert-butoxide (1.4 mmol). To this solution 204 mg of $Co(NO_3)_2.6H_2O$ (0.7 mmol) was added resulting in the immediate formation and precipitation of KNO_3. After filtration of a quantitative amount of potassium nitrate (140 mg) the isopropanol solution was evaporated until saturation occured. After four days dark red crystals were obtained. IR (KBr, cm^{-1}): 3633 (w), 3376 (mb), 2975 (m), 2935 (w), 1633 (s), 1606 (m), 1459 (m), 1414 (m), 1366 (m), 1331 (m), 1300 (m), 1242 (w), 1208 (s), 1178 (m), 1152 (s), 1016 (w), 1001 (w), 979 (w), 961 (w), 896 (w), 874 (w), 769 (m), 748 (w), 680 (w), 645 (w), 562 (w). E.A. : C 55.66 %, H 7.21 %, N 5.79 %, O 18.13 %, Co 5.83 %.

5.3.3 Europium (III) potassium tetra-quinoline-TEMPO (Eu-Q-T)

One half gram of quinoline-TEMPO (1.4 mmol) was dissolved in 200 ml of isopropanol in the presence of 157 mg of potassium tert-butoxide (1.4 mmol). To

this solution 118 mg of $Eu(NO_3)_3.6H_2O$ (0.35 mmol) was added with consequent precipitation of potassium nitrate. In this reaction only 90 mg (0.9 mmol) of potassium nitrate was obtained after filtration and this is indicative that some potassium atoms are contained in the complex. After evaporation of the solvent the orange compound was dissolved in acetonitrile and after 2 days, orange crystals were obtained. IR (KBr, cm^{-1}) : 3614 (w), 3378 (mb), 3937 (m), 1648 (s), 1548 (w0, 1434 (s), 1364 (m), 1334 (m), 1307 (m), 1252 (w), 1243 (w), 1208 (s), 1178 (m), 1153 9s0, 998 (w), 976 (w), 963 (w), 898 (w), 805 (w), 768 (m), 751 (w) 718 (w), 704 (w), 678 (w), 643 (w), 561 (w). E.A. : C 58.28 %, H 6.49 %, N 8.26 %, O 13.99 %, K 2.0 %.

5.3.4 Lantanum (III) potassium tetra-quinoline-TEMPO (La-Q-T)

One half gram of quinoline-TEMPO (1.4 mmol) was dissolved in 200 ml of isopropanol in the presence of 157 mg of potassium tert-butoxide (1.4 mmol). To this solution 151 mg of $La(NO_3)_3.6H_2O$ (0.35 mmol) was added with consequent precipitation of potassium nitrate. In this reaction only 90 mg (0.9 mmol) of potassium nitrate was obtained after filtration. After evaporation of the solvent the red-orange compound was dissolved in acetonitrile and after 2 days orange crystals were obtained IR (KBr, cm^{-1}) : 3411 (mb), 2975 (m), 2936 (m), 1649 (s), 1607 (m), 1546 (w0, 1431 (s), 1364 (m), 1333 (m), 1301 (m), 1178 (s), 1150 (s), 1016 (w), 1000 (w), 981 (w), 805 (w), 765 (m), 746 (w), 719 (w), 705 (w), 679 (w), 643 (w), 560 (w),476 (m). E.A. : C 57.15 %, H 7.05 %, N 6.10 %, O 13.99 %, K 3.03 %, La 0.08 %.

5.4 Crystal structures

5.4.1 Nickel (II) bis-quinoline-TEMPO

Nickel (II) bis-quinoline-TEMPO is monomeric with Ni having an octahedral geometry defined by two molecules of quinoline-TEMPO and two molecule of isopropanol. Each paramagnetic ligand chelates the central metal by two oxygen atoms. The oxygen-metal bond lengths for the two oxygen atoms in quinoline-TEMPO are respectively Ni (1) – O (1) = 1.9773 (17) Å and Ni (1) – O (2) = 2.0438

(18) Å with the angle O (1) – Ni – O (2) = 86.01° (17). The octahedral coordination geometry is completed by two molecules of isopropanol having bond lengths with the metal center Ni (1) – O (1A) = 2.039 (4) Å and Ni (1) – O (1B) = 2.0941 (13) Å and bond angles O (1A) – Ni (1) – O (1D) = 92.24° (15). The cordination geometry is slightly distorted with bond angles which are not perfectly at 90°. The crystal lattice contains an additional molecule of isopropanol which is not connected to the organometallic complex structure. Selected bond lengths and angles are reported in Table VI in the Appendix.

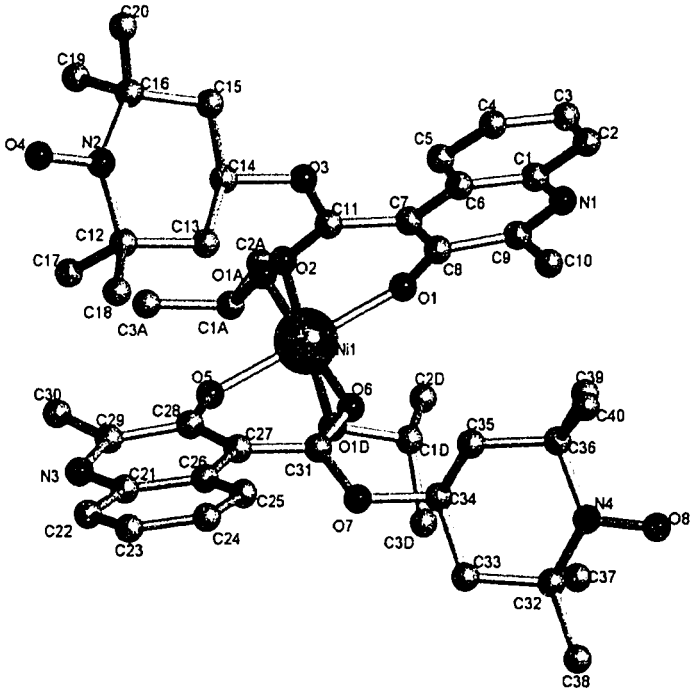

Figure 5-1 Crystal structure of nickel (II) bis-quinoline-TEMPO.

5.4.2 Cobalt (II) bis-quinoline-TEMPO

Cobalt (II) bis-quinoline-TEMPO and nickel (II) bis-quinoline-TEMPO have coordination-equal structures. Selected bond lengths and angles are reported in Table VI in the Appendix.

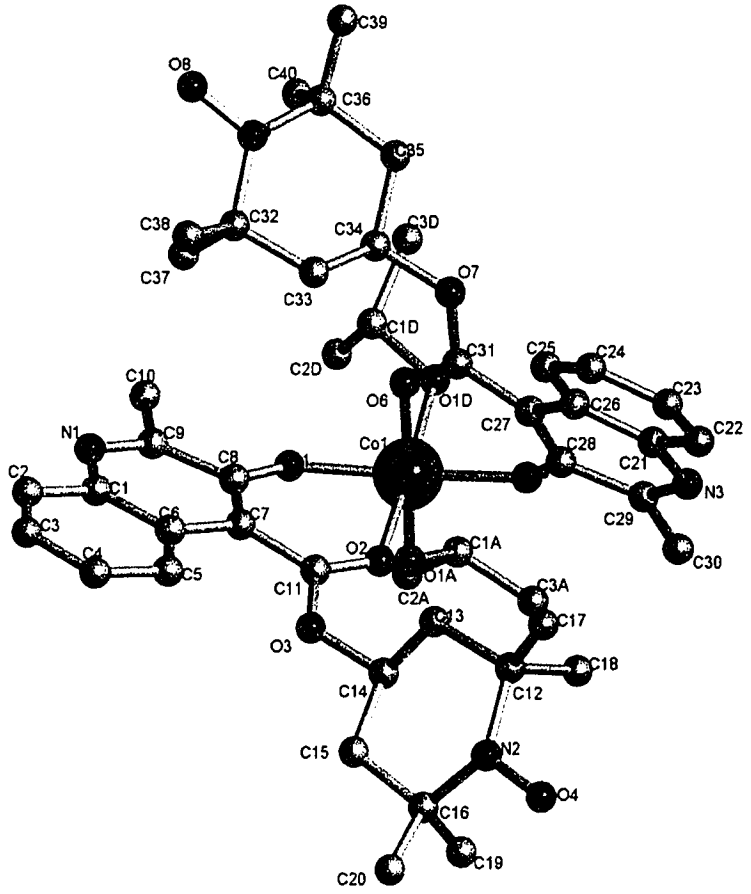

Figure 5-2 Crystal structure of cobalt (II) bis-quinoline-TEMPO.

5.4.3 Europium (III) potassium tetra-quinoline-TEMPO

The crystal structure of europium (III) potassium tetra-quinoline-TEMPO is a linear polymer composed of tetra-quinoline-TEMPO monomers bridged by potassium atoms. Selected bond lengths and angles are reported in Table VIII in the Appendix. Each quinoline-TEMPO chelates the trivalent lanthanide metal with two oxygen atoms as shown in Figure 5-3. The bond lengths are Eu (1) – O (1) = 2.303 (3) Å and Eu (1) – O (2) = 2.476 (3) Å and the angle is O (1) – Eu (1) – O (2) = 69.53°. Europium has square antiprism symmetry. The monomer of the polymer, as shown in Figure 5-4, it is composed by four quinoline-TEMPO ligands. Two moieties of the aromatic quinoline system are positioned anti-parallely to each other and in front of other two molecules of ligand. The central metal posses a 222 symmetry composed of 3 perpendicular two-fold axis. Four

oxygens of the two ligands on top and four oxygens of the two ligands on the bottom create two approximate squares twisted at 45° with respect to each other.

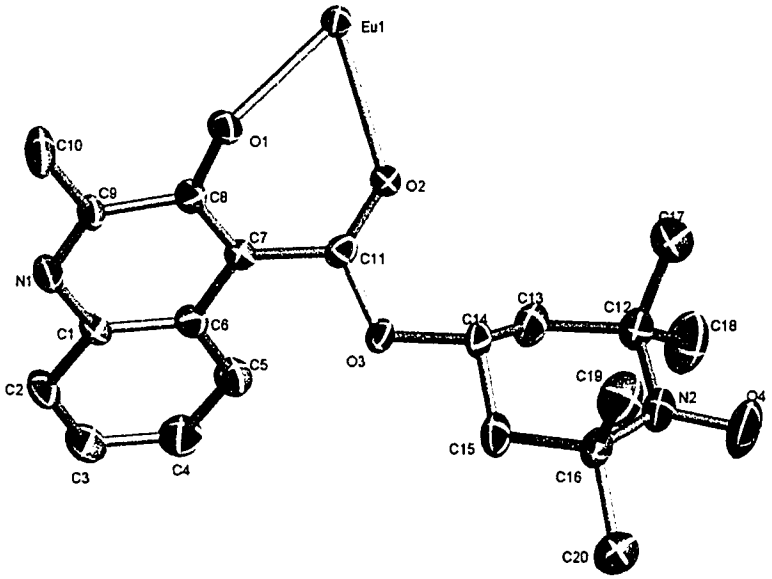

Figure 5-3 Crystal structure of the ligand-metal part of europium (III) potassium tetra-quinoline-TEMPO.

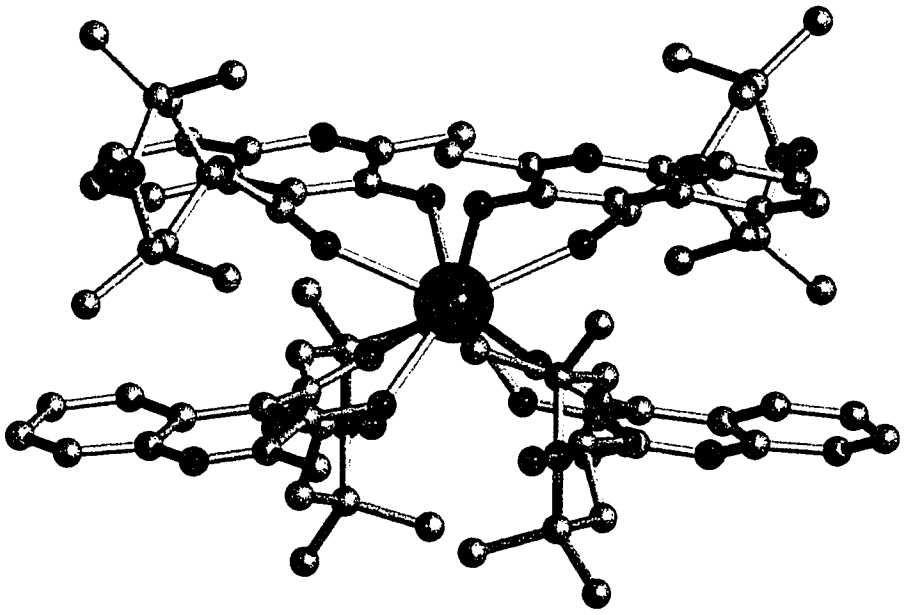

Figure 5-4 Crystal structure of the monomer tetra-quinoline-TEMPO in the europium (III) potassium tetra-quinoline-TEMPO polymer.

One potassium atom, disordered in three positions, bridges two monomer units in the polymer. In Figure 5-5 a section of the polymer structure is shown in

which two of the possible positions for the potassium atom are shown. Two molecules of acetonitrile and two molecules of water are coordinated to K.

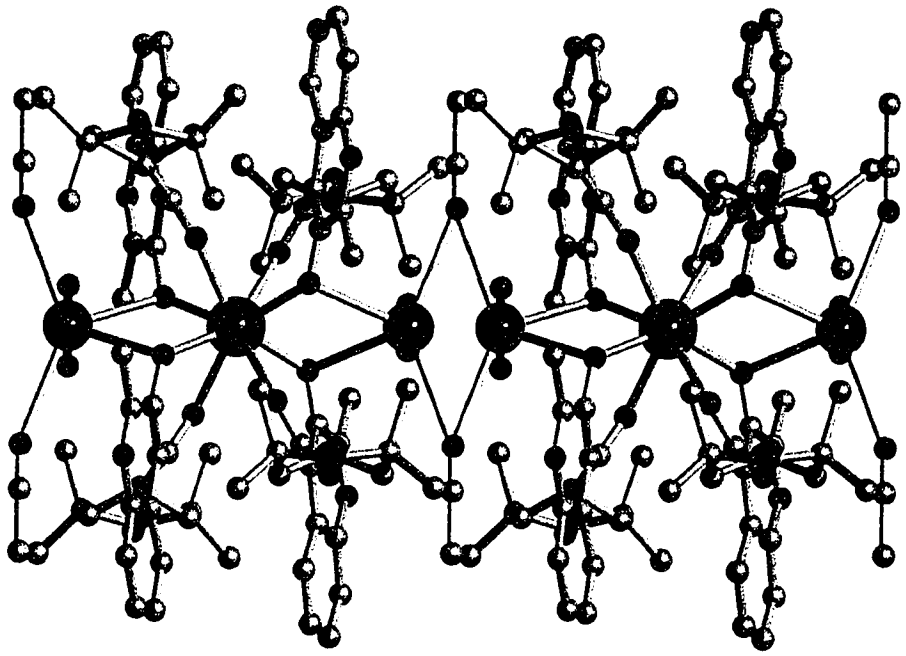

Figure 5-5 Crystal structure of the polymer europium (III) potassium tetra-quinoline-TEMPO.

5.5 Detection of the 2-cyano-e-propyl radical at 613 nm by europium (III) potassium tetra-quinoline-TEMPO

5.5.1 Introduction of energy transfer to the europium metal centre

Lantanides belong to the rare earth family of metals. They have attracted a lot of attention due to the *f-f* transitions that have been observed which, when the excited state is long-lived, cause metal-centered luminescence. Quantum yields of fluorescence are present in solution and in solid state for lanthanides[77]. The observation that enhancement of the luminescence of rare earth metals occurs in aqueous solutions by substituting the water by heavy water led to the conclusion that highly energetic vibrations of the OH groups were causing a deactivation of the *f-f* transitions[78,79]. From this point the conclusion that protection of the metal center from water molecules in solution would have brought an enhancement of the emission became a principle for the development of several applications in

biology and medicine[80,81] (fluoroimmunoassay and protein labeling). Some of the ions, in particular Eu^{3+} and Tb^{3+}, have shown long-lived excited states and intense emission and they have found applications in the fabrication of lasers[82], in phosphors for fluorescent lamps[83] or in electrochemiluminescent systems[84,85] for colour displays and for optical amplifiers. Several organometalic compounds have been reported as edifices for the encapsulation of the metal[86-88] and an "antenna effect" has been shown to be responsible for the emission from the metal center. Luminescent lanthanide β-diketonates are present in the literature[89,90] and recent interest is driven by their application as light-converting molecular devices. Energy transfer between the excited ligand molecule and the long-lived excited state of Eu^{3+} is one of the mechanisms of deactivation of the excited state of the ligand as shown in Figure 5-6, leading to luminescence from the europium center. The other deactivation pathways can be attributed to radiative and non-radiative processes from the excited states of the ligand and to low-lying ligand-to-metal charge transfer processes[91] (LMCT). The system cannot be considered as a result of interaction between one donor in its excited state and one acceptor in the ground state. Multiple interactions between ligands and the metal center occur during the deactivation process.

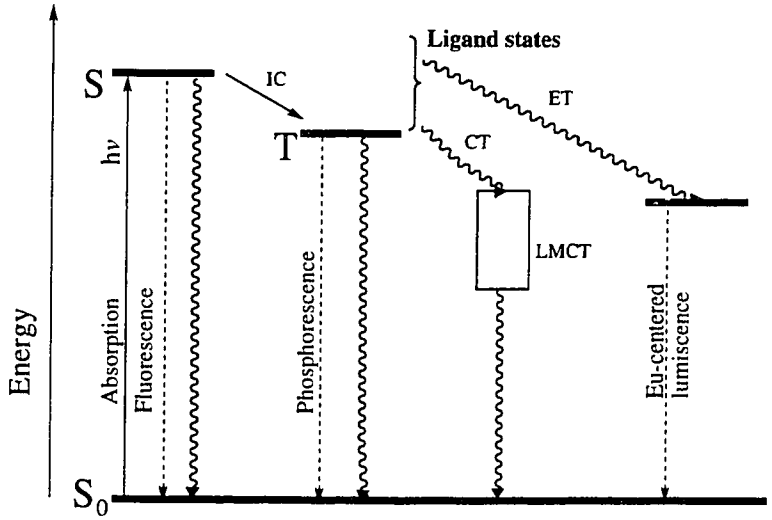

Figure 5-6 Jablonski diagram for the deactivation pathway of an organometallic lanthanide complex. IC intersystem crossing, CT charge transfer, LMCT ligand metal charge transfer.

5.5.2 *Results and discussion*

5.5.2.1 Absorption and emission of europium (III) potassium tetra-quinoline-TEMPO

The europium complex presented in this thesis has a deactivation pathway similar to the one described above in addition to the channel of intramolecular quenching of the excited states of the ligand due to the presence of the nitroxide moiety. The emission spectrum of Eu-Q-T in acetonitrile, exciting at 350 nm, showed two emissions bands . One due to the fluorescence of quinoline-TEMPO with a maximum at ~400 nm and and the other is a sharp peak at 613 nm which is easily attributed to the europium-centered fluorescence emission (Figure 5-7).

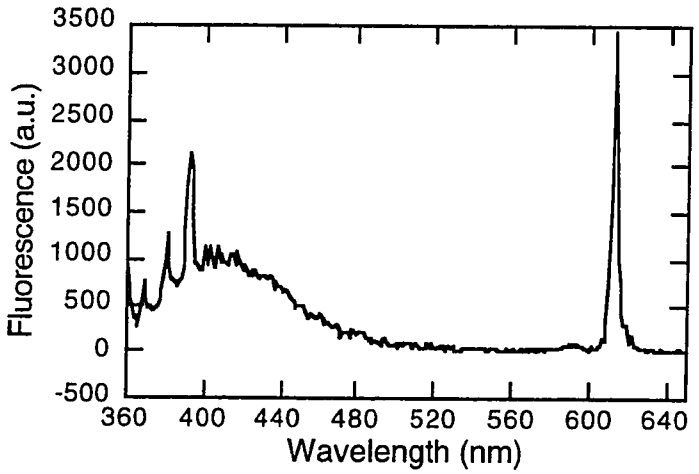

Figure 5-7 Fluorescence spectrum of europium (III) potassium tetra-quinoline-TEMPO (5×10^{-6} M , Abs < 0.1) in acetonitrile. λ_{ex} 350 nm.

The absorption spectrum in acetonitrile of the complex Eu-Q-T shows a shift to longer wavelengths with respect to the spectrum of the ligand in the same solvent (Figure 5-8). This is attributed to the fixation of the chelating group in a rigid conformation. The increased conjugation of the aromatic ring with the enolic part of the structure shifts the absorption to little more than 20 nm.

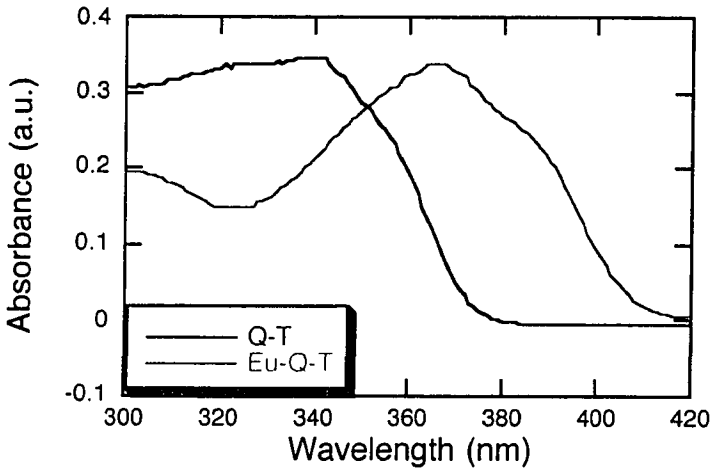

Figure 5-8 Absorption spectrum of europium (III) potassium tetra-quinoline-TEMPO (0.0216 mM) and quinoline-TEMPO (0.065 mM) in acetonitrile.

The extinction coefficients for Eu-Q-T, quinoline-TEMPO and Q-TAIBN at 350 nm, 370 nm and 385 nm are shown in Table 5-1.

	ε_{350} M^{-1} cm^{-1}	ε_{370} M^{-1} cm^{-1}	ε_{385} M^{-1} cm^{-1}
Eu-Q-T	14817	19847	15043
Quinoline-TEMPO	5070	< 50	< 50
Q-TAIBN	2981	< 50	< 50

Table 5-1 Extinction coefficients in acetonitrile of Eu-Q-T at 350, 370, 385 nm and quinoline-TEMPO and Q-TAIBN at 350 nm.

It is noticed that four times the value of ε_{350} for quinoline-TEMPO (5070 M^{-1} cm^{-1}) is more or less equal to the value of ε_{370} for the complex (19847 M^{-1} cm^{-1}). The complexation of europium metal did not change the capacity of the ligand to absorb light at its maximum band of absorption. Q-TAIBN has an absorption spectrum similar to the absorption spectrum of quinoline-TEMPO with the only difference being a smaller value of the extinction coefficient.

5.5.2.2 Fluorescent emission monitored at 400 nm and 613 nm

If we consider that the absorption of Q-TAIBN does not differ in position to the spectrum of quinoline-TEMPO we can also deduce that the resulting

hypothetical product from the reaction of the 2-cyano-2-propyl radical with Eu-Q-T will be maintained during the consecutive trapping of all four nitroxide groups (4 per molecule) giving a shifted absorption. This allows us to follow the course of the reaction by fluorescence detection from a dynamic point of view. The red emission became a useful monitoring tool, having a certain specification in the presence of the complexed form in solution. Decomplexation during the reaction results in the release of quinoline-TEMPO free molecules and europium free ions leading to a decrease of the europium-centered emission due to disappearance of the "antenna effect". The emission from the ligand cannot be affected by destruction of the structure if the excitation wavelength is fixed at 350 nm or 370 nm because both the ligand and the complex absorbs but it is a useful information if the excitation wavelength is set at 385 nm, as only the complex absorbs at this wavelength. The kinetics of radical trapping of carbon-centered radicals generated by decomposition of AIBN (1 mM) at 60 °C in the presence of Eu-Q-T (5×10^{-6} M) in acetonitrile were followed, in each experiment varying the excitation and emission wavelengths (λ_{ex} 350, 370, 385 nm; λ_{em} 400, 613 nm). The samples were prepared in the same way as described for the use of quinoline-TEMPO with AIBN as radical initiator (Chapter 3.4.1). In Figure 5-9 the fluorescence growth monitored at 400 nm is shown employing excitation wavelengths of 350 nm and 370 nm. In both cases the fluorescence emission increases gradually. This observation could suggest the formation of the lanthanide complex in which all four nitroxides traps have been coupled with a carbon-centered radical by formation of a sigma bond. The wavelength of excitation was then moved to 385 nm where only the complex can absorb. In Figure 5-10 the fluorescence emission at 400 nm during the reaction is shown with an excitation wavelength fixed at 385 nm. Fluorescence reaches a maximum intensity at around 4600 seconds and then decreases to a minimum value at around 8000 seconds.

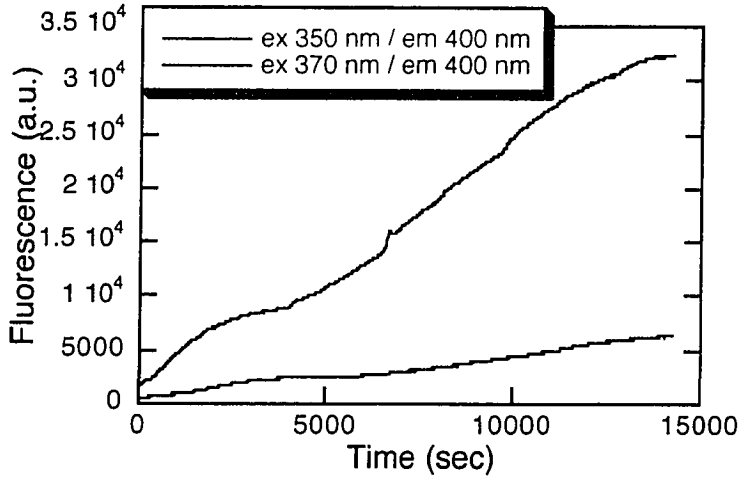

Figure 5-9 Fluorescence growth due to the scavenging of the 2-cyano-2-propyl radical by Eu-Q-T (5 x 10^{-6} M) in acetonitrile at T = 60 °C under a nitrogen atmosphere. AIBN concentration 1 mM. λ_{ex} 350, 370 nm ; λ_{em} 400 nm.

This is the first indication that during this reaction of radical coupling, decomplexation can occur. After the minimum is reached fluorescence grows again but at this point of the reaction the reaction system has become too complicated to be rationalized.

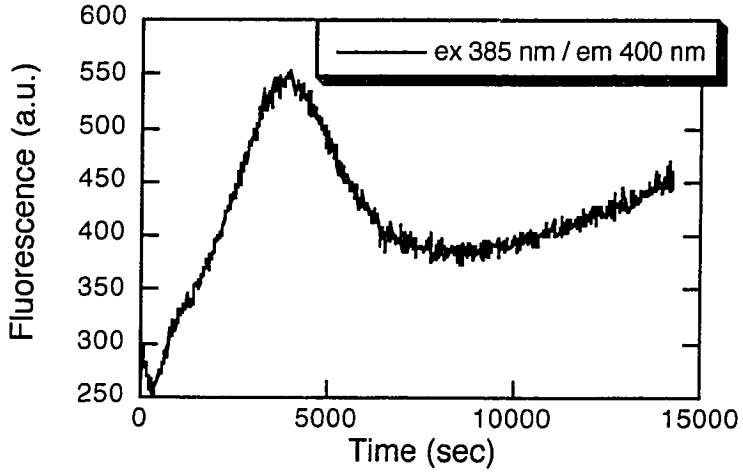

Figure 5-10 Fluorescence growth due to the scavenging of the 2-cyano-2-propyl radical by Eu-Q-T (0.025 mM) in acetonitrile at T = 60 °C under a nitrogen atmosphere. AIBN concentration 1 mM. λ_{ex} 385 nm ; λ_{em} 400 nm.

Similar behavior was observed for fluorescence emission monitored at 613 nm with the excitation wavelengths fixed at 350 nm and 370 nm (Figure 5-11). Prior to 5000 seconds, the intensity reaches a maximum and then starts decreasing until the signal is reset.

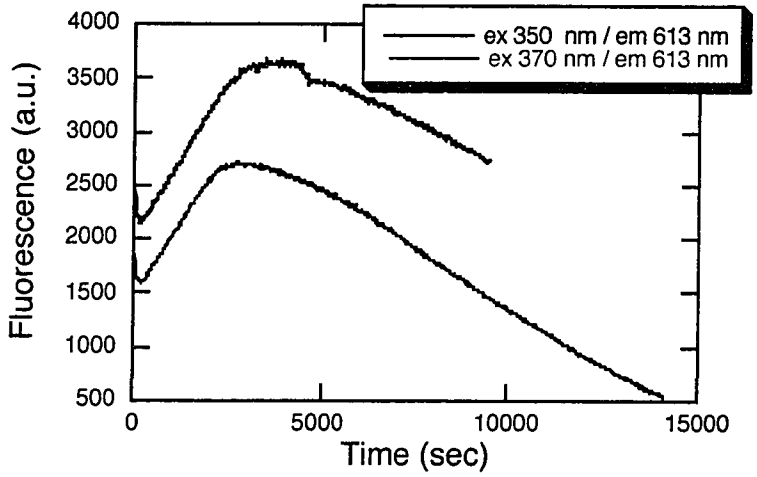

Figure 5-11 Fluorescence growth due to the scavenging of the 2-cyano-2-propyl radical by Eu-Q-T (0.025 mM) in acetonitrile at T = 60 °C under a nitrogen atmosphere. AIBN concentration 1 mM. λ_{ex} 350, 370 nm ; λ_{em} 613 nm.

This also supports the fact that Eu-Q-T is able to trap a carbon-centered radical with the structure of the complex remaining intact for an initial phase in the reaction. For the remaining time, every trapping event with a nitroxide group becomes a dissociation event of a molecule of the ligand from the europium-centered metal. Figure 5-12 shows three emission spectra at three different moments of the reaction with an excitation wavelength at 350 nm.

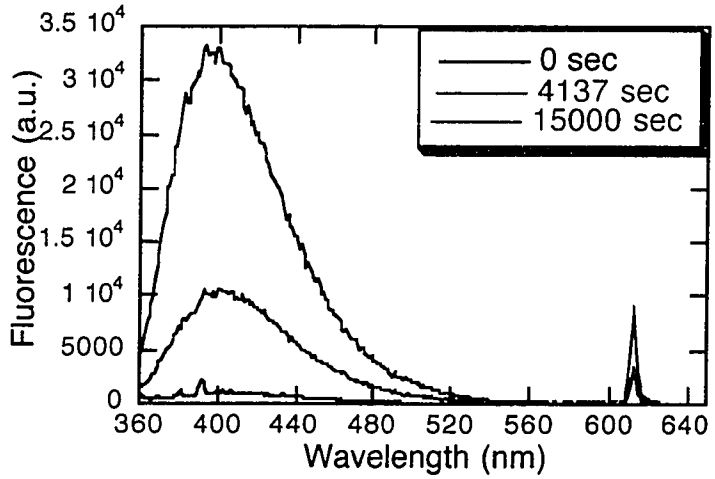

Figure 5-12 Fluorescence emission spectra of the reaction between AIBN (1 mM) radical initiator and Eu-Q-T (5 x 10^{-6} M) at 60 °C under a nitrogen atmosphere at 0, 4137 and 15000 seconds. λ_{ex} 350 nm.

The fluorescence increases due to the emission from quinoline-TEMPO and the metal for more than 4000 seconds but after a period of time the emission from the encapsulated europium starts decreasing until complete disappearance is achieved at the end of the reaction.

5.5.2.3 UV absorption dynamics of the reaction

In order to understand more about what is happening inside the system the reaction was followed using a UV spectrophotometer. The reaction conditions were the same as for the experiments of fluorescent detection of carbon-centered radicals produced by the thermal decomposition of AIBN.

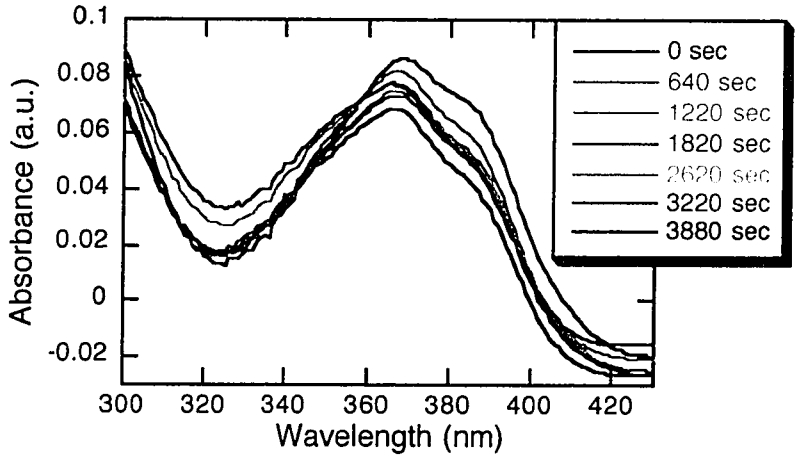

Figure 5-13 Absorption spectra of the reaction between AIBN (1 mM) and Eu-Q-T (5 x 10^{-6} M) at 60 °C under a nitrogen atmosphere. The scans were collected between 0 and 4000 seconds.

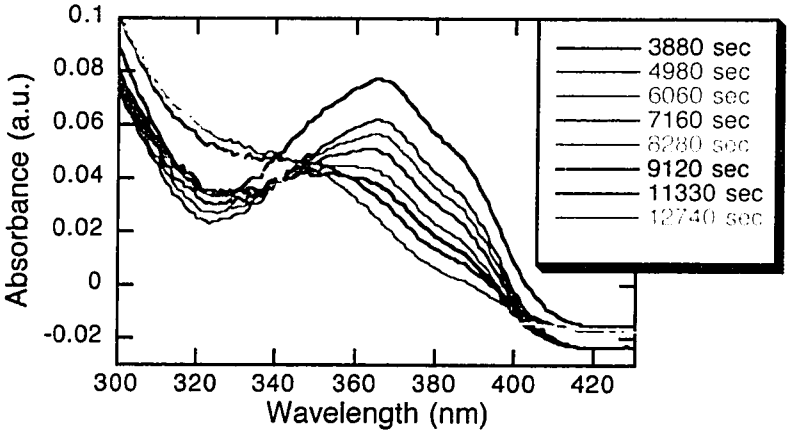

Figure 5-14 Absorption spectra of the reaction between AIBN (1 mM) and Eu-Q-T (5 x 10^{-6} M) at 60 °C under a nitrogen atmosphere. Scans collected between 4000 and 17000 seconds.

Figure 5-13 and Figure 5-14 show the evolution of the total absorbance of the reaction in two phases of the reaction. From zero to 4000 seconds, the absorption decreases a little in the first phase and then oscillates between similar values. In the second phase, from 4000 seconds to 17000 seconds, the absorption considerably decreases until it is possible to observe the disappearance of the band between 370 nm and 410 nm. This observation is consistent with the proposed mechanism of the reaction in which radical trapping by the Eu-Q-T occurs in the first part of the reaction. Coupling then with a radical occurs resulting in the ligand and the metal being released from the complex.

5.5.3 Conclusions

Complexation of metals employing quinoline-TEMPO as a ligand has been shown to be an efficient process to prepare organometallic probes for carbon-centered radicals. The testing reaction with one of the four sensors described in this chapter allows the detection of radicals by monitoring fluorescence from the ligand and from the metal center of the molecule. The trapping reaction of 2-cyano-2-propyl radicals produced by thermolysis at 60 °C of AIBN 1 mM was successfully monitored at 400 nm and 613 nm and the behavior of the intensities of emission was investigated by varying the excitation wavelengths from a part of the spectrum where the free ligand in solution absorbs to wavelengths at which only the complex can absorb. Scheme 5-3 represents the conclusion obtained from this study. In the first phase of the reaction of radical trapping the organometallic paramagnetic compound Eu-Q-T scavenges a radical by one of the four nitroxide switches present in the molecule. All trapping events then lead to the decomposition of the complex with consequent releasing of fluorescent molecules of Q-TAIBN and metal ions. The other organometallic pre-fluorescence probes prepared in this work did not show any metal-centered emission and investigation of their reactions of radical trapping were not investigated because of the difficulty in following the mechanistic dynamics of the reaction.

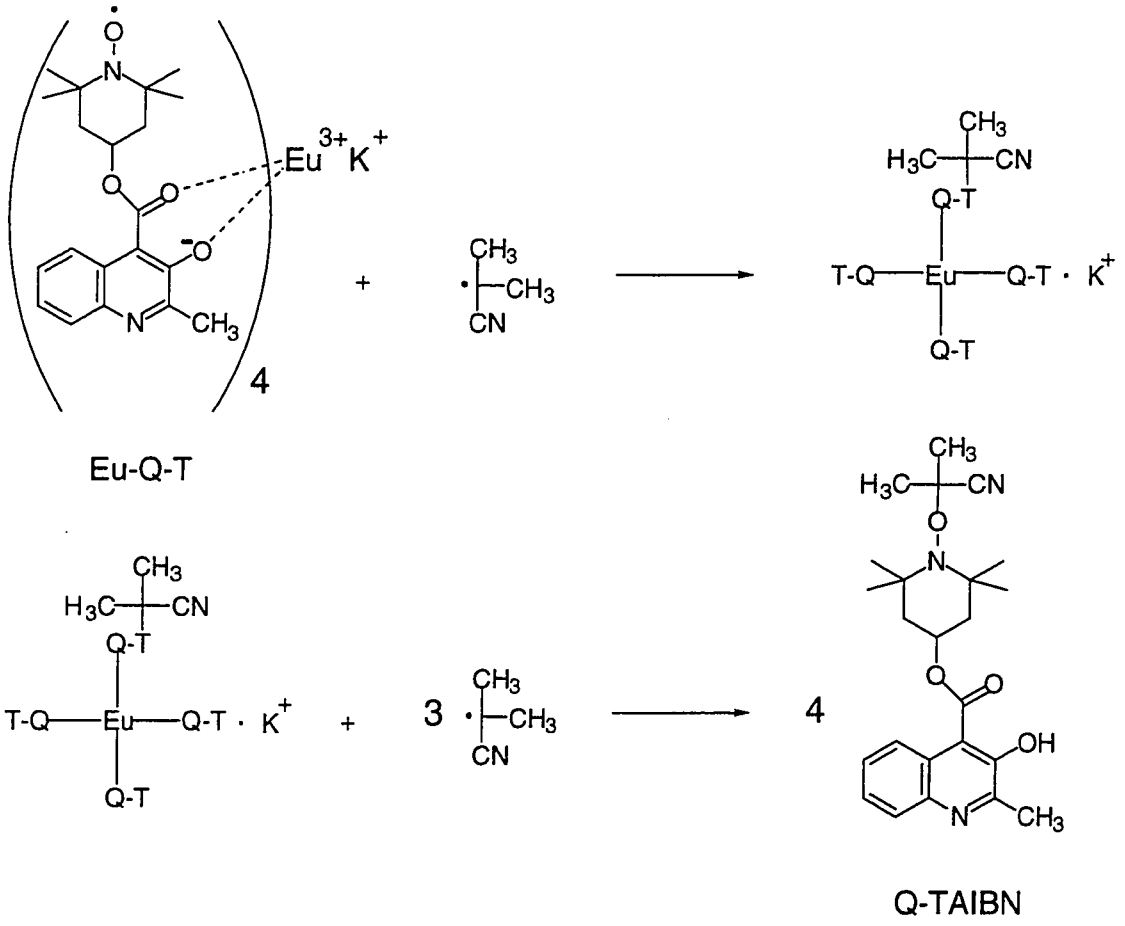

Scheme 5-3 Reaction showing the proposed mechanism of the radical trapping of the 2-cyano-2-propyl radical produced by thermal decomposition at 60 °C of AIBN in presence of Eu-Q-T.

Preliminary results confirm this mechanism, although a complete understanding of the process can only be reached by analyzing the products of the reaction of Eu-Q-T with AIBN. A preparative reaction, as described in Chapter 3.3.1.1 for the preparation of Q-TAIBN, will elucidate how radical chemistry interacts with this organometallic paramagnetic complex. In order to evaluate the electron exchange component of the quenching of the metal-centered fluorescence emission by the nitroxide moieties the complex Eu-Q-TAIBN could be prepared employing Q-TAIBN as a ligand for Eu^{3+}. This will lead to a fluorescent material with higher fluorescence quantum yield than the paramagnetic analogous.

6 Final comments and future directions

6.1 Conclusions

It is known that carbon-centered radicals are important intermediates in chemical and biochemical processes. Detection of these transients have been accomplished with several different spectroscopic techniques. The observation that nitroxide stable free radicals quench fluorescence emission from a fluorophore led to the development of sensors which can be applied to investigate the production and the behavior of radical intermediates in biological and artificial model systems. TEMPO and PROXYL stable free radicals have been used by the scientific community to fabricate pre-fluorescent probes for radicals. The nitroxide group with its unpaired electron acts as a fluorescence switch "off" when tethered to a fluorophore through a covalent chemical bond. This switch can then be tunned to the "on" mode by a coupling reaction with a radical through the formation of a sigma bond.

An important application has been achived employing a fluoresciamine-nitroxide adduct to quantify hydrodryl radicals production rates in biological systems. Hydroxyl radicals are strong oxidant species which are thought to be generated within cells and tissues where they can attack lipids, proteins and DNA molecules producing irreparable cellular damage. Detection of oxygen-centered radicals occurs in this case in an indirect way. This method employs the reaction between hydroxyl radicals and dimethyl sulfoxide to produce methyl radicals quantitatively, which are trapped by nitroxide moieties. Fluoresciamine-PROXYL and acridine-TEMPO adducts are presently supplied to the scientific community by Molecular Probes, and eventually new pre-fluorescent probes will soon be proposed. Development of new pre-fluorescent probes will lead to the imaging of radical chemical processes within complex and environmental matrices.

The work presented in this thesis all relates to the fluorescence detection of radicals and it has been demostrated the applicability of new pre-fluorescent probes to heterogenous and supramolecular systems such as zeolites, micelles or systems used in the field of free radical polymerization. In comparison with other spectroscopic techniques the fluorescence detection of radicals has greater sensitivity allowing detection of radicals in concentrations of 10^{-6}-10^{-7} M. This methodology does not require isolation of products because only radical chemistry is involved in the process. Fluorescence growth occurs due to the radical trapping reaction by the nitroxide group and it can be considered to be the only process responsible for the switching "on" of the probe. This allows easier investigation of radical processes in heterogenous systems where detection of radical transients by other spectroscopic techniques results difficult.

Carbon-centered radicals produced by thermal and photoinduced decomposition of radical initiators have been detected by fluorescence spectroscopy employing coumarin-TEMPO and quinoline-TEMPO pre-fluorescent nitroxide switches. The kinetics of radical scavenging in homogenous solutions depends on the number of radicals produced in the system. The concentrations of both sensor and radical initiator have been optimized to find the best conditions for the use of fluorescence spectroscopy as an analytical tool. It has been shown that at the excitation wavelength it is required for the sensor an absorbance value in the range 0.1-0.2 (a.u.). In the fluorescence detection of radicals produced by radical photoinitiation it has been shown that the radical initiator has to absorb photons predominantly without competing for photons with the sensor at the excitation wavelength. The use of only one lamp for these experiments has allowed monitoring the complete consumption of the probe and thus degradation of the coupled-product of trapping. Quinoline-TEMPO requires a protecting shield from the radical initiator because it tolerates only a small amount of irradiation light.

The probes synthesized in the present work have been applied to different systems. A novel methodology has been developed employing coumarin-TEMPO as pre-fluorescent sensor to determine the absolute kinetics for end-cap cleavage in TEMPO-capped polystyrene obtained by "living" free radical polymerization. Quinoline-TEMPO has been used to trap benzyl radicals

produced by photolysis of the symmetric ketone 1,3-diphenylacetone in supramolecular systems. Micelles and NaY zeolites have been used in order to encapsulate the sensor and the radical initiator in a constrained environment thus preventing quick separation of the radical pairs in random radicals. In the first case the slow reactivity of benzyl radicals with quinoline-TEMPO with respect to homogenous solutions shows evidence for "cage effects" inside the micellar system. Fluorescence radical detection has been observed from solid samples of NaY zeolites containing both the radical trap and the radical initiator. During photolysis light scattering considerably increased the time required to saturate the probe signal. For this reason a polymer dispersion of the aluminosilicate powder was prepared to increase the incident light reaching cavities in the framework. Biradicals produced by photodecomposition of cyclic ketones were trapped by quinoline-TEMPO. The kinetic study of radical trapping reaction suggests that the sensor is a good candidate for a better understanding of these intermediates if molecules with various aliphatic tail lengths are tested in this reaction.

Finally quinoline-TEMPO has been shown to be a very good paramagnetic ligand for metals. The europium (III) potassium tetra-quinoline-TEMPO has shown an "antenna effect" after excitation of the ligand moiety leading to a sharp emission in the red region of the visible spectrum due to the metal center. The behavior of the fluorescence emission bands from the ligand and from the metal have been monitored during the course of the radical trapping reaction of the 2-cyano-2-propyl radical. It has been shown that the decomposition of the organometallic structure occurs due to radical coupling of the nitroxide group leading to the formation of free molecules of the diamagnetic coupled product of the ligand.

6.2 Future directions

Other members of the research group have used quinoline-TEMPO and some of the systems for these applications are presently under investigation. Dr. Olga Garcia Ballesteros has employed the pre-fluorescent radical sensor to trap carbon-centered radicals in a poly-methyl methacrylate film. These radicals are

produced by the thermal decomposition of 2,2'-azobisbutyronitrile and by the photodecomposition of 1,3-diphenylacetone. The experiments of the thermal decomposition of the radical initiator were performed at different temperatures between 80 °C and 100 °C, and they all showed that the rate of fluorescence evolution increased as the temperatute of the reaction was increased, as expected. The main objective of this research project was to obtain photoimaging after irradiation based on the different fluorescence emission between the irradiated and non-irradiated areas. The polymeric films were irradiated through a standard resolution mask by using a high-performance collimated UV-light source system LS-60 series. The standard mask presents different sizes between lines and spaces and photoimaging of the polymer film has been achieved with resolution masks between 1 μm and 55 μm.

The behavior of bisbenzyl biradicals will be studied employing [3,n]paracyclophan-2-ones with different chain lengths and quinoline-TEMPO as the pre-fluorescent probe. In particular, two cyclic ketones with n = 2 and n = 4 will be prepared and analyzed by fluorescence spectroscopy in the reaction of photodecomposition in presence of the nitroxide switch. The radical trapping reactions, which are in competition with the self-quenching of the biradical intermediates due to the intersystem crossing mechanism of the triplet biradical to a singlet biradical leading to the decarbonylated cyclophane product, will give different kinetics. Rationalization of the results will give further information about these intermediates.

Fluorescence detection of carbon-centered radicals in micelles introduces the possibility of using pre-fluorescent probes to monitor the production of radicals and their permeability through the micellar system. Micelles are the simplest model for membranes and quinoline-TEMPO has shown the potential to monitor carbon-centered radicals produced within the micellar environment. Radicals could also be produced outside these aggregates by decomposition of water soluble radical initiators. Diffusion of radicals through the polar edges of micellar aggregates would result in them being intercepted by quinoline-TEMPO allowing fluorescence detection. Bilayer aggregates called liposomes could also

be prepared containing the sensor. Water-soluble radical initiators could be encapsulated in the core of the liposome or left in the external acqueous phase. Decomposition of the radical initiator will produce radicals which are now free to either recombine or to experience diffusion from both the inside of the bilayer to the outside and reverse. The presence of quinoline-TEMPO in the vesicles will allow fluorescence detection of radicals hence revealing information about the permeability of radicals through different surfactants.

Quinoline-TEMPO and a radical photoinitiator have been inserted into NaY zeolites and fluorescence growth has been observed during the photodecomposition reaction. Radical trapping by the pre-fluorescent sensor has shown the potential use of these probes in the study of radical intermediates produced inside the cavities by photolysis of suitable radical initiators. This methodology could now be applied to other more interesting organic substrates. During last few years the debate about the real photostability of organic molecules used as sunscreens has received considerable attention. Some of these optical filters have been reported to be very photoreactive, leading to in vivo phototoxicity or even photocarcinogenesis. For some of these molecules photodegradation pathways involving carbon-centered radicals have been invoked to explain observed phototoxicity. In order to prevent these problems, our group is working on the idea to encapsulate sunscreen filters in zeolites; such a different environment may lead to different photobehaviors of sunscreens and may prevent any possible interaction of reactive intermediates, formed during photodegradation, with target molecules such as DNA or lipids. Quinoline-TEMPO is a suitable probe to monitor radicals produced by photodegradation of sunscreens.

The organometallic paramagnetic compounds presented in this work can be used to prepare polystyrene polymers containing the metal center bridging long polymeric chains. The same experimental approach used for the radical trapping of polystyrene macroradicals by coumarin-TEMPO could be considered for this synthesis. Radical trapping of a polystyrene macroradical, produced by the uncapping of a TEMPO-capped polystyrene at high temperatures, by each of the

four nitroxides group present in the europium (III) potassium tetra-quinoline-TEMPO complex can produce a dendrimer with an emitting metal at the core. The molecule may not support such an extension due to bond formation with a macroradical tail at high temperatures. The choice of lower-molecular weight oligomers and working at milder conditions reducing the temperature from the value of 125 °C increases the possibility of the molecule not degrading.

Enzyme-mediated free radical polymerization is a novel field which gives us new options in the preparation of polymers using more environmental compatible approaches[92,93]. This includes the reduction in the use of heavy metals, the use of ambient or near ambient temperatures and the non-requirement of special equipment. It has been reported recently that horseradish peroxidase (HRP) mediates the free radical polymerization of both methyl methacrylate and styrene using solvent mixtures of water and a water-soluble organic solvents in the presence of hydrogen peroxide and β-diketones as initiator for the polymerization. HRP is an oxido-reductase that acts on hydrogen peroxide and on organic reducing substrates. The hydroxyl radicals produced within the enzyme catalytic system abstract a hydrogen from β-diketones with the consequent formation of water and a carbon-centered radical which, in presence of monomer, can start the polymerization process. In our laboratory the Masters student Marius Gabriel Ivan is carrying out a project determining the rates of production of carbon-centered produced in HRP enzyme catalytic systems.

6.3 Claims to original research

Fluorescence detection of carbon-centered radicals has been examined during the course of this thesis including the development of the applications of pre-fluorescent radical sensors in different systems.

Coumarin-TEMPO and quinoline-TEMPO pre-fluorescent sensors for radicals have been prepared, characterized and tested in radical trapping reactions in

homogenous solutions employing radical initiators activated by light and by heat.

Coumarin-TEMPO was used for the development of a novel methodology in the field of "living" free radical polymerization. The absolute kinetics for end-cap cleavage in TEMPO-capped polystyrene were determined. From this data the Arrhenius parameters and the corresponding bond dissociation energy for the terminal TEMPO group in the polymeric chain were obtained.

Micelles have been used to confine the elements of the reaction system of photoproduction of radicals in closer space. Caging of triplet-radical pairs by solvent molecules has been observed in micellar environment.
Fluorescence detection of carbon-centered radicals has been achieved inside the cavities of NaY zeolites. The radical photoinitiator and the pre-fluorescent probe were included in the zeolite framework and fluorescence increments were observed after irradiation of solid samples and polymeric suspensions.

Bisbenzyl biradicals have been detected using quinoline-TEMPO as a pre-fluorescent probe.

Organometallic paramagnetic compounds were prepared employing quinoline-TEMPO as a ligand for metals. The europium complex was tested in the radical trapping reaction of carbon-centered radicals. The mechanism dynamics of the reaction were outlined by rationalization of the evolution of the fluorescence emissions from the ligand and the metal during the thermal decomposition of 2,2′-azobisbutyronitrile radical initiator.

Appendix

Table I Crystal data and structural analysis results of 4-(3-Hydroxy-2-methyl-quinolinoyloxy)-2,2,6,6-tetramethylpiperidine-1-oxyl free radical (quinoline-TEMPO) monoclinic and triclinic.

Complex	Quinoline-TEMPO	
	Monoclinic	Triclinic
Empirical formula	C20 H25 N2 O4	C40 H50 N4 O8
Formula weight	357.42	714.84
Crystal color	red	red
Crystal system	monoclinic	triclinic
Space group	P2 (1)/n	P-1
a (Å)	8.3137 (6)	7.9277 (9)
b (Å)	25.0697 (2)	9.7800 (11)
c (Å)	9.5088 (7)	25.596 (3)
α (deg)	90	88.008 (2)
β (deg)	111.15 (1)	85.392 (2)
γ (deg)	90	72.299 (2)
V ($Å^3$)	1848.3 (2)	1884.4 (4)
Z	4	2
Radiation:		
λ(Mo Kα) (Å)	0.71073	0.71073
T °C	173 (2)	203 (2)
D_{calcd} ($mg\ m^{-3}$)	1.284	1.260
μ_{calcd} (mm^{-1})	0.090	0.088
R, wR^2	0.0507, 0.0965	0.0450, 0.1140

Table II Selected bonds and angles for quinoline-TEMPO monoclinic and triclinic.

Quinoline-TEMPO

Monoclinic	Triclinic
N (1) – C (9) = 1.305 (2)	N (1) – C (9) = 1.2995 (16)
N (1) – C (1) = 1.376 (2)	N (1) – C (1) = 1.3752 (16)
N (2) – O (4) = 1.2863 (16)	N (2) – O (4) = 1.2838 (12)
N (2) – C (12) = 1.495 (2)	N (2) – C (12) = 1.4815 (14)
O (1) – C (8) = 1.3467 (19)	O (1) – C (8) = 1.3468 (14)
O (2) – C (11) = 1.2226 (18)	O (2) – C (11) = 1.2193 (14)
C (7) – C (8) = 1.382 (2)	C (7) – C (8) = 1.3803 (16)
C (8) – C (9) = 1.436 (2)	C (8) – C (9) = 1.4359 (15)
C (12) – C (13) = 1.530 (2)	C (12) – C (13) = 1.5279 (15)
C (13) – C (14) = 1.506 (2)	C (13) – C (14) = 1.5027 (16)
O (4) – N (2) – C (12) = 115.54 (12)	O (4) – N (2) – C (12) = 116.06 (9)
O (1) – C (8) – C (7) = 124.44 (14)	O (1) – C (8) – C (7) = 124.59 (10)
O (2) – C (11) – C (7) = 121.83 (14)	O (2) – C (11) – C (7) = 122.95 (10)
O (2) – C (11) – O (3) = 121.83 (14)	O (2) – C (11) – O (3) = 122.06 (10)
C (9) – N (1) – C (1) = 119.04 (14)	C (9) – N (1) – C (1) = 119.43 (10)
C (1) – C (2) – C (3) = 121.49 (17)	C (1) – C (2) – C (3) = 121.23 (11)
C (8) – C (7) – C (11) = 116.38 (14)	C (8) – C (7) – C (11) = 116.40 (10)

Table III Crystal data and structural analysis results of 4-(3-hydroxy-2-methyl-4-quinolinoyloxy)-2,2,6,6-tetramethylpiperidine-1-hydroxyl (Q-TH) and 4-(3-p-toluensulfonyloxy-2-methyl-4-quinolinoyloxy)-2,2,6,6-tetramethylpiperidine-1-oxyl free radical (QTs-T).

Complex	Q-TH	QTs-T
Empirical formula	C20 H26 N2 O4	C27 H31 N2 O6 S
Formula weight	358.43	511.60
Crystal color	transparent	orange
Crystal system	monoclinic	monoclinic
Space group	P2 (1)/n	P2 (1)/n
a (Å)	15.7292 (17)	8.7798 (19)
b (Å)	6.0842 (7)	29.311 (6)
c (Å)	19.615 (2)	10.501 (2)
α (deg)	90.00	90.00
β (deg)	96.647 (2)	107.428 (2)
γ (deg)	90.00	90.00
V ($Å^3$)	1864.5 (4)	2578.2 (9)
Z	4	4
Radiation:		
λ(Mo Kα) (Å)	0.71073	0.71073
T °C	203 (2)	203 (2)
D_{calcd} ($mg\ m^{-3}$)	1.277	1.318
μ_{calcd} (mm^{-1})	0.089	0.170
R, wR^2	0.0534, 0.1399	0.0512, 0.1337

Table IV Selected bond lengths and angles for Q-TH and QTs-T.

Q-TH	QTs-T
N (1) - C (9) = 1.303 (3)	N (1) – C (9) = 1.314 (3)
N (1) - C (1) = 1.384 (2)	N (1) – C (1) = 1.365 (3)
N (2) – O (4) = 1.447 (2)	N (2) – O (4) = 1.284 (2)
N (2) – C (12) = 1.488 (2)	N (2) – C (12) = 1.494 (2)
O (1) – C (8) = 1.338 (2)	O (1) – C (8) = 1.402 (2)
O (2) – C (11) = 1.219 (2)	O (2) – C (11) = 1.198 (2)
C (7) – C (8) = 1.387 (3)	C (7) – C (8) = 1.362 (3)
C (8) – C (9) = 1.433 (3)	C (8) – C (9) = 1.418 (3)
C (12) – C (13) = 1.533 (3)	C (12) – C (13) = 1.531 (3)
C (13) – C (14) = 1.507 (3)	C (13) – C (14) = 1.505 (3)
O (4) – N (2) – C (12) = 106.83 (14)	S – O (1) = 1.6165 (13)
O (1) – C (8) – C (7) = 124.58 (18)	S – O (5) = 1.4234 (15)
O (2) – C (11) – C (7) = 123.03 (17)	S – O (6) = 1.4151 (16)
O (2) – C (11) – O (3) = 122.01 (17)	O (4) – N (2) – C (12) = 115.73 (15)
C (9) – N (1) – C (1) = 119.18 (17)	O (1) – C (8) – C (7) = 119.88 (16)
C (1) – C (2) – C (3) = 120.96 (19)	O (2) – C (11) – C (7) = 122.46 (17)
C (8) – C (7) – C (11) = 115.61 (17)	O (2) – C (11) – O (3) = 125.67 (17)
	C (9) – N (1) – C (1) = 119.75 (17)
	C (1) – C (2) – C (3) = 120.2 (2)
	C (8) – C (7) – C (11) = 123.61 (17)
	C (8) – O (1) – S = 121.24 (11)

Table V Crystal data and structural analysis results of Nickel (II) bis-quinoline-TEMPO and Cobalt (II) bis-quinoline-TEMPO.

Complex	Nickel (II) bis-quinoline-TEMPO	Cobalt (II) bis-quinoline-TEMPO
Empirical formula	C49 H72 N4 Ni O11	C49 H72 Co N4 O11
Formula weight	951.82	952.04
Crystal color	yellow	dark red
Crystal system	triclinic	triclinic
Space group	P-1	P-1
a (Å)	13.8604 (7)	13.7869 (8)
b (Å)	14.2600 (10)	13.9421 (8)
c (Å)	16.7426 (8)	16.4727 (10)
α (deg)	109.5070 (10)	107.220 (1)
β (deg)	94.5520 (10)	96.470 (1)
γ (deg)	119.0680 (10)	118.379 (1)
V ($Å^3$)	2606.5 (3)	2537.1 (3)
Z	2	2
Radiation:		
λ(Mo Kα) (Å)	0.71070	0.71070
T °C	173 (2)	173 (2)
D_{calcd} ($mg\ m^{-3}$)	1.213	1.246
μ_{calcd} (mm^{-1})	0.431	0.398
R, wR^2	0.0588, 0.1559	0.0867, 0.2606

Table VI Selected bond lengths and angles for Nickel (II) bis-quinoline-TEMPO and Cobalt (II) bis-quinoline-TEMPO.

Nickel (II) bis-quinoline-TEMPO	Cobalt (II) bis-quinoline-TEMPO
Ni (1) – O (1) = 1.9773 (17)	Co (1) – O (1) = 1.9907
Ni (1) – O (2) = 2.0438 (18)	Co (1) – O (2) = 2.0959
Ni (1) – O (5) = 1.9776 (17)	Co (1) – O (5) = 1.9928
Ni (1) – O (6) = 2.0386 (19)	Co (1) – O (6) = 2.0957
N (1) – C (9) = 1.299 (3)	N (1) – C (9) = 1.298 (2)
N (1) – C (1) = 1.380 (4)	N (1) – C (1) = 1.3837
N (2) – O (4) = 1.275 (3)	N (2) – O (4) = 1.292 (4)
N (2) – C (12) = 1.481 (4)	N (2) – C (12) = 1.509 (4)
O (1) – C (8) = 1.283 (3)	O (1) – C (8) = 1.288 (2)
O (2) – C (11) = 1.225 (3)	O (2) – C (11) = 1.227 (2)
C (7) – C (8) = 1.409 (3)	C (7) – C (8) = 1.415 (3)
C (8) – C (9) = 1.471 (3)	C (8) – C (9) = 1.471 (3)
C (12) – C (13) = 1.533 (4)	C (12) – C (13) = 1.542 (3)
C (13) – C (14) = 1.506 (5)	C (13) – C (14) = 1.515 (5)
O (4) – N (2) – C (12) = 116.7 (3)	O (4) – N (2) – C (12) = 115.0 (3)
O (1) – C (8) – C (7) = 127.4 (2)	O (1) – C (8) – C (7) = 127.36 (18)
O (2) – C (11) – C (7) = 127.3 (2)	O (2) – C (11) – C (7) = 126.48 (19)
O (2) – C (11) – O (3) = 118.4 (2)	O (2) – C (11) – O (3) = 118.77 (16)
C (9) – N (1) – C (1) = 119.04 (14)	C (9) – N (1) – C (1) = 119.43 (10)
C (1) – C (2) – C (3) = 121.2 (3)	C (1) – C (2) – C (3) = 121.12 (13)
C (8) – C (7) – C (11) = 117.8 (2)	C (8) – C (7) – C (11) = 117.9 (2)
O (1) – Ni (1) – O (2) = 86.01 (7)	O (1) – Co (1) – O (2) = 84.4
O (1) – Ni (1) – O (6) = 90.04 (8)	O (1) – Co (1) – O (6) = 89.3
O (1) – Ni (1) – O (5) = 175.12 (7)	O (1) – Co (1) – O (5) = 173.0
O (1) – Ni (1) – O (1A) = 94.56 (13)	O (1) – Co (1) – O (1A) = 92.24
O (1) – Ni (1) – O (1D) = 94.00 (6)	O (1) – Co (1) – O (1D) = 93.7

Table VII Crystal data and structural analysis results of Europium (III) tetra-quinoline-TEMPO and Lantanum (III) tetra-quinoline-TEMPO.

Complex	Europium (III) potassium tetra-quinoline-TEMPO
Empirical formula	C84 H102 Eu K N10 O18
Formula weight	1730.82
Crystal color	orange
Crystal system	tetragonal
Space group	P-4n2
a (Å)	20.390 (5)
b (Å)	20.390 (5)
c (Å)	10.366 (3)
α (deg)	90
β (deg)	90
γ (deg)	90
V (Å^3)	4309 (2)
Z	2
Radiation:	
λ(Mo Kα) (Å)	0.71073
T °C	203 (2)
D_{calcd} (mg m^{-3})	1.334
μ_{calcd}(mm^{-1})	0.847
R, wR^2	0.0471, 0.1275

Table VIII Selected bond lengths and angles for Europium (III) tetra-quinoline-TEMPO.

Europium (III) potassium tetra-quinoline-TEMPO	Symmetry transformations used to generate equivalent atoms
Eu (1) – O (1), #1, #2, #3 = 2.303 (3)	#1 -y+3/2, -x+3/2, -z+5/2
Eu (1) – O (2)), #1, #2, #3 = 2.476 (3)	#2 –x+1, -y+2, z
Eu (1) – K (2), #3 = 4.087 (3)	#3 y-1/2, x+1/2, -z+5/2
N (1) – C (9) = 1.288 (6)	#4 y-1/2, x+1/2, -z+3/2
N (1) – C (1) = 1.372 (5)	#5 –y+3/2, -x+3/2, -z+3/2
N (2) – O (4) = 1.270 (5)	
O (1) – C (8) = 1.318 (6)	
O (2) – C (11) = 1.230 (5)	
C (7) – C (8) = 1.375 (6)	
C (8) – C (9) = 1.477 (6)	
C (12) – C (13) = 1.553 (6)	
C (13) – C (14) = 1.490 (8)	
O (4) – N (2) – C (12) = 115.9 (4)	
O (1) – C (8) – C (7) = 125.5 (4)	
O (2) – C (11) – C (7) = 124.5 (4)	
O (2) – C (11) – O (3) = 121.5 (4)	
C (9) – N (1) – C (1) = 120.4 (4)	
C (1) – C (2) – C (3) = 121.0 (4)	
C (8) – C (7) – C (11) = 117.7 (4)	

References

(1) Gilbert, A.; Baggott, J. *Essentials of Molecular Photochemistry*; Black Well Scientific Publications: Berlin, 1991.

(2) Forrester, A. R. *Landolt-Bornstein*; Springer: Berlin, 1979; Vol. Vol. 9, Magnetic Properties of Free Radicals, Part c1: Nitroxide Radicals.

(3) Patai, S.; Rappoport, Z. *Nitrones, Nitronates, Nitroxides*, 1989.

(4) Gijzeman, O. L. J.; Kaufman, F.; Porter, G. *J. Chem. Soc. Faraday Trans. 2* **1972**, *69*, 727-737.

(5) Gijzeman, O. L. J.; Kaufman, F.; Porter, G. *J. Chem. Soc. Faraday Trans. 2* **1972**, *69*, 708-720.

(6) Gijzeman, O. L. J.; Kaufman, F. *J. Chem. Soc. Faraday Trans. 2* **1972**, *69*, 721-726.

(7) *Nitric Oxide - Biology and pathology*; Ignarro, E. b. L. J., Ed.; Academic Press: San Diego, 2000.

(8) Korth, H.-G.; Sustmann, R.; Ernst, A.; de Groot, H.; Hughes, L.; Ingold, K. U. *J. Am. Chem. Soc.* **1994**, *116*, 2767-2777.

(9) Chattopadhyay, S. K.; Das, P. K.; Hug, G. L. *J. Am. Chem. Soc.* **1983**, *105*, 6205-6210.

(10) Watkins, A. R. *Chem. Phys. Lett.* **1974**, *29*, 526-528.

(11) Kuzmin, V. A.; Tatikolov, A. S. *Chem. Phys. Lett.* **1977**, *51*, 45-47.

(12) Green, S. A.; Simpson, D. J.; Zhou, G.; Ho, P. S.; Blough, N. V. *J. Am. Chem. Soc.* **1990**, *112*, 7337-7346.

(13) Blough, N. V.; Simpson, D. J. *J. Am. Chem. Soc.* **1987**, *110*, 1915-1917.

(14) Moad, G.; Shipp, D. A.; Smith, T. A.; Solomon, D. *J. Phys. Chem. A* **1999**, *103*, 6580-6586.

(15) Blough, N. V.; Herbelin, S. E. *J. Phys. Chem. B* **1998**, *102*, 8170-8176.

(16) Pou, S.; Huang, Y.; Bhan, A.; Bhadti, V. S.; Hosmane, R. S.; Wu, S. Y.; Cao, G.; Rosen, G. M. *Analytical chemistry* **1993**, *212*, 85-90.

(17) Li, B.; Gutierrez, P. L.; Blough, N. V. *Anal. Chem.* **1997**, *69*, 4295-4302.

(18) Johnson, C. G.; Caron, S.; Blough, N. V. *Anal. Chem.* **1996**, *68*, 867-872.

(19) Jockusch, S.; Dedola, G.; Lem, G.; Turro, N. J. *J. Phys. Chem. B* **1999**, 9126-9129.

(20) Kawai, A.; Okutsu, T.; Obi, K. *J. Phys. Chem* **1991**, *95*, 9130-9134.

(21) Goudsmit, G.; Paul, H.; Shushin, A. I. *J. Phys. Chem.* **1993**, *97*, 13243-13249.

(22) Kobori, Y.; Kawai, A.; Obi, K. *J. Phys. Chem.* **1994**, *98*, 6425-6429.

(23) Conti, F.; Corvaja, C.; Toffoletti, A.; Mizuochi, N.; Ohba, Y.; Yamauchi, S.; Maggini, M. *J. Phys. Chem. A* **2000**, *104*, 4962-4967.

(24) Ishii, K.; Fujisawa, J.; Adachi, A.; Yamauchi, S.; Kobayashi, N. *J. Am. Chem. Soc.* **1998**, *120*, 3152-3158.

(25) Chateauneuf, J.; Lusztyk, J.; Ingold, K. U. *J. Org. Chem.* **1988**, *53*, 1629-1632.

(26) Beckwith, A. L. J.; Bowry, V. W.; Moad, G. *J. Org. Chem.* **1988**, *53*, 1632-1641.

(27) Beckwith, A. L. J.; Bowry, V. W.; Ingold, K. U. *J. Am. Chem. Soc.* **1992**, *114*, 4983-4992.

(28) Bowry, V. W.; Ingold, K. U. *J. Am. Chem. Soc.* **1992**, *114*, 4992-4996.

(29) Sobek, J.; Martschke, R.; Fisher, H. *J. Am. Chem. Soc.* **2001**, *123*, 2849-2857.

(30) Turro, N. J.; Kraeutler, B. *Acc. Chem. Res.* **1980**, *13*, 369-377.

(31) Korolenko, E. C.; Cozens, F. L.; Scaiano, J. C. *J. Phys. Chem.* **1995**, *99*, 14123-14128.

(32) Turro, N. J.; Anderson, D. R.; Chow, M.; Chung, C.; Kraeutler, B. *J. Am. Chem. Soc.* **1981**, *103*, 3892-3896.

(33) Turro, N. J.; Chow, M.; Chung, C.; Kraeutler, B. *J. Am. Chem. Soc.* **1981**, *103*, 3886-3891.

(34) Kleinman, M. H.; Shevchenko, T.; Bohne, C. *Photochemistry and Photobiology* **1998**, *67(2)*, 198-205.

(35) Skene, W. G.; Scaiano, J. C.; Listigovers, N. A.; Kazmaier, P. M.; Georges, M. K. *Macromolecules* **2000**, *33*, 5065-5072.

(36) Borbat, P. P.; Costa-Filho, A. J.; Earle, K. A.; J. K. Moscicki; Freed, J. H. *Science* **2001**, *291*, 266-269.

(37) Balcon, B. J.; Petersen, N. O. *J. Org. Chem.* **1988**, *54*, 1922-1927.

(38) Fossey, J.; Lefort, D.; Sorba, J. *Free Radicals in Organic Chemistry*; John Wiley & Sons: Singapore, 1995.

(39) Ram, S.; Ehrenkaufer, R. E. *Tetrahedron Lett.* **1984**, *25*, 3415-3418.

(40) Hamilton, W. C.; Ibers, J. A. *Hydrogen bonding in solids* New York, 1968.

(41) *Controlled radical polymerization*; Matyjaszewski, K., Ed.; American Chemical Society: Washington, 1998.

(42) Robbins, W. K.; Eastman, R. H. *J. Am. Chem. Soc.* **1970**, *92*, 6077-6079.

(43) Step, E. N.; Buchachenko, A. L.; Turro, N. J. *J. Am. Chem. Soc.* **1994**, *116*, 5462-5466.

(44) Veregin, R. P. N.; Odell, P. G.; Michalak, L. M.; Georges, M. K. *Macromolecules* **1996**, *29*, 2246-3352.

(45) Georges, M. K.; Veregin, R. P. N.; Kazmaier, P. M.; Hamer, G. K. *Macromolecules* **1993**, *26*, 2987-2988.

(46) Rizzardo, E.; Solomon, D. H. *Polymer Bulletin* **1979**, *1*, 529-534.

(47) Moad, G.; Rizzardo, E.; Solomon, D. H. *Macromolecules* **1982**, *15*, 909-914.

(48) Georges, M. K.; Veregin, R. P. N.; Kazmaier, P. M.; Hamer, G. K.; Saban, M. *Macromolecules* **1994**, *27*, 7228-7229.

(49) Benoit, D.; Harth, E.; Fox, P.; Waymouth, R. M. *Macromolecules* **2000**, *33*, 363-370.

(50) Skene, W. G.; Belt, S. T.; Connolly, T. J.; Hahn, P.; Scaiano, J. C. *Macromolecules* **1998**, *31*, 9103-9105.

(51) Skene, W. G.; Scaiano, J. C.; Yap, G. P. A. *Macromolecules* **2000**, *33*, 3536-3542.

(52) Baldovi, M. V.; Mohtat, N.; Scaiano, J. C. *Macromolecules* **1996**, *29*, 5497-5499.

(53) Hawker, C. J. *J. Am. Chem. Soc.* **1994**, *116*, 11185-11186.

(54) Turro, N. J.; Lem, G.; Zavarine, I. S. *Macromolecules* **2000**, 9782-9785.

(55) Tsentalovich, Y. P.; Morozova, O. B.; Avdievich, N. I.; Ananchenko, G. S.; Yurkovskaya, A. V.; Ball, J. D.; Forbes, M. D. E. *J. Phys. Chem. A* **1997**, *101*, 8809-8816.

(56) Zimmit, M. B.; Doubleday, C.; Gould, I. R.; Turro, N. J. *J. Am. Chem. Soc.* **1985**, *107*, 6724-6726.

(57) Scaiano, J. C. *Tetrahedron* **1982**, *38*, 819-824.

(58) Tanaka, R.; Kuriyama, Y.; Itoh, H.; Sakuragi, H.; Tokumaru, K. *Chem. Lett.* **1993**, *8*, 1447-1450.

(59) Barton, D. H. R.; Charpiot, B.; Ingold, K. U.; Johnston, L. J.; Motherwell, W. B.; Scaiano, J. C.; Stanforth, S. *J. Am. Chem. Soc.* **1985**, *107*, 3607-3611.

(60) Miranda, M. A.; Font-Sanchis, E.; Perez-Prieto, J.; Scaiano, J. C. *J. Org. Chem.* **1999**, *64*, 7842-7845.

(61) Miranda, M. A.; Font-Sanchiz, E.; Perez-Prieto, J.; Scaiano, J. C. *J. Org. Chem.* **2001**, *66*, 2717-2721.

(62) Grissom, J. W.; Gunawardena, G. U. *Tetrahedron Lett.* **1995**, *36*, 4951-4954.

(63) Turro, N. J.; Cherry, W. R. *J. Am. Chem. Soc.* **1978**, *100*, 7431-7432.

(64) Garcia-Garibay, M. A.; Zhang, Z.; Turro, N. J. **1991**, *113*, 6212-6218.

(65) Turro, N. J.; Cheng, C.; Lei, X. **1985**, *107*, 3739-3741.

(66) Ramamurthy, V.; Corbin, D. R.; Turro, N. J.; Sato, Y. *Tetrahedron Lett.* **1989**, *30*, 5829-5832.

(67) Turro, N. J. *Acc. Chem. Res.* **2000**, *33*, 637-646.

(68) Jockusch, S.; Liu, Z.; Ottaviani, M. F.; Turro, N. J. *J. Phys. Chem. B* **2001**, *105*, 7477-7481.

(69) Scaiano, J. C.; Kaila, M.; Corrent, S. *J. Phys. Chem. B* **1997**, 8564-8568.

(70) Vostrikova, K. E.; Luneau, D.; Wernsdorfer, W.; Rey, P.; Verdaguer, M. *J. Am. Chem. Soc.* **2000**, *122*, 718-719.

(71) Ishii, K.; Fujisawa, J.; Ohba, Y.; Yamauchi, S. *J. Am. Chem. Soc.* **1996**, *118*, 13079-13080.

(72) Stroh, C.; Turek, P.; Rabu, P.; Ziessel, R. *Inorg. Chem.* **2001**, *40*, 5334-5342.

(73) Osiecki, J. H.; Ullman, E. F. *J. Am. Chem. Soc.* **1968**, *90*, 1078-1079.

(74) Caneschi, A.; Gatteschi, D.; Lalioti, N.; Sangregorio, C.; Sessoli, R.; Venturi, G.; Vindigni, A.; Pini, G. M.; Rettori, A.; A., N. M. *Angew. Chem. Int. Ed.* **2001**, *40*, 1760-1761.

(75) Forbes, G. C.; Kennedy, A. R.; Mulvey, R. E.; Rodger, P. J. A. *Chem. Commun.* **2001**, 1400-1401.

(76) Rowe, R. A.; Jones, M. M. *Inorganic Syntheses* **1990**, 114.

(77) Stein, G.; Wurzberg, E. *J. Chem. Phys.* **1974**, *62*, 208-212.

(78) Heller, A. *J. Am. Chem. Soc.* **1965**, *88*, 2058-2059.

(79) Haas, Y.; Stein, G. *J. Phys. Chem.* **1971**, *75*, 3677-3681.

(80) Selvin, R.; Rana, T. M.; Hearst, J. E. *J. Am. Chem. Soc.* **1994**, *116*, 6029-6030.

(81) Xiao, M.; Selvin, P. R. *J. Am. Chem. Soc.* **2001**, *123*, 7067-7073.

(82) Georgescu, S.; Lupei, V.; Petraru, A.; Hapenciuc, C.; Florea, C.; Naud, C.; Porte, C. *J. of Luminescence* **2001**, *93*, 281-292.

(83) Ternane, R.; Trabelsi-Ayedi, M.; Kbir-Agriguib, N.; Piriou, B. *Journal of luminescence* **1999**, *81*, 165-170.

(84) Muyamoto, Y.; Uekawa, M.; Ikeda, H.; Kaifu, K. *J. of Luminescence* **1999**, *81*, 159-164.

(85) Zhao, D.; Li, W.; Hong, Z.; Liu, X.; Liang, C.; Zhao, D. *J. of Luminescence* **1999**, *82*, 105-109.

(86) Petoud, S.; G. Bunzli, J.-C.; Glanzman, T.; Piguet, C.; Xiang, Q.; Thummel, R. P. *J. of Luminescence* **1999**, *82*, 69-79.

(87) Panigrahi, B. S. *J. of Luminescence* **1999**, *82*, 121-127.

(88) Steemers, F. J.; Verboom, W.; Reinhoudt, D. N.; van der Tol, E. B.; Verhoeven, J., W. *J. Am. Chem. Soc.* **1995**, *117*, 9408-9414.

(89) Voloshin, A. I.; Shavaleev, N. M.; P., K. V. *Journal of Luminescence* **2001**, *93*, 191-197.

(90) Voloshin, A. I.; Shavaleev, N. M.; Kazakov, V. P. *Journal of Luminescence* **2001**, *93*, 199-204.

(91) Froidevaux, P.; Bunzli, J. *J. Phys. Chem.* **1994**, *98*, 532-536.

(92) Singh, A.; Ma, D.; Kaplan, D. L. *Biomacromolecules* **2000**, *1*, 592-596.

(93) Kaira, B.; Gross, R. A. *Biomacromolecules* **2000**, *1*, 501-505.